



TAMPEREEN TEKNILLINEN YLIOPISTO  
TAMPERE UNIVERSITY OF TECHNOLOGY

Joni Backas

**Energy Efficient Control of Hydrostatic Drive Transmissions**  
A Nonlinear Model-Based Approach



Julkaisu 1559 • Publication 1559

Tampere 2018

Tampereen teknillinen yliopisto. Julkaisu 1559  
Tampere University of Technology. Publication 1559

Joni Backas

## **Energy Efficient Control of Hydrostatic Drive Transmissions**

A Nonlinear Model-Based Approach

Thesis for the degree of Doctor of Science in Technology to be presented with due permission for public examination and criticism in Konetalo Building, Auditorium K1702, at Tampere University of Technology, on the 28<sup>th</sup> of September 2018, at 12 noon.

Tampereen teknillinen yliopisto - Tampere University of Technology  
Tampere 2018

Doctoral candidate: Joni Backas  
Laboratory of Automation and Hydraulic Engineering  
Faculty of Engineering Sciences  
Tampere University of Technology  
Finland

Supervisor: Prof. Kalevi Huhtala  
Laboratory of Automation and Hydraulic Engineering  
Faculty of Engineering Sciences  
Tampere University of Technology  
Finland

Instructor: Associate Prof. Reza Ghabcheloo  
Laboratory of Automation and Hydraulic Engineering  
Faculty of Engineering Sciences  
Tampere University of Technology  
Finland

Pre-examiners: Prof. Kari Tammi  
Department of Mechanical Engineering  
Aalto University, School of Engineering  
Finland

Prof. Marcus Geimer  
Institute of Vehicle System Technology  
Karlsruhe Institute of Technology  
Germany

Opponents: Prof. Kari Tammi  
Department of Mechanical Engineering  
Aalto University, School of Engineering  
Finland

Prof. Petter Krus  
Department of Management and Engineering  
Linköping University  
Sweden

ISBN 978-952-15-4177-3 (printed)  
ISBN 978-952-15-4245-9 (PDF)  
ISSN 1459-2045

## **Abstract**

The high standard of living in industrial countries is based on the utilization of machines. In particular, the tasks performed with hydraulic work machines (HWMs) are essential in numerous industrial fields. Agriculture, mining, and construction are just a few examples of the lines of business that would be inconceivable today without HWMs. However, rising oil prices and competing technologies are challenging the manufacturers of these machines to improve their fuel economy.

Despite the fact that energy efficiency research of hydraulic systems has been active for more than a decade, there seems to be a significant gap between industry and academia. The manufacturers of HWMs have not adopted, for example, novel system layouts, prototype components, or algorithms that require powerful control units in their products.

The fuel economy of HWMs can be increased by utilizing system information in control algorithms. This cost-effective improvement enables operation in challenging regions and closer to the operating boundaries of the system. Consequently, the information about the system has to be accurate. For example, reducing the rotational speed of the engine has proven effective in improving the energy efficiency, but it increases the risk of even stalling the engine, for instance in situations where the power generation cannot meet the high transient demand. If this is considered in the controller with low uncertainty, fuel economy can be improved without decreasing the functionality of the machine.

This thesis studies the advantages of model-based control in the improvement of the fuel economy of HWMs. The focus is on hydrostatic drive transmissions, which is the main consumer of energy in certain applications, such as wheel loaders.

We started by developing an instantaneous optimization algorithm based on a quasi-static system model. The control commands of this fuel optimal controller (FOC) were determined based on cost function, which includes terms for fuel economy, steady-state velocity error, and changes in the control commands.



Although the use of quasi-static models is adequate for steady-state situations, the velocity tracking during transients and under load changes has proven to be inadequate. To address this issue, a high-performance velocity-tracking controller was devised. Full state feedback was assumed, and we resorted to a so-called D-implementation, which eliminates, for example, the need for the equilibrium values of pressure signals. The nonlinearities of the system were considered with the state-dependent parameters of the linear model.

In the next step, a nonlinear model predictive controller combined fuel economy control and velocity tracking. To the best of the author's knowledge, this is the first time that the model predictive control scheme has been utilized with such a detailed system model that also considers the hydraulic efficiencies and torque generation of the engine. This enables utilizing the controller as a benchmark of control algorithms for non-hybrid hydrostatic drive transmissions that do not require information about the future.

The initial tests of all the controllers were conducted with a validated simulation model of a research platform machine, a five-ton municipal tractor. In addition, the FOC and velocity-tracking controller were implemented into the control system of the machine. The practical worth of the FOC was proven with a relatively unique field experiment set-up that included, for example, an online measurement system of fuel consumption and autonomous path following. The fuel economy improved up to 16.6% when compared with an industrial baseline controller. The devised velocity-tracking concept was also proven as a significant reduction of error was observed in comparison with classic literature solutions, namely state feedback and proportional-integral-derivative controllers.

## Preface

This research was conducted during years 2013-2018 at the Laboratory of Automation and Hydraulics (AUT) (formerly known as the Department of Intelligent Hydraulics and Automation (IHA)) at the Tampere University of Technology (TUT).

I would like to express my sincere and deep gratitude for my instructor Reza Ghabcheloo and supervisor Kalevi Huhtala (also the head of AUT). Your guidance and understanding during this process has been truly invaluable.


I wish to thank the preliminary examiners Professor Marcus Geimer and Associate Professor Kari Tammi for the evaluation of this thesis and their constructive feedback. Your expertise helped to improve the work notably.

In addition, I am grateful to all my colleagues at AUT who contributed to the unique working atmosphere, offered their scientific knowledge and participated also in many “counterbalancing” discussions over the years. In particular, M.Sc. Miika Ahopelto, Dr. Tech Otso Karhu, Dr. Tech. Mika Hyvönen and M.Sc. Antti Kolu provided their unselfish assistance for this research.

The financial support provided by the Finnish Cultural Foundation and TUT’s graduate school has been essential for completing this study. In addition, supportive grants from Henry Ford Foundation, TUT Industrial Research Fund, Walter Ahlström Foundation and Suomen Konepajainsinööriyhdistys are gratefully acknowledged.

To my sons Aapo and Elias, thank you for occupying my mind with non-scientific matters and my daughters Ella and Venla, thank you for lifting the heaviest burdens with your joyful greetings. Finally, I would like to express my heartfelt gratitude to Heidi, my wife. You both enable this effort and make it worthwhile.

Lempäälä, August 2018.



Joni Backas

# Contents

|  |             |
|--|-------------|
| <b>Abstract</b> .....  | <b>iii</b>  |
| <b>Preface</b> .....   | <b>v</b>    |
| <b>Contents</b> .....  | <b>vi</b>   |
| <b>List of Abbreviations</b> .....   | <b>viii</b> |
| <b>List of Publications</b> .....  | <b>ix</b>   |
| <b>Unpublished Manuscript</b> .....  | <b>ix</b>   |
| <b>1 Introduction</b> .....  | <b>1</b>    |
| 1.1 Research Problem.....  | 2           |
| 1.2 Contributions of the Thesis .....                                      | 4           |
| 1.3 Author’s Contribution to the Publications .....                        | 5           |
| 1.4 Assumptions and the Scope of Validity of the Conclusions .....         | 5           |
| <b>2 Review of the State of the Art</b> .....                              | <b>7</b>    |
| 2.1 Control of Hydrostatic Drive Transmissions .....                       | 7           |
| 2.1.1 Energy Management of Hydrostatic Drive Transmissions .....           | 7           |
| 2.1.1.1 Rule-Based Control .....   | 8           |
| 2.1.1.2 Model-Based Control .....  | 9           |
| 2.1.1.3 Optimal Control .....  | 10          |
| 2.1.2 Velocity Tracking of Hydraulic Drive Transmissions .....             | 15          |
| 2.1.2.1 Predictive Control .....   | 15          |
| 2.1.2.2 State Feedback and Classical Control .....                         | 15          |
| 2.1.2.3 Fuzzy Logic Control.....   | 16          |
| 2.2 Methods for Measurement, Analysis and Comparison of Fuel Economy ..... | 16          |
| 2.2.1 Baseline Controllers.....  | 16          |
| 2.2.1.1 Dynamic Programming.....   | 17          |
| 2.2.1.2 Commercial Control Algorithms .....                                | 17          |
| 2.2.2 Experimentation .....  | 19          |
| 2.2.2.1 Simulations .....  | 19          |

|   |           |
|---|-----------|
| 2.2.2.2 Laboratory Testing .....  | 19        |
| 2.2.2.3 Field Experiments .....   | 20        |
| 2.2.2.4 Test Cycles.....  | 20        |
| 2.2.3 Methods for Measuring Fuel Consumption and Economy .....  | 21        |
| 2.3 Summary .....   | 22        |
| <b>3 Research Platform Machine .....</b>  | <b>24</b> |
| 3.1 Systems of the Machine .....  | 25        |
| 3.1.1 Hydraulics .....  | 25        |
| 3.1.2 Control System and Architecture .....   | 26        |
| 3.1.3 Online Fuel Consumption Measurement System .....  | 27        |
| 3.2 Validation of Simulation Models .....   | 30        |
| <b>4 Summary of Publications.....</b>   | <b>33</b> |
| 4.1 P.I: Fuel Optimal Controller for Hydrostatic Drives – A Simulation Study and Model Validation.....                  | 34        |
| 4.2 P.II: Fuel Optimal Controller for Hydrostatic Drives and Real-World Experiments on a Wheel Loader .....             | 35        |
| 4.3 P.III: Gain Scheduled State Feedback Velocity Control of Hydrostatic Drive Transmissions.....                       | 36        |
| 4.4 P.IV: Nonlinear Model Predictive Energy Management of Hydrostatic Drive Transmissions (unpublished manuscript)..... | 36        |
| <b>5 Discussion.....</b>  | <b>38</b> |
| 5.1 Energy efficiency (RQ1).....  | 38        |
| 5.2 Practical importance (RQ2).....   | 40        |
| 5.3 Adaptability and flexibility (RQ3) .....  | 42        |
| <b>6 Conclusion and Future Work.....</b>  | <b>44</b> |
| <b>Bibliography.....</b>  | <b>46</b> |
| <b>Publication P.I.....</b>   | <b>53</b> |
| <b>Publication P.II.....</b>  | <b>65</b> |
| <b>Publication P.III.....</b>   | <b>81</b> |
| <b>Unpublished Manuscript P.IV.....</b>   | <b>93</b> |

## List of Abbreviations

|      |  |
|------|--|
| CAN  | Controller area network                      |
| CCC  | Control command combination                  |
| CVT  | Continuously variable transmission           |
| DP   | Dynamic programming                          |
| ECMS | Equivalent consumption minimization strategy |
| EM   | Energy management                            |
| FOC  | Fuel optimal controller                      |
| GSVC | Gain-scheduled velocity controller           |
| HEV  | Hybrid electric vehicle                      |
| HHV  | Hydraulic hybrid vehicle                     |
| HSD  | Hydrostatic drive transmission               |
| HWM  | Hydraulic work machine                       |
| IBLC | Industrial baseline controller               |
| ICE  | Internal combustion engine                   |
| IMU  | Inertial measurement unit                    |
| MPC  | Model predictive control                     |
| NMPC | Nonlinear model predictive control           |
| OBE  | On-board electronics                         |
| OOL  | Optimal operating line                       |
| PID  | Proportional-integral-derivative             |
| PLC  | Programmable logic controller                |
| PM   | Power management                             |
| RB   | Rule-based                                   |
| RQ   | Research question                            |
| SDP  | Stochastic dynamic programming               |

## List of Publications

This thesis is a compendium that includes three publications and one unpublished manuscript. In the text, these are referred to as **P.I**, **P.II**, **P.III**, and **P.IV**.

- P.I** Backas, J., Ghabcheloo, R., Hyvönen, M. & Huhtala, K. 2014. Fuel Optimal Controller for Hydrostatic Drives – A Simulation Study and Model Validation. Proceedings of the Bath/ASME 2014 Symposium on Fluid Power & Motion Control, FPMC2014. September 10–12, 2014, Bath, United Kingdom.
- P.II** Backas, J., Ghabcheloo, R., Tikkanen, S. & Huhtala, K. 2016. Fuel Optimal Controller for Hydrostatic Drives and Real-World Experiments on a Wheel Loader. *International Journal of Fluid Power*, 17 (3). DOI: 10.1080/14399776.2016.1202081. pp. 187–201.
- P.III** Backas, J., Ghabcheloo, R. & Huhtala, K. 2017. Gain Scheduled State Feedback Velocity Control of Hydrostatic Drive Transmissions. *Control Engineering Practice* 58. DOI: 10.1016/j.conengprac.2016.10.016. pp. 214–224.

## Unpublished Manuscript

- P.IV** Backas, J. and Ghabcheloo, R. Nonlinear Model Predictive Energy Management of Hydrostatic Drive Transmissions.

# 1 Introduction

Hydraulic work machines (HWMs) are an essential part of several industrial fields. Their impact is unreplacable, for example, in applications that require transferring high loads, and operating with high forces and on relatively difficult terrains or remote locations. Numerous machines can be classified as HWMs, but probably some of the most familiar are agricultural and municipal tractors, excavators, wheel loaders, a variety of forest machines, and modern mining equipment. A central factor for the competitive edge of HWMs, and hydraulic systems in general, is their superior power-to-weight ratio. This means that, for example, a comparatively lightweight boom can be equipped with a powerful actuator, which also keeps the size of the actual machine reasonably small.

The advantage of power density has been so significant that the energy efficiency aspects of hydraulic systems were neglected for decades, even though basic system layouts combined with traditional control methods often resulted in unnecessary low fuel economy. However, due to increasing oil prices and stringent emission regulations, the research for improving the energy usage of HWMs has been extremely active, especially during the last 10 years.

Modern HWMs are equipped with numerous sensors that provide real-time data about the operation of the machine to networks accessible from all over the world. This offers the machine owners a convenient way of supervising their fleet, but the possibilities are not limited to unidirectional monitoring. With computer-controlled drive-by-wire machines, this data can be utilized to change the operation of the machine. For example, information about the state of the systems enables both a considerable increase in the automation level and optimal control of HWMs. Such features can improve the quality of work and lower the operational costs.

Innovative products are a necessity for machine manufacturers that are striving to increase their global market share. Moreover, there seems to be growing interest towards advanced features also among the customers, who are beginning to realize that there is more in the electric control of HWMs than just a reduced number of hydraulic hoses.



Figure 1. Different types of hydraulic work machines (Photo provided by M. Ketonen).

Probably one of the most beneficial things in computer-controlled drive-by-wire machines is that the hydraulic installations are decoupled from the system controls. Therefore, changing the operation of the system does not usually require physical modifications. In addition, improvements of certain features, such as fuel economy or even safety, can be updated via a network connection. This enables both cost reductions and increased uptime of machines.

## 1.1 Research Problem

While both the industry and academia are developing solutions to the challenges of HWMs, it seems that the gap between these communities is quite significant. There is a considerable amount of research in the academic fluid power community related especially to the energy management (EM) of hydraulic hybrid vehicles (HHV). These are usually conducted with advanced system layouts or controller algorithms that require high calculation power. At the same time, most commercial manufacturers focus on improving the robustness and operability of their machines that are hydromechanically controlled even today. There are some hybrid machines in the market, but majority of them are electrical as the forklift of Still [1] or the hybridization is included in 1-dimensional work functions as in the crane of Liebherr [2].

The difference between these two worlds was a significant motivator for this thesis. It seems that for the cost-conscious machine-building industry the acquired benefits, for example in energy efficiency, might not cover the costs of substantial modifications fast enough. This is especially the case if the mechanical design of the machines has to be changed, for example to fit in an energy storage. Therefore, as large-scale hybridization of HWMs is not yet in prospect, the improvements can be achieved, for example, via intelligent control. For drive-by-wire machines, this means only changes in the control software that is a one-time expense. Even though such algorithms have already been developed in the Academia especially for the work functions of HWMs, they usually require very advanced control units not available in cost-effective prices. In addition,



these solutions tend to focus on improving the numeric results and ignoring for instance facility of commissioning and aspects of compliance. Therefore, developing commercial products based on them requires considerable effort.

Municipal tractors are one of the most versatile HWMs because they can be equipped with a variety of implements, such as buckets, snowplows or brushes. Regardless of the tool attached, the majority of the energy of wheel loaders [3], and especially municipal tractor applications, is consumed in the translational motion of the machine also referred to as traction drives. This encourages the pursuit for improving the fuel economy of hydrostatic drive transmissions (HSD).

*In this work, HSD includes the entire power transfer system of a traction drive beginning from the shaft of the internal combustion engine (ICE) and ending at the axle of the wheel of the machine.*

The main objective of this thesis is to improve the energy efficiency of HSDs with cost-effective solutions. This is formulated into the following research questions (RQs):

**Energy efficiency (RQ1):** How much the fuel economy of non-hybrid HSDs can be improved only by control algorithms without impairing the functionality of the system? What is the benefit of utilizing dynamic system models instead of steady-state equations?

**Practical importance (RQ2):** How to demonstrate that the control solutions developed for **RQ1** have also practical worth?

**Adaptability and flexibility (RQ3):** Can the controllers of drive-by-wire machines be designed in way that enables reduction of costs via faster control design and commissioning of HWMs?

In order to answer these research questions, this thesis involves the design of EM and velocity-tracking controllers for HSDs with the following features:

- F1 Fuel economy:** The designed EM solutions should improve the fuel economy of HSDs by means of control algorithms. Systems with energy storage are beyond the scope of this thesis.
- F2 High performance:** The response of the system should not be significantly impaired in order to increase fuel economy.
- F3 Experimentally verified:** Field tests are essential in the evaluation of the benefits of the developed controllers. Moreover, as the focus is on improving the fuel economy of HSDs, fuel consumption should be measured instead of predicting it with a model. Successful experimental testing also guarantees a certain level of robustness, as the utilized models are never perfectly consistent with the reality.
- F4 Credible comparison:** The performance of the developed controllers should be assessed by comparing both of them with feasible textbook solutions and state-of-the-art commercial algorithms of similar applications when viable.

- F5**      **Real-time implementable:** The primary requirement for the controllers is that the information about the future should not be mandatory. This enables real-time implementation that is necessary for **F3**.
- F6**      **Generality and modularity:** Structures of the devised controllers should be applicable to multiple system layouts of HSDs, and the number of tunable parameters should be kept to a minimum. In addition, the design has to enable the controller of an individual system to be integrated into the upper level EM of the machine.

## 1.2 Contributions of the Thesis

The scientific contributions of this thesis are as follows:

- An experimentally verified controller for improving the fuel economy of HSDs based on instantaneous optimization.
- An experimentally verified velocity-tracking controller for HSDs. This controller is based on gain-scheduling and state feedback. Here, D-implementation [4] was utilized to lift the uncertain pressure-based estimation of friction by replacing the measured pressure values with their derivatives.
- Developing a nonlinear model predictive controller (NMPC) scheme of HSDs that includes both EM and velocity tracking. This controller is able to serve as a benchmark for evaluating the fuel economy of non-hybrid HSDs with controllers that do not utilize information about the future.
- Plausible experimental verification with:
  - measured online fuel consumption that also enables comparing the momentary fuel economy of different controllers;
  - utilization of credible baseline controllers;
  - removing the operator influence for fuel economy with an autonomous drive algorithm introduced in [5]; and
  - meticulous evaluation of the functionality of the designed EM controller in extreme operability tests.

Such a thorough set-up for experimental tests is relatively unique in the literature.

- Validated simulation model of the research platform machine also in terms of fuel consumption.
- A modular structure of the EM controller for which the required calculation power can be adjusted (e.g., based on the available resources of the control unit in order to achieve feasible real-time implementation).
- Modifications to the control system of the machine that enable integration and implementation of the designed controllers.

### 1.3 Author's Contribution to the Publications

In this section, the contributions of the author of this thesis (later referred to as *the author*) to the publications and the unpublished manuscript are briefly explained.

- P.I** The author wrote the paper and designed the controller, tuned the parameters as well as implemented it on the real-time simulation environment, GIMsim. The responsible designer of GIMsim is M. Hyvönen who provided assistance during the model validation process. Measurements for collecting the validation data were planned and conducted by the author. R. Ghabcheloo suggested improvements for the structure of the controller and reviewed the paper together with Professor K. Huhtala.
- P.II** The author wrote the paper and was responsible for the changes required for the research platform machine. The author also modified the controller to enable implementation and conducting the experiments. In addition, the author installed the fuel measurement system after receiving information from the manufacturer of the engine. R. Ghabcheloo suggested improvements and made corrections to the paper. The author planned the tests and developed the baseline controller. Professors R. Ghabcheloo and S. Tikkanen made suggestions for the test plan and reviewed the paper together with Professor K. Huhtala.
- P.III** The author wrote the paper as well as developed and implemented the controller to the research platform machine. Professor R. Ghabcheloo presented the initial idea of utilizing gain scheduling for the velocity-tracking controller. The author derived the equations of the system model, and further developed the model (e.g., by adding a state in order to improve the response). Required signal processing and parameter tuning was conducted by the author. Professor R. Ghabcheloo suggested major improvements and made corrections to the paper. Professor K. Huhtala reviewed the paper.
- P.IV** The author wrote the manuscript and developed the models for the model predictive controller (MPC) framework. The basic structure of MPC is based on the script written by Grüne and Pannek [6]. This template was heavily modified by the author to implement, for example, reference tracking. The author designed and conducted the simulations to determine the most feasible structure and parameters for the controller. Professor R. Ghabcheloo suggested solutions, especially for improving the convergence of the optimization, made corrections, and reviewed the paper.

### 1.4 Assumptions and the Scope of Validity of the Conclusions

Controlling the hydraulic systems of HWMs encompasses an extensive field of research for which the main topics range from the modelling accuracy of these systems in various operating situations to the utilization of divergent control methods. Moreover, the practical implementations of the designed controllers are likely to impose restrictions (e.g., for the resolution of control commands or available computing resources). Especially the latter might have a significant effect on achievable real-time operation. In addition, the manufacturers of

commercially available components do not usually allow major changes to their products. For instance, some undesired features cannot be deactivated, and the tuning of the parameters of low-level controllers might not be enabled. Thus, it is important to delineate the scope in which the contributions listed in Section 1.2 are applicable.

- The presented methods for EM and velocity tracking require a modern drive-by-wire HWM. Additionally to these electrical operator (or computer-generated) commands, the information about certain state variables is essential for the control algorithms. For EM, pressure values are the most important ones, and for the velocity tracking, naturally the speed of the machine has to be measured.
- Pure rolling is assumed for the wheels of the machine (i.e., no slipping or skidding is present).
- For the system models, the hydraulic efficiencies are measured and the consumption of the engine is determined in steady-state operation points. These values cannot be considered entirely accurate in transient conditions, as demonstrated, for example, in [7]. However, the comparison of fuel rate values together with the validation data of the machine presented in Chapter 3, indicate that the accuracy of the predicted fuel consumption is adequate.
- The engine model utilized in **P.I** is validated for the maximum positive and negative loads of 50 and -20 kW, respectively, due to the limitations of the available laboratory equipment. The rated power of the engine is 100 kW.
- Even though the structures of the controllers are designed generic, the research is conducted with one machine in which the HSD does not have mechanical transmission, and the displacement of the hydraulic motors can be changed between two discrete settings. This system layout is quite uncommon in commercially available municipal tractors and wheel loaders.
- The scope of the research is limited to HSDs with no hybrid capabilities (i.e., no energy storages or secondary power sources). Therefore, if the designed controllers are utilized in a system with multiple consumers of power, high-level power management is required. To this end, the controllers include an interface for such a solution presented in [8].
- Comparisons between the fuel consumption of the designed controllers and globally optimal strategies, for example, dynamic programming (DP), are not conducted. This is because the focus is on empirical testing of the controllers from which collecting the required data (e.g., load profile), is not a trivial matter. In addition, the model utilized in DP would be significantly different from the real machine. Therefore, such comparisons would be unreliable. Furthermore, the computation time of DP increases exponentially with the number of variables. Due to this “curse of dimensionality,” it has not been utilized as a benchmark in **P.IV**.
- The devised controllers improve the fuel economy while tracking a given velocity reference trajectory and penalizing the velocity error. Thus, optimal control commands are not task-based as the reference is pre-determined. Alternatively, the problem could be set, for example, to “drive 100 meters and minimize the amount of consumed fuel.” This would also require including time in the optimization.

## **2 Review of the State of the Art**

This chapter provides a review of the state of the art in the field of control of HSDs. The main focus is in the different aspects of EM ranging from control algorithms (Section 2.1.1) to testing methods (Section 2.2.2). In addition, baseline controllers (Section 2.2.1) and means of evaluating success (Section 2.2.3) are discussed. Even though the test cycles of HWMs are not as standardized as those of automobiles, some references are made and commonly used practices described in Section 2.2.2.4. Section 2.1.2 presents solutions for the velocity tracking of HSDs.

### **2.1 Control of Hydrostatic Drive Transmissions**

#### **2.1.1 Energy Management of Hydrostatic Drive Transmissions**

This section presents control schemes that can be utilized in EM of the traction drives of HWMs to improve their fuel economy. The review is limited to approaches that do not require accurate information about the future and, therefore, are implementable to real machines.

The majority of the published EM research has been conducted with hybrid electric vehicles (HEV), but in recent years, studies of HHV have also emerged. In addition, the number of solutions for automotive applications is extensive when compared to HWM. Fortunately, the principles of the cited EM research can be applied also to different applications.

The most utilized problem formulation in EM research assumes that the velocity reference trajectory is given but not entirely known in advance. For example, all the standardized drive cycles of on-road vehicles contain this information. Thus, the control objective can be expressed as follows:

1. Minimize the amount of fuel consumed.
2. Minimize the velocity error for a given reference trajectory.

Alternatively, an optimal velocity reference trajectory could be generated for a given task, but solving this problem is excluded from this thesis and related research and, therefore, omitted here.

Generally speaking, EM controllers can be divided into reactive [9] and predictive ones [10]. The former type relies solely on measured variables and reacts (i.e., changes control commands) to the observed changes in the states of the system. The controllers devised in **P.I** and **P.II** belong to this class. In **P.III**, the controller is also reactive, but EM is not considered. The controllers of the latter type utilize information about the future references or dynamic system models, and predict the system's response. These controllers usually generate a trajectory of control commands instead of calculating only the ones applied in the next execution cycle. The controller presented in **P.IV** is of the predictive type.

The main difference between reactive and predictive control schemes is, therefore, the amount of required information. Consequently, if certain data is not available, the value has to be predicted. Otherwise, the performance of the controller will be reduced.

The following sections (2.1.1.1–2.1.1.3) present literature covering a variety of EM controllers from which all rule-based (Section 2.1.1.1) and model-based (Section 2.1.1.2) solutions can be classified as reactive together with instantaneous optimization (Section 2.1.1.3.1). In addition, two predictive control schemes are reviewed, namely model predictive control (MPC, Section 2.1.1.3.2) and stochastic dynamic programming (SDP, Section 2.1.1.3.3).

#### **2.1.1.1 Rule-Based Control**

Probably the most utilized method for controlling drive transmissions is determining a set of static rules, for example based on expert knowledge ([11], [12]) or extensive simulations [12]. Rule-based (RB) controllers are usually designed to meet the requirements of the operator in a way that all work cycles can be completed (i.e., emphasizing functionality over fuel economy [13]).

Probably, the simplest RB method is the one in which the control commands of the actuators are changed one at a time according to a specified signal (e.g., velocity reference of the machine). The idea is utilized, for example, in [14], in which the hydraulic pump and motor are the variable displacement type. In addition, the rotational speed of the diesel engine is controlled. The control sequence is divided into three parts according to the mentioned components. At the first stage, the displacement of the pump is increased to maximum after which the displacement of the motor is reduced to minimum at stage 2. Finally, the speed of the engine is increased, assuming that it is not already set to maximum. In this thesis, this controller is referred to as the sequential RB controller.

According to Jähne et al., they utilized the state-of-the-art hydromechanical control of wheel loaders in which the pump and the motor were controlled simultaneously as a function of the gas pedal [13]. No explicit information about the algorithm or time-domain simulation results are presented, but based on their description, the used method is similar to the one named Automotive Drive and Anti-Stall Control (DA) by Bosch Rexroth [15]. DA control, described in Section 2.2.1, can be implemented hydromechanically.

In [12], a preliminary rule base was designed based on engineering intuition. The approach utilizes three control modes (braking, power-split, and recharging) from which the most suitable is chosen according to the requested power (i.e., gas pedal position and two constant power values). This controller was further developed with rules extracted from DP simulations (see Section 2.2.1.1 for more information). A similar approach was also taken in [12], [16], and [17].

Fuzzy reasoning has also been used in creating rules for driveline control. These approaches are often based on mimicking skilled drivers; for example, Omid et al. [18] and Naranjo et al. [19] defined their rule bases this way. In their studies, Langari and Wong ([11], [20]) presented a situation awareness-based fuzzy rule set that distributed the torque requirement between the combustion engine and the electric motor according to expert knowledge. Other studies in which hydraulic drive transmissions are controlled with fuzzy logic controllers are, for example, [21] and [22].

### 2.1.1.2 Model-Based Control

Usually, rules derived by expert knowledge on the system result in adequate fuel economy only in certain operation points or conditions. If higher performance is required, information about the controlled system can be included in the control algorithm with a mathematical model. This enables calculating control commands based on numerical values rather than ad hoc methods. Such a control scheme in which the system model is utilized, but no future predictions are made (as for example with MPC), is here referred to as model-based control.

A common practice in model-based EM is utilizing the efficiencies of driveline components to determine the control command combination (CCC) that results in the highest system efficiency. Concentrating on the entire system is important, because the CCC that maximizes the efficiencies of hydraulic components can be highly suboptimal for the engine or vice versa.

Vanwalleghem et al. devised a controller based on steady-state efficiencies of the components and tested their algorithm with an experimental laboratory set-up in several steady-state operating points. They compared the efficiencies achieved with their optimal control values to those obtained with the sequential RB controller described in Section 2.1.1.1. According to them, the total efficiency of the system can be significantly improved if the engine is operated in regions of optimal specific fuel consumption. [14] While this obviously has a major effect on their results, the decreased losses of hydraulic components also contribute to the improvements. However, the value of the study is hindered as it is limited to steady-state operations.

Jähne et al. determined an “energetically optimal engine speed” based on required power calculated with constant efficiencies but dependent on the load situation. They conducted simulations for two different work cycles of a wheel loader and compared the results to a constant engine speed controller. The reported reduction in fuel consumption was up to 15% when the adaptive engine speed controller was compared to a constant speed controller. [13]

It is not explicitly stated in [13], but the author believes that the optimal engine speed is chosen from the best efficiency curve of the engine. This method is also exploited, for example, in [23] for controlling continuously variable transmissions (CVT), and it is based on determining a specific rotational speed of the engine that results in the best fuel economy for all feasible values of power. When these optimal points are connected, the authors term the result Optimal Operating Line (OOL) of the engine. This method is also referred to as a single-track strategy in the literature. It is notable that the single-track strategy also considers only the efficiency of the engine. Therefore, it can be assumed that fuel economy is improved when the efficiencies of the entire transmission are included in the controller. Still, Ahn et al. reported improvements of only 0.8% and 1.8% in simulations and empirical experiments, respectively, with such modifications in their controller [24]. In addition to the single-track strategy, other methods (e.g., speed envelope and off-the-beaten-track) are reviewed in [25].

In [12], the original rule base was improved with DP-based simulations of a hybrid electric truck. However, the results were not utilized directly, mainly because DP-generated control commands resulted in too frequent gear shifting, which decreases the drivability of the machine. Further, in their improved rule base, the power split ratio could obtain four different control modes: motor only, engine only, power assist, and recharge. In addition, a charge-sustaining rule was determined with DP. This enhanced algorithm decreased the combined fuel consumption and emission value by 5.57–20.46% in four simulated test cycles when compared to a controller with “engineering intuition-based” rules. With DP, the same value was improved by 10.66–35.03%, which represents the global optima of the simulations. Identifying different operation modes for energy saving was utilized also in [26].

Bender et al. utilized recorded drive cycle information in order to decide the most beneficial situations to use the hydraulic part of their power split transmission. They compared their algorithm to a method in which torque was generated as much as possible with the hydraulic system. The reported improvement in fuel consumption was approximately 6%. [27]

### 2.1.1.3 Optimal Control

Optimality is a concept that is directly linked to the utilized problem setting. Therefore, an optimal solution might not be the one that results in the lowest fuel consumption, because, for example, component wear [28], trajectory tracking [29], or particle emissions [30] might also be considered. In most studies, the optimization problem is formulated as a minimization of a cost function that may include any terms the researchers consider relevant. Thus, optimality is defined differently in almost all the studies in the literature. In addition, functionality of the system should not decrease significantly due to the improvements in fuel economy. In **P.II**, the results are presented both in terms of fuel economy and functionality.

#### 2.1.1.3.1 Instantaneous Optimization

Instantaneous optimization (also static optimization) is a method that is used to determine the optimal control commands of actuators  $\mathbf{u}^*$  at every calculation cycle based only on measured variables. This means that no



information about the future is required, and the commands are calculated one step forward. Usually, this is achieved by determining  $\mathbf{u}$  that minimizes a cost function  $J$  with

$$\mathbf{u}_{N_u \times 1}^*(\mathbf{x}) = \operatorname{argmin} J(\mathbf{x}, \mathbf{u}) \quad (1)$$

where  $\mathbf{x}$  and  $\mathbf{u}$  are vectors of the states and control commands, respectively.  $N_u$  is the number of control inputs. The controller utilized in **P.I** and **P.II** is of this type, but due to the discretized control command space  $U$ , Equation (1) is rewritten as

$$\mathbf{u}_{N_u \times 1}^*(\mathbf{x}) = \operatorname{argmin}_{\mathbf{u} \in U} J(\mathbf{x}, \mathbf{u}) \quad (2)$$

If a driveline includes an accumulator, its charging and discharging can be considered in the optimization with an equivalency factor that is the relation between the used energy of the secondary power source to the power demand. The Equivalent Consumption Minimization Strategy (ECMS) is also one branch of instantaneous optimization strategies.

Kumar and Ivantysynova controlled a hydraulic hybrid power split drive with instantaneous optimization in a laboratory test rig. They utilized a Toyota Prius engine model and managed to exceed the fuel economy of this electric hybrid passenger car with its hydraulic alternative. In this study, any pressure of the accumulator above its reference was considered available energy, and the possible remaining power request was generated with the engine. The operation point (i.e., torque and speed) of the engine was determined with instantaneous optimization, and the displacements of hydrostatic units were controlled to maintain the pressure of the accumulator and the load of the engine at desired values. [31] This implies that, despite the obtained results, there seems to be room for improvement as hydraulic units are only used to optimize the operating point of the engine. In addition, the utilized driver model, effecting especially in transient situations, is left unexplained.

ECMS is widely researched with HEV. Liu and Peng developed customary ECMS with DP simulations and decreased the gap to global optima by reducing the penalty of battery power (i.e., equivalency factor) during accelerations [32]. In [33], GPS data was utilized to change the equivalency factor according to the current road load. In addition, driving pattern recognition can be used to estimate this value [34]. Analogous strategies to ECMS can be used also with HHVs. For example, Wu et al. added a penalty term for the state of charge (SOC) of the accumulator [35].

### 2.1.1.3.2 Model Predictive Control

The most significant defect of the EM approaches described above is that they are mainly based on steady-state models. Therefore, operation under transient situations cannot be optimal. In model predictive control (MPC), the response of the system is predicted with its dynamic model. The timespan for which the prediction is made is called the prediction horizon. Moreover, control command trajectories are calculated in advance for

a pre-determined number of samples  $N_c$  called the control horizon, but only the first CCC is sent to the actuators of the system.

A common practice is to determine  $\mathbf{u}^*$  by minimizing a cost function over the horizons. Mathematically, this can be expressed, for example, with

$$\mathbf{u}_{N_u \times N_c}^*(\mathbf{x}) = \underset{\mathbf{u}}{\operatorname{argmin}} \left( \sum_{i=1}^{N_c} J(\mathbf{x}_i, \mathbf{u}_i) + \sum_{i=N_c+1}^{N_p} J(\mathbf{x}_i, \mathbf{u}_{N_c}^*) \right) \quad (3)$$

subject to  $\begin{aligned} \dot{\mathbf{x}} &= \mathbf{f}(\mathbf{x}, \mathbf{u}) \\ g(\mathbf{x}, \mathbf{u}) &\leq 0 \end{aligned}$

where  $\mathbf{f}(\mathbf{x}, \mathbf{u})$  and  $g(\mathbf{x}, \mathbf{u})$  are a set of functions that define the dynamics of the system and applied constraints, respectively.  $N_p$  is the number of samples of the prediction horizon. Note that in Equation (3), the cost after the control horizon (i.e.,  $i > N_c$ ) is calculated with constant control commands, here the last CCC of  $\mathbf{u}^*$ .

Nilsson et al. discovered in their simulation study that the fuel-optimal command trajectory for the engine is to first accelerate or decelerate the speed of the engine beyond the optimal steady-state value, and then approach the optimum value from the opposite direction from where the transition started. [36] Despite the fact that they focus on the engine, instead of having, for example, a hydraulic system as a load, and that their controller is able to prepare for the upcoming change in loading, the results indicate that it is worthwhile to develop controllers for optimizing transient situations.

In [28] and [37], the MPC scheme is exploited in the hydraulic drive transmission of a passenger vehicle. The utilized objective function includes terms for velocity-tracking error and the efficiencies of the controllable components. Too frequent starts and stops of the engine are handled with a dwell-time constraint, but penalties are not placed on any other control changes. The controller is implemented using a state machine that, for example, changes the mode of the engine to idle under deceleration or when the accumulator is able to provide the requested power. The utilized sample time and prediction horizon were 1 and 5 seconds, respectively. While these values might be suitable for on-road applications, at least the 1-Hz update rate is highly suboptimal with HWMs and might even result in unfeasible predictions of MPC.

Their test system is a laboratory set-up of an open hydraulic circuit, which is quite unusual in drive transmissions. Moreover, the volumetric flow seems to be controlled both with the displacement of the pump and a throttling valve. The hybridization is done by placing an accumulator to the outlet of the pump after a check valve. [28] Although this configuration allows for controlling the accumulator pressure to some extent, it cannot be considered representative of any commonly used HSD. Arguably, the main contribution of this work is in simplifying the optimization to a convex quadratic programming problem.

In [10], Vu et al. utilized MPC to track optimal references of a simulated HHV. These values were determined with a supervisory controller that optimized the operation point of the engine and hydraulic components were

constrained to serve this purpose, along with the minimization of velocity error. A linearized model was utilized in minimizing a quadratic cost function, which included penalties for the reference errors and the changes of control commands. Weighting factors for the latter terms were tuned by observing step responses of the system. The utilized model included three states—engine speed, accumulator pressure and vehicle speed—and three control inputs—engine speed, pump displacement and motor displacement. The researchers used a sample time of 0.1 seconds, and the prediction and control horizons of 2 and 0.5 seconds, respectively. There was no information about the real-time capability of the controller in the paper.

Vu et al. reported fuel economy improvements of 35% and 10% in urban (Japan 1015) and highway (HWFET) drive cycles when the devised controller was compared to a proportional-integral-derivative– (PID–) based tracking of the optimal references. However, their baseline controller (three PIDs) required that the minimum accumulator pressure be raised from the value utilized with MPC in order to prevent depletion. This had a major effect on the results as the engine had to generate more power and less volume was available for capturing the energy of regenerative braking. [10] No value for global optima was presented. As stated above, the control method was based on optimizing the operation point of the engine. Thus, the results might be improvable, as the maximum system efficiency is not usually found in the same operation point as the one of the engine. However, including the highly nonlinear hydraulic efficiencies in the optimization will significantly increase the complexity of the problem.

Borhan et al. controlled the power split transmission of on-road HEV with MPC. They linearized the nonlinear system model at every execution cycle in the current operation point, but also applied nonlinear MPC (NMPC) to the same EM problem (simulated Toyota Prius in four different drive cycles). The NMPC increased the fuel economy by 9.2–9.7 % when compared to their linear MPC. Both controllers were real-time executable with a sample time of one second. [38] In this study, the results were not compared to the global optima, but it is unique because of the utilized NMPC approach.

The MPC scheme has also been exploited with mechanical transmissions, as Meyer et al. optimized the fuel economy of their CVT drive. They simulated an on-road CVT drive with a 0.25-second sample time and 1-second prediction horizon. No comparison was made to baseline controllers, but the engine operated in the high-efficiency region for the majority of the trapezoidal test cycle. [39]

### 2.1.1.3.3 Stochastic Dynamic Programming

Dynamic programming (see Section 2.2.1) requires information about the future and, therefore, cannot be implemented in the control systems of human-operated machines. Stochastic dynamic programming (SDP) is an attempt to tackle this major shortcoming. The idea of SDP is to predict the future drive cycle based on the operations done in the past. For this, transition probabilities from one state to another are required and often modelled as a Markov chain. In on-road applications, an adequate number of these probabilities can be obtained, for example from standardized drive cycles as implemented in [40] and [41]. For HWMs, a similar database could be gathered during a typical workday.

Again, a typical approach for determining  $\mathbf{u}^*$  is by minimizing a cost function  $J$ . The control objective of SDP can be expressed with

$$\mathbf{u}_{N_u \times N_c}^*(\mathbf{x}) = \operatorname{argmin} \left( p(\mathbf{x}_0, \mathbf{u}_0, \mathbf{x}_1)J(\mathbf{x}_0, \mathbf{u}_0, \mathbf{x}_1) + \alpha \sum_{i=1}^{N_c} p(\mathbf{x}_i, \mathbf{u}_i, \mathbf{x}_{i+1})J(\mathbf{x}_i, \mathbf{u}_i, \mathbf{x}_{i+1}) \right) \quad (4)$$

where  $p(\mathbf{x}_i, \mathbf{u}_i, \mathbf{x}_{i+1})$  is the probability that the system makes the transition from state  $\mathbf{x}_i$  to  $\mathbf{x}_{i+1}$  with CCC  $\mathbf{u}_i$ .  $\alpha$  is the discount factor that decreases the effect the future transitions have on the  $\mathbf{u}^*$ .

In the comparative study of Deppen et al., the SDP controller achieved better fuel economy (approximately 23% in highway and 19% in urban drive cycles) than their MPC solution did. They observed that even though the SDP was more efficient, the MPC strategy is more reliable in highly uncertain applications. This was supported by a significantly smaller root mean square (RMS) of velocity error. [41]

No recorded data was presented from the test cycles in [41], but clearly larger RMS errors suggest that the velocity-tracking of their SDP controller requires improvement. Due to this, it is not that evident that the results are even comparable, because the responses might not be similar enough in terms of drivability. Furthermore, the drive cycles of the experiments were generated from the probability maps of the same standard cycles that were used in the SDP design. It would be interesting to see the performance of the SDP controller with a test cycle that has not been used at all in its design process. Their test set-up and MPC are described in Section 2.1.1.3.2.

Also, Kumar implemented an SDP-based EM strategy to simulate on-road HHV in [40]. Similarly to [41], the probabilities of power demand were modelled with “many standard drive cycles,” but no explicit information was provided. The strategy was found nearly optimal in three different standard cycles. [40] However, Kumar emphasized the essentiality of a representative probability model, and based on his excellent results, it can be assumed that the test cycles were included in the probability database. This approach is valid for on-road vehicles for which multiple standard cycles exist and operation is more predictable than those of HWMs. Therefore, the applicability of the SDP controller for HWMs requires further research.

Nilsson et al. controlled a diesel-electric wheel loader that included a super capacitor, a mechanical drive train, and hydraulic lift and tilt functions with SDP. They reported 3–4% increase in energy efficiency with predictive control compared with a controller that kept the engine speed reference constant. Furthermore, the amount of energy not delivered to the consumers (i.e., drive train and work functions) increased significantly if the experiment was not identical from the utilized probability maps. For example, if lifting was performed at different distance values than in the recorded cycles. [42]

In [43], drivability was also included in the cost function of the presented shortest path SDP algorithm. In addition, there were separate terms for engine and gear events, which are aimed to reduce the number of changes between engine ON and OFF states as well as back and forth gear changes. The authors achieved an

11% increase in fuel efficiency with the same level of drivability, when compared with their quite complex baseline industrial controller. [43]

### 2.1.2 Velocity Tracking of Hydraulic Drive Transmissions

Closed-loop velocity control, also known as cruise control in the automobile industry, is a function that improves the quality of work with inexperienced drivers and enables experts to concentrate better on their task. Combine-tractor synchronization and convoying in mining machinery are just a few examples of where accurate speed tracking is essential for safety and performance.

Similar to EM solutions, published research related to the velocity-tracking of HSDs is very limited as the majority of the research on hydraulic systems is conducted with linear actuators (i.e., hydraulic cylinders). Unlike HSDs, these systems are usually valve controlled and, therefore, omitted here.

#### 2.1.2.1 Predictive Control

Several teams have developed cruise control systems and some of these are intended for HSDs, such as the MPC solution for combine harvesters by Coen et al. [44]. They controlled both engine speed and pump displacement, but presented results only for a one-step response with a 6-km/h velocity reference. In this study, the control design was validated with field tests in which the HSD was composed of a variable pump, hydraulic motor, and mechanical transmission. [44]

Still, most cruise control solutions are developed for on-road vehicles with no hydraulic components. For example, Shakouri et al. used NMPC [45] and detailed their design to switch between velocity and distance tracking modes in [46]. Meyer et al. controlled their mechanical CVT with MPC and achieved adequate tracking performance while operating the engine in high-efficiency regions [39].

#### 2.1.2.2 State Feedback and Classical Control

Velocity tracking of hydraulic systems has also been realized with methods utilizing more established control practices (e.g., state feedback). Some of the presented research is not conducted with drive transmissions, but they all are pump controlled.

Lennevi and Palmberg developed a linear quadratic (LQ) control design in their research covering the velocity control of HSDs. The tests were conducted with a laboratory test rig, but also simulations with different constant settings for the displacement of the HSD motor were performed. Supported by the latter part, they concluded that the responses could be improved by gain scheduling. [47] This is not surprising as the LQ design assumes a linear system. Gain-scheduled velocity-tracking of HSDs based on a state-dependent system model was investigated in **P.III**. Approaches based on state-dependent models for hydraulic systems have been developed, for example, Strano and Terzo [48] and Taylor et al. [49].

Hu et al. used linear control theory, namely PD control, feedforward, and feedback in the velocity-tracking of a hydraulic elevator. The system was realized with an electric motor, constant displacement hydraulic pump,

and hydraulic cylinder. They improved the response of classical PD control by integrating feedforward and feedback terms in the control loop. The gains of these additional parts were determined with system models linearized at the different elevations of the system. [50] Zhang and Li also controlled a hydraulic cylinder by altering the flow of a hydraulic pump. However, they combined feedback linearization with PID control. [51]

State feedback and a combined inverse model plus a PID controller were designed for the tracking control of a hydrostatic dynamometer by Wang et al. in [52]. Both of their solutions provided fast and precise tracking, but there was no obvious improvement with a more complex state-feedback controller. However, according to them, this controller enables, for example, the utilization of robust control methodologies to further improve the accuracy of tracking. [52] Li et al. used an  $H_\infty$  controller to consider parameter uncertainties and disturbance torque for a pump-controlled hydraulic motor. In addition, their solution was also robust to measurement noise. [53]

### 2.1.2.3 Fuzzy Logic Control

Fuzzy logic controllers have also been utilized in the velocity tracking of HSDs. Guo and Hu utilized an adaptive fuzzy PD method for the speed control of a tractor. Their approach requires defining many rules and membership functions for the controller, which is quite common for fuzzy systems. The demonstrated operating speed in this research was 0.8–1.4 m/s. [54] Yadav and Gaur combined internal model control and fuzzy logic for speed control of heavy-duty vehicles [55].

In [56], Do et al. designed an adaptive fuzzy sliding mode controller for a secondary controlled HSD of an HHV. Their experiments were conducted with a laboratory set-up in which the hydraulic pump was operated with an electric motor. The performance of their controller exceeded that of a classical PID controller utilized as a baseline. However, steady-state error was observed in all the tests, while the most significant differences of the controllers occurred during transients. As none of the presented operation points were adequately managed with the PID, it is doubtful whether the tuning of parameters was sufficient. In fact, the authors admit that good tracking performance could also be obtained with the PID controller if the parameters were changed (e.g., according to the velocity reference).

## 2.2 Methods for Measurement, Analysis and Comparison of Fuel Economy

After developing a novel EM scheme, its success has to be evaluated. This section covers different aspects of testing, ranging from controllers used in comparison to the ways of conducting the experiments. In addition, test cycles and different measurement methods are presented.

### 2.2.1 Baseline Controllers

Accurate information of controllers implemented in commercial HSDs is basically non-existent. Thus, the algorithms described in this section offer merely potential guidelines to consider when designing comparative

controllers used as baselines. In this thesis, these are referred to as baseline controllers. Furthermore, the control methods described in Section 2.1.1 can also be utilized in comparisons, but their descriptions are not repeated in this section.

### 2.2.1.1 Dynamic Programming

Dynamic programming (DP) (see, e.g., [57]) is a method that enables calculating the global optima of, for example, fuel consumption. This is conducted by utilizing the principle of optimality (also known as the Bellman equation), according to which the optimal solution for the current time step can be computed given the initial state of the system, cost function and the optimal decisions of the future [58]. Therefore, for the control of HSDs, it is required for DP that the loading conditions and velocity profile of the work cycle are known a priori.

Because the future events are completely known, the procedure of DP begins from the end of the cycle. First, the investigation turns to the second last step, and utilizing the dynamic equations of the system, the costs of all possible CCCs are evaluated. This evaluation is usually based on a cost function determined by the designer. Therefore, optimality is not a univocal concept as discussed in Section 2.1.1.3. Next, another step is taken towards the beginning of the cycle, but this time the number of evaluated costs has multiplied, because now all the feasible CCCs that precede the penultimate ones have to be investigated.

It is easy to see that the total number of calculations will grow exponentially at every step towards the beginning of the cycle. Moreover, if the system model has several states, this “curse of dimensionality” might even limit the feasible utilization of DP, as the required computational power increases exponentially also with the number of states and control command variables.

Theoretically, DP provides a limit to the fuel economy that any causal controller cannot beat. For that reason, it is one of the few methods that provides an easily interpretable baseline. It is a completely different matter whether the same control sequence is optimal in reality, due to the uncertainties and simplifications of modeling. Nevertheless, as long as the model used in DP and simulations are identical, the scientific value of research can be reliably verified.

### 2.2.1.2 Commercial Control Algorithms

Accurate information about commercially utilized controllers is very limited since all manufacturers want to maintain their competitive edge. In this section, three commercial control algorithms are described in as much detail as the available information allows and according to the author’s best educated guesses.

In applications that consume a major part of their energy in drive transmission (e.g., wheel loaders and municipal tractors), a commonly utilized control algorithm is based on adjusting the displacements of hydraulic components according to the actual rotational speed of the engine. The sequence has been named DA control by Bosch Rexroth [15] and can be implemented hydromechanically (see Figure 2). DA control has inspired the rule-based controller utilized as the baseline in **P.II**.





Commercial manufacturers have also developed electronic control solutions of HSDs. For example, Eaton [60], Bosch Rexroth [61], and Danfoss [62] have systems that decouple the control commands of individual actuators from control devices of the operator. Therefore, the gas pedal, for example, can determine machine velocity instead of setting the speed command of the engine. This allows for improving the fuel economy of HSDs. Danfoss announced that with their Best Point Control, fuel consumption is reduced by up to 25% [62]. However, evaluation of these controllers is difficult, because no specific information about the utilized algorithms is publicly available.

### 2.2.2 Experimentation

After designing a new controller, one has to conduct experiments to demonstrate its efficacy. There are three commonly utilized testing methods in the scientific community, each enabling something that the others might be lacking. Here, the methods are classified into simulations, laboratory testing and field experiments.

#### 2.2.2.1 Simulations

Perhaps most of the published research results are obtained with simulations. This is possibly because the experiment set-up is completely controlled by the designer, and all the signals can be easily recorded. After designing and validating the model of the system, simulations are also the fastest and most cost-effective way of conducting multiple tests. In addition, conditions and disturbances are exactly known, which guarantees repeatability and enables determining global optima (e.g., for known cycles).

In [13], a verified simulation model of a wheel loader was utilized in two different loading cycles. Scheider et al. derived an operation point-dependent loss map from a detailed simulation model in their similar study [63]. Pffner et al. [23] analyzed the fuel saving potential of a downsized and supercharged engine connected to a CVT with the simulations of an on-road vehicle, and Kache simulated hydraulic hybrid rail cars with real route data [64]. In **P.I**, a simulation model is first validated and then utilized in the evaluation of the FOC of HSDs. Other simulation studies considering EM of hydraulic power trains are, for example, [14], [26], [35], [10], [65], and [66].

The results of Ahn et al. showed significant differences in the efficiency of a power split drive transmission between simulations and laboratory tests. They explained the 17.2-percentage unit difference with increased frictions of the transmission that was in the development stage. [24] In addition, Cheong et al. reported discrepancies due to unmodeled frictions [67].

#### 2.2.2.2 Laboratory Testing

Testing can be taken a step further towards real plants with laboratory set-ups. Yet occasionally, some parts of reality can still be simulated. When the focus is on the control of drive transmissions, loading conditions are probably the most obvious thing to emulate. This can be implemented by using a hydraulic pump and pressure relief valve as a loading unit, and connecting it to the hydraulic motor of the tested transmission. This approach was taken, for example, in [68]. A more realistic test rig was utilized by Wu et al., who generated load for a

hydraulic hybrid propulsion system with a dynamometer and inertia [69]. This enabled also simulating negative loads (i.e., downhill for HSDs).

The number of laboratory experiments conducted with combustion engines is significantly lower than those with electric motors. This is probably due to their emissions, namely exhaust fumes and noise. Still, ICEs are undoubtedly the most important power sources of drive transmissions, and their torque generating characteristics have to be modelled with high accuracy for representative testing. For example, in [28], [31], and [68], this deficiency was compensated by emulating the characteristics of diesel engines with a simulation model and electric motor. Deppen et al. utilized the same set-up also in [37] and [41]. It is also possible to connect an entire vehicle to a dynamometer for testing as was done in [70].

### 2.2.2.3 Field Experiments

If a research platform machine exists, it can be utilized in field tests. In that case, the available landscape limits possible drive cycles as additional positive and negative loading can be generated only by driving uphill and downhill, respectively. However, the scenario will definitely be realistic and offers an opportunity to evaluate, for example, the drivability and robustness of the designed control algorithm. Still, real-world experiments will always contain multiple sources of uncertainties.

Despite the high level of infrastructure that real machines require, some research groups consider them valuable for their EM studies. At Purdue University, they have a mini excavator [71] and a compact wheel loader [72]. That same group has also reported results with a sports utility vehicle [73] and they intend to also implement their algorithms into a railway machine [74]. Another research platform wheel loader has been engineered at Aachen University [63], but according to the author's knowledge, no experimental results have been published yet.

In Scandinavia, Linköping University has a wheel loader and Tampere University of Technology has municipal tractors as research platforms. While Eriksson and other researchers in Linköping attempt to improve energy efficiency with optimal trajectories and operator behavior [75], the research group at Tampere focuses on controllers [76].

Among manufacturers of HWMs, the research and development team of AB Volvo has probably published the most articles related to the control systems of HWMs. They have conducted tests with real machines (see, e.g., [77] and [78]), but precise information about the utilized algorithms are technical business secrets and, presumably, are therefore not presented.

### 2.2.2.4 Test Cycles

Although several different standardized drive cycles exist for automobiles, for HWMs, there have only been attempts to design such test procedures. The main challenge is that the concept covers a large variety of different machines. Some efforts have been made to define cycles separately for specific types of machines, for example, Japanese JCMAS H 020 ([79]) and H 022 ([80]) for excavators and wheel loaders, respectively.

However, the described test procedures do not offer completely realistic fuel economy data because they demand that working motions are executed in the air without any interaction between the bucket and the soil. For example, a large study by AB Volvo included 80 drivers of different skill levels, and indicated that the filling of the bucket was the main source for variations in fuel economy and productivity among the participants [81].

The United States Environmental Protection Agency has also defined different kinds of non-road test cycles. Their database includes four cycles for wheel loaders. However, the procedures comprise a series of operation points for the engines, and no specific maneuvers of the machine are defined. [82]

Still, a couple of cycles exist that are commonly used to test drive transmissions and wheel loaders in particular. In a short loading cycle (see, e.g., [75], [81] and [83]), also known as the Y-cycle, the wheel loader drives into a pile of soil to fill the bucket, which is followed by reverse motion to the initial starting point and acceleration towards a truck in which the bucket is emptied. The cycle ends when the machine reverses back to the initial starting point. Total travelled distance is approximately 10–15 meters. In [80], a similar cycle is described, but no distances are specified. Available information is that the angle between the digging simulation place and the loading bar should be 60 degrees, the height of the loading bar should be 2.2 meters, and the additional weight in the bucket should be equivalent to the fully loaded bucket of clay [80].

Another representative test scenario, load and carry, is described in [81]. This cycle can be used to simulate, for example, the handling application in which gravel is loaded onto a conveyor belt. The travelled distance is 10 times longer than the one in the Y-cycle, and it also contains steady-state driving. For traction drive, JCMAS H 022 states that, for example, a mid-size wheel loader should be driven for five 100-meter cycles on hard clay or an asphalt road from which the longest and shortest distances should be neglected. In the results, the average fuel consumption per travelled distance should be calculated [80]. No mention of the slope grade is made in the document.

In **P.II**, three 180-meter cycles were driven that included both uphill and downhill parts on asphalt and gravel roads. The JCMAS procedure was not followed exactly in **P.II**, because the utilized test area did not have adequate long and level roads for the test.

The briefly described tests of JCMAS H 022 were designed to evaluate the energy consumption of typical wheel loader operations. Because these machines are used for various purposes, defining “typical operation” is practically impossible. In fact, according to [77], larger machine-owner companies perform their own testing before placing any substantial purchase orders. In these tests, machine manufacturers compete at a real worksite in productivity and energy efficiency. The machines are driven by the specific manufacturers’ professional drivers, which ensures proper operation. Naturally, this kind of external benchmarking is probably extremely rare in the research and development of a machine manufacturer.

### 2.2.3 Methods for Measuring Fuel Consumption and Economy

When testing methods, comparative controllers and test cycles are determined, the only major decision left is how to measure the consumed energy or if it is required to evaluate productivity or even the total cost of

ownership. In this section, different methods used in the scientific community are described. The focus is limited to measurement-based approaches and neglects pure simulations.

If the objective of a study is to measure energy consumption, arguably one of the simplest ways is to measure the torque and angular speed of an electric motor. The product of these two values equals the output power of the motor that can be integrated into energy. This approach was taken, for example, in [84]. Alternatively, if the interest is on fuel economy, a brake-specific fuel consumption (BSFC) map can be utilized to calculate the consumption of the engine as was done in [31], [24], and [70]. However, the BSFC maps are measured in steady-state conditions and, therefore, they are not accurate during transients. In fact, the resulting error might be extremely large. In [7], the consumption calculated with a BSFC model differed by up to 50% from the measured value.

Actual measurement methods of consumed fuel can be divided into the determination of total value and dynamic measurement. The former can be conducted gravimetrically by weighting an external fuel tank as in [72] and [85], or measuring the added volume when filling an integrated tank as, for example, in [86]. Contrary to these methods, dynamic measurement also offers information about the situations in which consumption differences occur. This data might be provided by the electronic control unit of the engine, as in [87], or via an individual measurement device as utilized in [88]. In **P.II**, the improvements of fuel economy were measured with an online measurement device described in detail in Section 3.1.3.

When considering work machines, contrary to automobiles, another metric of success is the productivity of the machines. The concept can be translated into measuring how much soil is loaded or transferred within a certain amount of time, resulting in kg/h as the unit of productivity. This value was used with excavators in [85] and with wheel loaders in [81]. Furthermore, if productivity (kg/h) is divided by fuel consumption (liter/h), yet another measuring unit is obtained. Both in [85] and [81], this is referred to as fuel efficiency (kg/liter), and it is analogous to values used in automotive studies (i.e., liter/km).

It might be difficult to estimate whether productivity should be valued over fuel consumption. However, as indicated in [81], a decreased production rate of a machine might slow down the whole site, resulting in a very expensive loss of income. Finally, if the monetary values of all expenditures, such as operators' wages and the prices of loaded materials, are available, the total cost of ownership can be calculated, but only for individual cases.

## 2.3 Summary

Above, different EM control methods were presented together with aspects related to their testing. The focus was mainly on real-time implementable algorithms, but also globally optimum solutions were mentioned for benchmarking purposes. As the published research of HWMs is very limited, some important publications about on-road vehicles were included. Even scarcer is research on HSDs, especially those on non-hybrid systems. Therefore, quite a few papers from these fields of research (HHV and HEV) are also cited.

Simulation studies dominate the fluid power community, but during this decade, the number of field test studies has increased. The complexity of the utilized models varies greatly, but to the best of the author's knowledge, none of the ones utilized in controllers include the torque generation dynamics of diesel engines. On this account, the speed of the engine might be increased too rapidly due to the assumption that the values of maximum torque curve are instantly available. This can lead to a situation in which the high load demand and the acceleration of engine speed are simultaneously active, which is extremely detrimental to fuel economy, especially if the boost pressure unit (i.e., turbo charger) of the engine is not able to provide enough air to the cylinders [7]. It is also notable that the performance of model-based algorithms will deteriorate if the values of the parameters are inaccurate as stated, for example, in [28].

MPCs enable constraint optimization during transients of the system. Therefore, the full functionality can be utilized. In **P.IV**, a nonlinear MPC is designed for the simultaneous velocity-tracking and fuel-optimal control of HSDs. A thorough search of the relevant literature yielded no articles that address this topic with a comparable implementation.

SDP is an interesting alternative between causal controllers and solutions that require information about the future, as the control commands are determined based on probabilities obtained from recorded work cycles. Several researchers have developed SDP-based controllers, and they all have improved the fuel economy of the systems. However, it seems that outside the generated probability maps, the performance deteriorates notably. Therefore, though effective for machines with specific tasks, SDP is not suitable for a generic EM solution.

In conclusion, one should recall that the control algorithms of drive transmissions are only part of the energy efficiency of HWMs. Supervisory control of multi actuator machines [89], operator behavior [81], and worksite optimization [78] are just a few examples of the factors that have an effect on fuel economy, but are beyond the scope of this thesis.

### 3 Research Platform Machine

The experimental testing of the developed controllers is conducted with a five-ton municipal tractor (see Figure 3) equipped with various systems that enable different types of research. This research platform machine is described in the following sections with the level of detail relevant to this thesis. An interested reader is referred to [76] for further details (e.g., about the localization and communication systems of the machine).



Figure 3. Research platform machine.

Despite the fact that the machine is referred to as a wheel loader in publications **P.I**, **P.II**, and **P.III**, the commercial machine that it is based on is a municipal tractor. The largest differences between these two types of HWM are their geometry and the typical size of their engines. Wheel loaders are designed for lifting heavy loads in areas outside public roads. Therefore, their maximum speed is usually lower than that of municipal tractors, which enables utilizing engines with lower maximum power. However, the effect on the presented research is negligible as the designed controllers are model-based and consider the characteristics of the engine.

In addition to the main systems of the machine, the online fuel consumption measurement system is depicted (see Section 3.1.3 for details). This device enables, for example, comparing the momentary fuel economy of different controllers, which is extremely rare in the published research as explained in Section 2.2.3.

Section 3.2 provides validation tests of the utilized simulation models, in addition to the figures included in **P.I** and **P.IV**. Some of these have been published in [90].

### 3.1 Systems of the Machine

#### 3.1.1 Hydraulics

The machine has a pure hydraulic drive transmission; that is, there is no mechanical connection in the system apart from the axles of the engine and hydraulic motors. Figure 4 presents the HSD of the machine together with the hydraulics of the articulated steering.

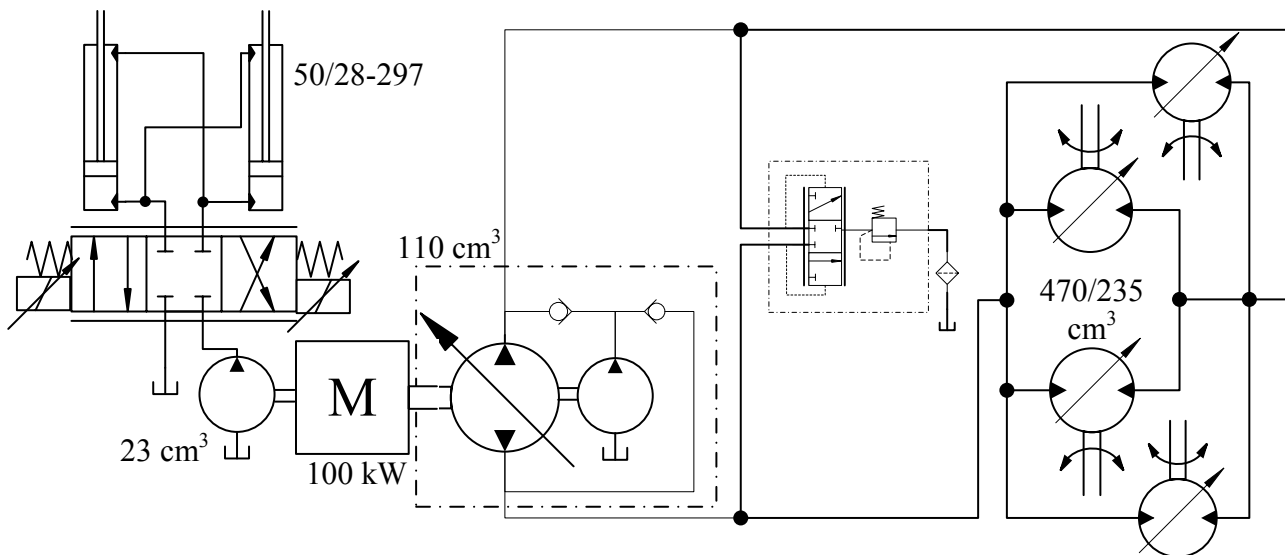


Figure 4. Simplified hydraulic circuits of the HSD and steering systems of the research platform machine.

The flow of the HSD pump can be controlled by changing the swivel angle (displacement) of the pump or the rotational speed of the engine to which the pump is directly connected. Furthermore, the structure of the pump also allows for changing the direction of the flow, which enables the forward and reverse motion of the machine. The displacement of the HSD motors can be changed between two discrete settings, namely 100% and 50% of the maximum.

The mechanism that operates the swivel angle of the HSD pump is presented in Figure 5. The force exerted by the control actuator results in changing the angle of the swash plate (i.e. the swivel angle). When this control force is in the direction of the presented arrow, the angle increases and more fluid is pumped with every rotation of the drive shaft. In the figure, the lower cylinder chamber (highlighted in grey) is the high pressure side of the pump.

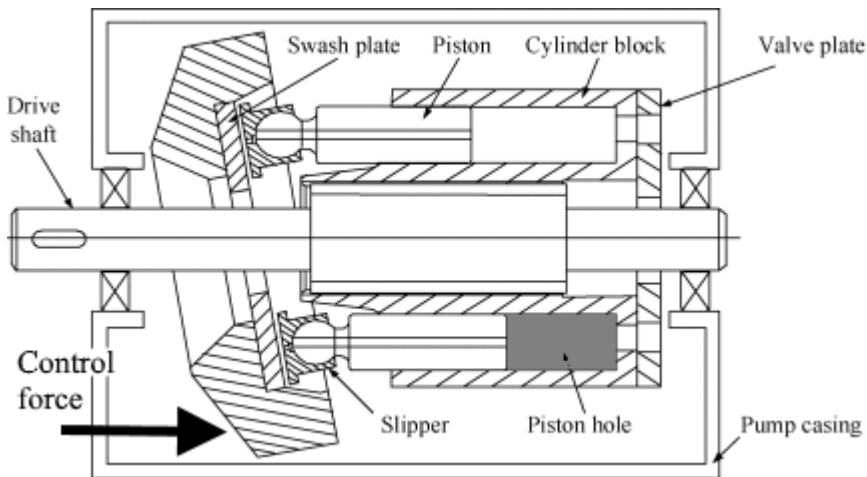


Figure 5. Displacement change mechanism of swash plate type axial piston pump. Figure adopted by the author from [91].

In Figure 4, there is also a flushing valve that directs part of the flow to the tank. This is important, for example, in terms of temperature control, as the returning fluid from the motors goes to the low-pressure side of the pump. This kind of system layout is called a closed hydraulic circuit. The flushing flow is replenished by the boost pump that also provides pressure to the displacement setting mechanism of the HSD pump. The pumps are integrated into the same casing.

The valve-controlled cylinders presented in Figure 4 are utilized in the articulated steering system of the machine. This system is also operated in the experiments of the research, but it is not considered, for example, in the fuel-optimal control of the HSD.

The movements of the implement hydraulics (i.e., lift and tilt) require yet another hydraulic system that is implemented with digital hydraulic valves. This technology is beyond the scope of this research and, therefore, it is not described here. For more information, the reader is referred to [92].

### 3.1.2 Control System and Architecture

The control system of the research platform machine is designed to enable rapid prototyping. To this end, an embedded computer with an xPC Target environment (QM-57 in Figure 6) is chosen for the control unit running advanced algorithms. The acquired benefit is that the controllers designed in a Matlab Simulink environment and tested with offline simulations can be easily compiled into a suitable format and uploaded to the control system of the machine. The structure of the control system is presented in Figure 6. The essential units for this research are depicted with grey blocks.



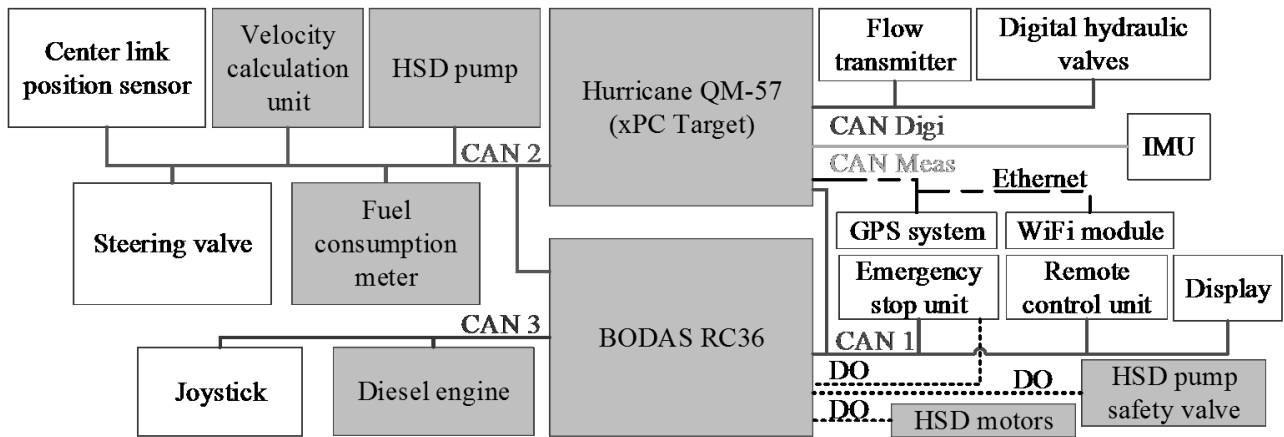


Figure 6. Diagram of the control system of the machine.

A major part of the signals is transmitted in digital form via Controller Area Network (CAN) buses. These include both control commands and measurement values. For example, the HSD pump includes on-board electronics (OBE), which implement closed-loop control of the displacement setting mechanism and send, for example, the values of pressures and relative displacement to the CAN bus. Therefore, these have to be discretized, which supports the choice made for the control command space in **P.II**.

As the QM-57 does not have any analog input or amplified output ports, a commercial control unit (see RC36 in Figure 6) is installed in the machine. The main safety features of the machine are implemented with this programmable logic controller (PLC). In addition, the control commands of HSD motors and diesel engine have to be transmitted with this unit. This is because QM-57 cannot control valve coils directly and does not have enough CAN bus interfaces in order to connect to all the buses of the machine. Furthermore, there is an on-going research about utilizing RC36 for running compiled Simulink models in a unit with less calculation power, but the presented algorithms of this thesis are not tested with RC36.

In **P.II**, the field experiments to evaluate fuel economy were conducted using an autonomous machine. This means that there was no operator present as the machine followed a pre-determined route and velocity trajectory. For this, the position measurement of the center link, steering valve, GPS system and inertial measurement unit (IMU) were utilized (see Figure 6). The path-following algorithm was based on the one developed by Ghabcheloo et al. in [5]. All the recorded data was first saved to the QM-57 and downloaded via Wi-Fi connection after each experiment.

### 3.1.3 Online Fuel Consumption Measurement System

The fuel economy improvements of the field tests of **P.II** were evaluated with a system that measures the amount of consumed fuel online. This enabled comparing the momentary engine consumption with different controllers that also rigorously expose the situations, for example, in which the devised controller is less optimal than the baseline controller. If only the total consumption is measured, it is more difficult to estimate how much the cycle contributes to the fuel economy results.

The installed measurement system is the KMA Mobile Type 075 developed by AVL. The device utilizes the Pierburg Luftfahrt Union (PLU) measuring principle that is insensitive to changes in the density, viscosity, and temperature of the fuel. This is achieved by controlling a servo motor-driven gear pump in order to maintain a zero pressure difference over the pump. Therefore, the rotational speed of the motor is proportional to the fuel flow, and no leakages due to pressure differences are present. [93]

The KMA system is capable of measuring flows up to 75 l/min with an uncertainty of  $\pm 0.1\%$  (of the reading) [93]. The maximum fuel consumption of the research platform machine was approximately 30 l/min in the experiments of **P.II**, in which the analog voltage output of the KMA system was utilized. However, this value was converted into digital form with a resolution of 0.75 ml/min and the 10-millisecond mean value was transmitted via CAN bus.

The engine of the research platform machine has a high-pressure fuel rail (or common rail). Thus, only part of the pumped fuel is injected into the cylinders. This means that in order to measure the consumed fuel, the returning flow has to be considered. In the KMA system, the returning flow is directed to the input port of the outlet pump (see Figure 7), and is therefore fed back without adding the amount to the measurement. In other words, the outlet pump of the KMA system forms a “closed circuit” with the fuel rail of the engine, and only the added fuel flow to this circuit is measured. This amount corresponds to the fuel injected into the cylinders of the engine.

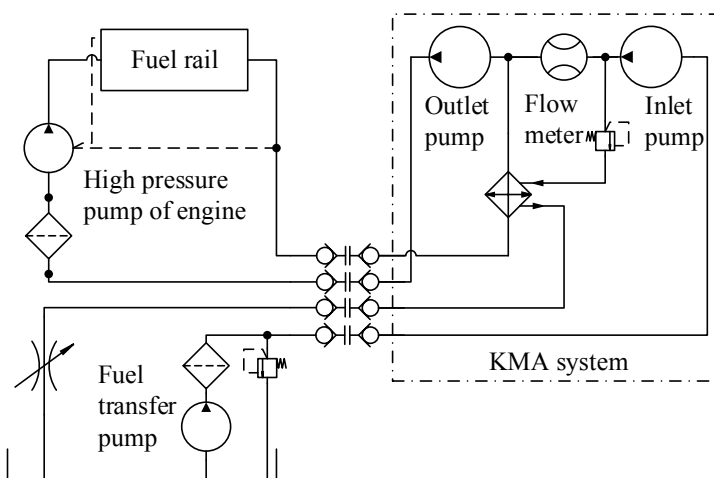


Figure 7. Simplified diagram of the fuel system of the engine with KMA system installed.

The fuel consumption of the simulation model utilized in **P.I** was validated with the consumption value available in the engine ECU. Figure 8 presents a part of a fuel economy test of **P.II**, where this data is compared to the one obtained with the KMA system.

The differences in the consumptions is shown on the right-hand side plot of Figure 8. Throughout all the tests, higher consumption values were measured with the KMA system. The average and standard deviation of the variations in this test were 1.17 l/h and 1.52 l/h, respectively. The largest differences occurred in situations in which the consumption increased rapidly. These might be related to the dynamics of the utilized methods, even

though the data of the KMA system is further filtered in Figure 8 to match the 100-millisecond interval of the engine ECU data.

More importantly, there seemed to be significant deviations in consumption during steady-state and low transient phases of the experiments. It has to be noted that the data provided by the engine ECU is calculated based on the control signal of the injection valves, while the data of the KMA system is measured. Still, it is not clear where this dissimilarity originated, as there might have been, for example, inaccuracies in the injection model, but also disturbances that had an effect on the measurement.

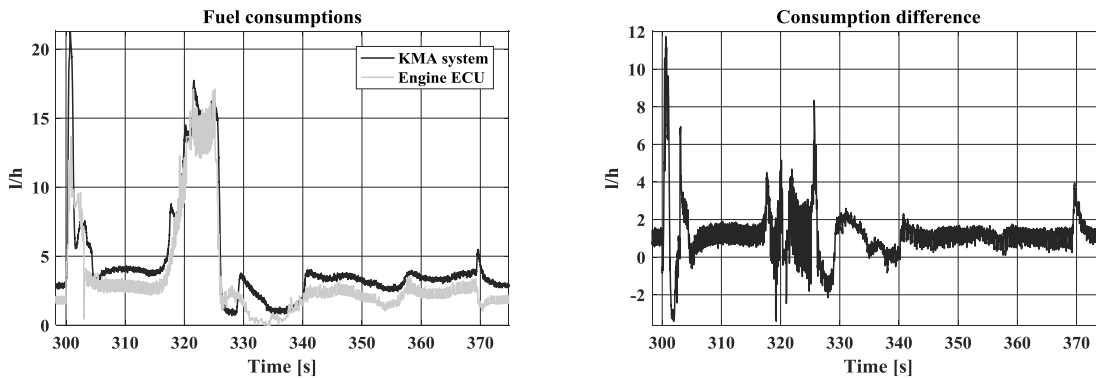


Figure 8. Comparison of fuel consumption values of KMA system and engine ECU.

If the final results of **P.II** had been calculated based on the consumption value of engine ECU, the fuel economy of the devised optimal controller would have increased more than the one obtained with the rule-based controller used as baseline. Modified results are presented in Table 1. In the fuel economy tests of **P.II**, the difference would increase from 16.6% to 17.5% (mass 5,000 kg) and from 12.4% to 15% (mass 6,000 kg). In the hill climbing tests utilized to evaluate the functionality of the controllers, the changes would be 1.7% (4 m/s), 0.5% (5 m/s), and 2.1% (6 m/s).

Table 1. The results of **P.II** evaluated with the consumption data of the engine ECU.

| Test             | Mass [kg] | Optimal controller |              |              |                    | Rule-based controller |              |              |
|------------------|-----------|--------------------|--------------|--------------|--------------------|-----------------------|--------------|--------------|
|                  |           | $m_f$ [ml]         | Distance [m] | Cons. [ml/m] | $\Delta$ cons. [%] | $m_f$ [ml]            | Distance [m] | Cons. [ml/m] |
| Autonomous drive | 5000      | 215.3              | 550.1        | 0.39         | -17.5 %            | 260.1                 | 548.1        | 0.47         |
|                  | 6000      | 244.3              | 538.8        | 0.45         | -15.0 %            | 287.1                 | 538.2        | 0.53         |
| Hill, 6 m/s      | 5000      | 61.3               | 71.9         | 0.85         | -1.5 %             | 60.5                  | 69.8         | 0.87         |
| Hill, 5 m/s      | 5000      | 54.2               | 72.3         | 0.75         | -1.4 %             | 52.7                  | 69.3         | 0.76         |
| Hill, 4 m/s      | 5000      | 60.1               | 70.6         | 0.85         | 6.7 %              | 57.0                  | 71.4         | 0.80         |

### 3.2 Validation of Simulation Models

This section presents validation tests for the models utilized in the research. First, the highly detailed model of the research platform machine, referred to as GIMsim, is validated with experimental data. This is followed by tests in which the responses of GIMsim are compared to those obtained with a simplified model utilized in **P.IV**.

In GIMsim, all the main hydraulic systems and mechanics of the research platform machine are modelled. In addition, it includes a model for tire-terrain interaction and graphical user interface. The models are executed in separate desktop PCs to enable real-time operation.

Some validation tests of GIMsim are also presented in **P.I**. However, the model of the hydraulic motors utilized in these simulations was based on the measurement report of the manufacturer. In this document, the value of the reduced displacement of the motors was  $282 \text{ cm}^3/\text{r}$  (i.e., 60% of the maximum). Recall that the motors have only two discrete settings for the displacement as explained in Section 3.1.1. In fact, the correct value is  $235 \text{ cm}^3/\text{r}$  (50% of the maximum), which was also later confirmed by the manufacturer. As a result, the pressure differences recorded with the reduced displacement of the motors are higher than the simulated ones in **P.I**.

Figure 9 presents a validation test of GIMsim, in which the displacement of the hydraulic motors is reduced at approximately time 7.9 s. The correspondence between the measured and simulated data is good especially with the rotational speed ( $n_e$ ) and fuel consumption (cons) of the engine. These are probably the most important values in the testing of EM controllers, while the accuracy of pressures ( $p_A$  and  $p_B$ ) is the best indicator for appropriate modelling.

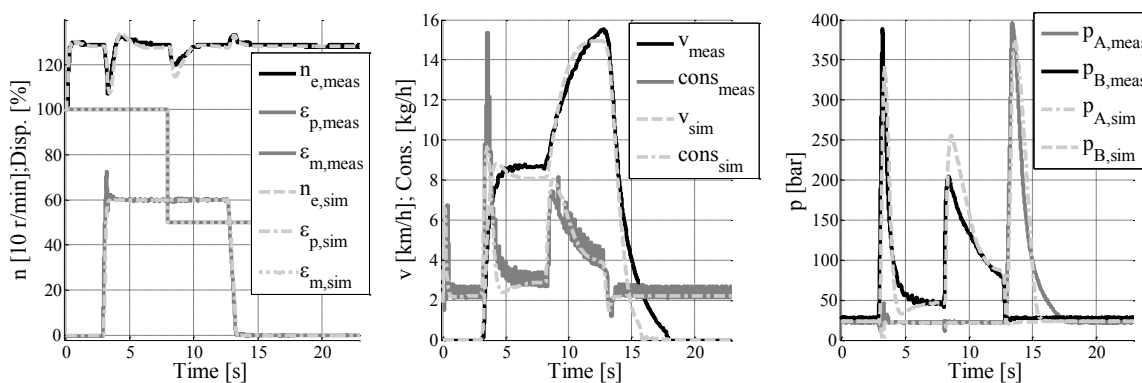


Figure 9. Validation test of GIMsim with decreasing motor displacement. The figure is modified from [90]. Reprinted with permission from TUT/AUT.

In the initial acceleration, the displacement of the pump is increased stepwise from 0% to 60%. This rapid change with relatively low engine speed (1200 r/min) is challenging for the boost pump (see Figure 4). As the displacement setting mechanism requires such a high volumetric flow, the pressure in the suction port of the

main pump ( $p_A$ ) falls below the minimum allowed value. Consequently, due to a safety function, the displacement starts to reduce before the pressure rises again to an admissible value. This feature is not included in the simulation model, which can be observed in the curves of  $\varepsilon_p$  at time 3.2 s.

Another validation test is depicted in Figure 10, in which the rotational speed of the engine is increased from 1,000 r/min to 1,900 r/min at time 7.5 s. In the beginning of the test, the displacement of the pump is increased from 0% to 70% with a two-second ramp command. Again, the simulated curves correspond well to the measured ones. Negligible differences can be observed with presented pressures that are most likely related to the modelling of friction.

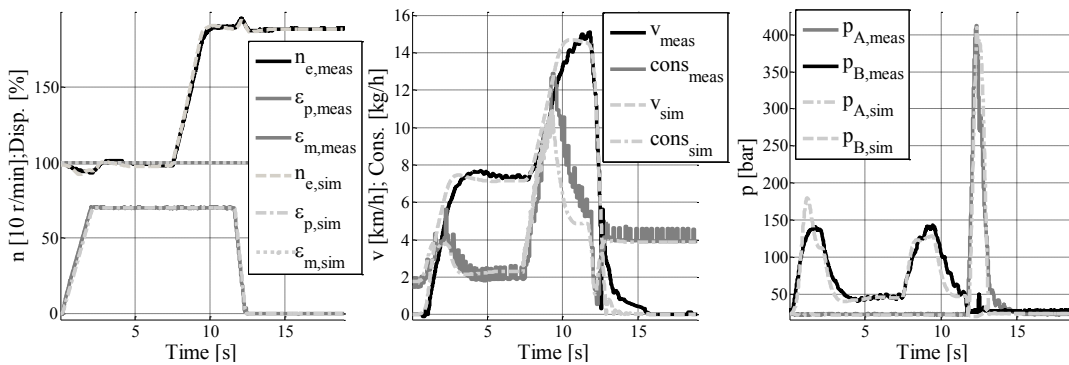


Figure 10. Validation test of GIMsim with increasing engine speed. The figure is modified from [90]. Reprinted with permission from TUT/AUT.

Another model of the HSD system was also developed for the NMPC presented in **P.IV**. Figure 11 presents a validation test in which the responses of this model are compared with the ones from GIMsim.

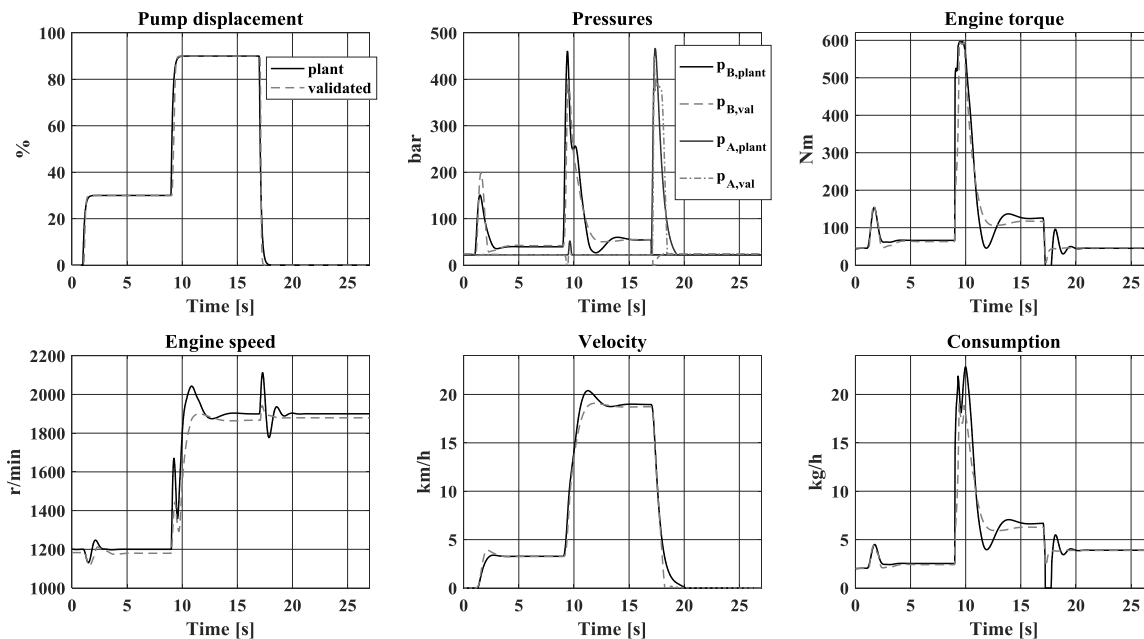


Figure 11. Validation test of the system model utilized in the controller of **P.IV**.

For the test in Figure 11, the machine starts from a standstill with  $n_e = 1,200$  r/min. At time = 1 s,  $\varepsilon_{p,com}$  is increased to 30%, resulting in approximately 3.3-km/h velocity. It can be observed that the engine speed of the NMPC model (referred to as “plant”) follows accurately that of GIMsim (referred to as “validated”) under an increasing load. This is important for the EM controller as significant uncertainties might, for example, result in loads increasing too rapidly, which can even stall the engine.

At time = 9 s,  $n_{e,com}$  and  $\varepsilon_{p,com}$  are increased to 1,900 r/min and 90%, respectively. This is a demanding situation for the engine model, because the set-point is changed under disturbance transient. As shown in the lower left plot, the  $n_e$  of NMPC overreacts, and the difference to the validated response becomes notably large. A similar effect is also observed during deceleration. In addition, the steady-state engine speeds are divergent due to the fact that the NMPC model does not include engine droop.<sup>1</sup> A more detailed discussion is found in the appendix of **P.IV**.

---

<sup>1</sup> Droop is a function of the engine controller that reduces the  $n_{e,com}$  as a function of the load.

## 4 Summary of Publications

This chapter provides brief summaries of publications **P.I–P.III** and the unpublished manuscript **P.IV** included in this compendium. In **P.I**, the HSD system is modelled and validation tests are presented. In addition, the FOC based on the quasi-static system model is tested. **P.II** presents the experimental results obtained when the controller of **P.I** is implemented into the research platform machine described in Chapter 3. The notable velocity-tracking error observed in publications **P.I** and **P.II** is addressed with gain-scheduling velocity control in **P.III**. **P.IV** is a simulation study in which EM and velocity-tracking are simultaneously considered with NMPC.

Table 2 summarizes the features of the devised controllers in order to provide a brief overview of the conducted research.

Table 2. Summary of the controllers.

| Controller  | Operating principle    | Intended use |                   | Real-time | Testing method |             | Fuel economy |
|-------------|------------------------|--------------|-------------------|-----------|----------------|-------------|--------------|
|             |                        | EM           | Velocity tracking |           | Simulation     | Field tests |              |
| <b>IBLC</b> | Rule-based             | X            | ---               | X         | X              | X           | Standard     |
| <b>FOC</b>  | Steady-state equations | X            | ---               | X         | X              | X           | High         |
| <b>GSVC</b> | Dynamic model          | ---          | X                 | X         | (X)            | X           | ---          |
| <b>NMPC</b> | Dynamic model          | X            | X                 | ---       | X              | ---         | High         |

As presented in Table 2, three of the controllers were designed for the energy management of HSDs. The baseline was set with an industrial baseline controller (IBLC), a rule-based solution that included no closed-loop velocity control features. FOC and NMPC resulted in very similar fuel economy that clearly exceeded the one achieved with the IBLC. The most important benefit of the NMPC, when compared with the FOC, is the achieved flexibility that facilitates balancing of high performance velocity-tracking and fuel economy.

## 4.1 P.I: Fuel Optimal Controller for Hydrostatic Drives – A Simulation Study and Model Validation

In this paper, the efficacy of a fuel economy improving optimal controller is evaluated with an HSD of a simulated wheel loader. The contributions are twofold as, in addition to the devised controller, a real-time simulation model is also developed and validated.

The controller determines the control commands of the actuators of HSD based on a cost function. The terms included in the decision-making are consumed fuel per travelled distance, velocity error, and the changes of control commands of the actuators. The control concept can be seen as instantaneous optimization in which only the current inputs are utilized in the calculation of the outputs of the controller, and the references are determined only for the next calculation step (i.e., one step ahead). For this reason, the fuel economy part of the cost has to be of the power type, instead of energy. In addition, some additional features (for example load limiting) was included in the controller in order to improve functionality.

During the research, the simulation model of the machine was validated. To accomplish this, 50 different acceleration/deceleration tests were conducted, and the response of the simulated machine was matched with the collected data. The correspondence of the measured and simulated data was high for the majority of the experiments. In a few tests, the accuracy of steady-state pressures was evaluated adequate. Therefore, the simulated and experimental fuel consumption were also equivalent.

Figure 12 presents the integrated fuel consumptions of the simulations conducted with the optimal and rule-based (referred also as baseline) controllers. The height of the hill is different in each subplot, which results in a steeper slope. Four different velocity trajectories were tracked with every hill height. Yet, the rule-based controller used as the baseline could not reach the hilltop in all tests. With such occasions, the corresponding bar is not plotted in the figure.

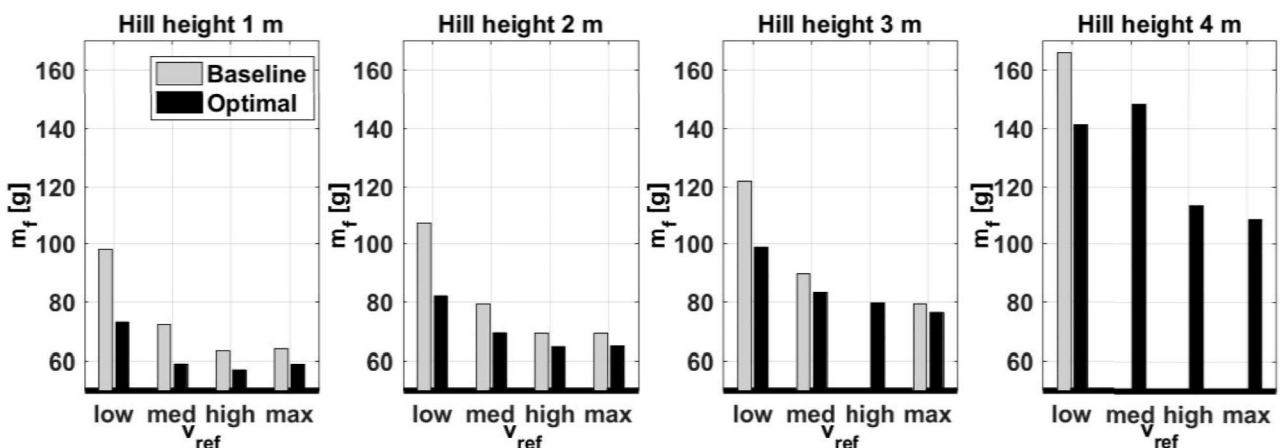


Figure 12. Total fuel consumptions of the simulation experiments of P.I.



The results indicate the efficacy of the designed optimal controller as the fuel economy is improved in every test when compared with the baseline controller. The relative improvement is larger with low velocity references, which originates from the fact that the optimal controller can utilize the reduced displacement of the hydraulic motors also in this operating region. Therefore, the displacement of the HSD pump can be increased and the engine speed decreased. Both of these actions improve the efficiency of the system. For example, with low velocities and a 1-meter hill, the optimal controller reduced the total consumption by 25.9%.

## 4.2 P.II: Fuel Optimal Controller for Hydrostatic Drives and Real-World Experiments on a Wheel Loader

This paper extends the design of the FOC of **P.I** for implementation to the control system of the research platform machine described in detail in [76]. In addition, the formulation of the problem is more detailed.

The most important changes in the controller are related to considering the features not included in the model of the machine, namely displacement changes of the HSD motors and the pressure cut-off of the HSD pump. The former is dealt with by preventing the optimal control commands from reaching the actuators during the displacement change. For the pressure cut-off that forces the pump displacement to decrease if maximum pressure is reached, the solution is to place an additional cost on the reduced displacement near the maximum pressure difference. The extra cost is removed when the pressure difference decreases to values of steady-state driving on level ground. Therefore, the machine climbs the steepest hills always with full displacement of the motors and allows reduction when reaching the hilltop.

There were two sets of experiments conducted that tested both the fuel economy and functionality of the controller. In the first set, a pre-recorded route was driven autonomously with and without an additional 1,000-kg load. The functionality was evaluated with extreme hill climbing tests in which the steepest slope was measured at 20 degrees.

The efficacy of the optimal controller was evaluated by comparing the gathered data to the one obtained with a rule-based controller serving as baseline. This controller was inspired by the DA control (see Section 2.2.1.2 for details) that can be implemented also hydromechanically. In terms of fuel economy, it is a more realistic and more efficient baseline than the controller utilized in **P.I**. In addition, the functionality is better due to the in-built load limiting function.

The research platform machine was equipped with an online fuel consumption measurement system (see Section 3.1.3) that enables accurate data, but more importantly also the possibility to investigate which situations contribute most to fuel economy. In the tests with and without an additional load, consumption per travelled distance improved 12.4% and 16.6% with the optimal controller, respectively.

### **4.3 P.III: Gain Scheduled State Feedback Velocity Control of Hydrostatic Drive Transmissions**

This paper addresses the velocity-tracking of HSDs. The solution incorporates the nonlinear characteristics of the system with a state-dependent (SD) model. The devised full state feedback controller is based on pole placement and gain-scheduling; that is, the gains are calculated utilizing measured speed and pressures, as well as approximated volumetric flow.

The challenge related to state estimation via measured pressures, originating from uncertain friction modelling, is tackled with so-called D-implementation developed by Kaminer et al. in [4]. With D-implementation, a measured state can be replaced by its derivative without changing the closed-loop properties of the design. This lifts the requirement of utilizing the actual measured pressure values that might cause uncertainties in the estimation of the states and, therefore, induce inaccurate controller gains.

The devised gain-scheduled velocity control (GSVC) is able to provide a solution to the velocity error under positive and negative loads experienced with the FOC in **P.I** and **P.II**. This is demonstrated with a test that includes both uphill and downhill parts driven with constant velocity reference. In addition, the reference tracking performance of the GSVC is shown with a stepwise sequence of four reference values ranging from 0.5 to 5 m/s. Both tests were conducted with the research platform machine (see Section 3 for details) at the test area of IHA.

In addition, the devised controller was compared to two well-known control concepts, namely constant gain state feedback and classical PID controllers. The investigations proved the concept, as the velocity error with the GSVC was explicitly reduced in both experiments when compared with the two baseline controllers.

However, the GSVC has to be further developed before combining it with the optimal controller of **P.II**. This is because in this research, control commands of the engine and HSD motors were held constant at 1,650 r/min and 100%, respectively.

### **4.4 P.IV: Nonlinear Model Predictive Energy Management of Hydrostatic Drive Transmissions (unpublished manuscript)**

In this paper, we address both velocity tracking and EM of HSDs with an NMPC approach. The designed NMPC framework aims to provide a benchmark for the controllers of non-hybrid HSDs that do not require information about the future.

According to our review of the relevant literature, no articles that address the MPC of traction drives with comparable implementation have been published. A number of MPC-based velocity-tracking solutions are

available, but research with EM features of HWMs is quite scarce. In addition, the utilized models are extremely simplified and, therefore, it is uncertain how much the performance is decreased due to the choices made.

In MPC, a dynamic system model is used for predicting the response of the system. Our solution utilizes a validated model that includes as few compromises as possible. However, some nonlinear features related to the dynamics of the back-pressure of HSD motors had to be omitted in order to guarantee convergence. The control commands are determined 25 samples ahead whereas the system response is predicted for the next 200 samples. The sample time of the controller is 10 milliseconds. The choices for the most essential parameters of the controller are discussed in the paper.

Our solution is unique especially in terms of determining stabilizing terminal constraints for control commands and distinctive terminal cost, which cleverly exploit the optimal steady-state solution. The choices made have a significant effect on the smoothness of control trajectories, and thus, in the stability of the control system that is not a certainty with complex nonlinear systems.

The simulations where the responses of the NMPC are compared with those obtained with the controllers of **P.II** prove the concept, as achieved velocity-tracking can be improved without the fuel economy of the machine deteriorating. In addition, the NMPC is considerably more versatile than, for example, the FOC of **P.II** in terms of balancing the tradeoff between fast velocity-tracking and high energy efficiency. This is because the NMPC does not require additional parts, such as the load limiter of the engine, as the features are easily included with the system model and constraints.

## 5 Discussion

This section summarizes how the research questions of this thesis **RQ1–RQ3** are addressed with the presented features of the controllers (**F1–F6**) as described in Section 1.1.

### 5.1 Energy efficiency (RQ1)

*How much the fuel economy of non-hybrid HSDs can be improved only by control algorithms without impairing the functionality of the system? What is the benefit of utilizing dynamic system models instead of steady-state equations?*

The benefits of performance obtained with sophisticated control depend naturally on the initially utilized algorithm (i.e. the baseline). Therefore, presenting a single value as the one and only truth is not feasible. Nevertheless, the developed model-based controllers enable significant improvements of fuel economy without degraded functionality.

The utilization of dynamic system models, here NMPC, offers simultaneously high fuel economy and fast velocity-tracking. However, probably the most essential benefits acquired are the increased versatility and configurability of the system.

This answer is justified by discussing the features **F1** and **F2**.

#### **Fuel Economy (F1)**

*The designed EM solutions should improve the fuel economy of HSDs by means of control algorithms. Systems with energy storage are beyond the scope of this thesis.*

Traditional system layouts and conventional control algorithms have created an unfavorable impression about the energy efficiency of hydraulic systems. The results presented in **P.I**, **P.II**, and **P.IV** show that significant

improvements of fuel economy can be achieved with model-based control of HSDs without any additional components or major changes in drive-by-wire HWMs.

An instantaneous optimization scheme was implemented with the quasi-static FOC, in which performance was demonstrated in real-time simulations and field experiments in publications **P.I** and **P.II**, respectively. In hill-climbing simulations of **P.I**, fuel economy improved from 5% to 25% when the devised controller was compared with a rule-based solution. The largest benefits were obtained with low velocities due to the rules that determine the applied displacements of HSD pump and motors. The comparative controller lacked any load limiting functions, which resulted in the engine stalling on the steepest hills.

The same control concept was also verified with the research platform machine in **P.II**. In these tests, a route that included asphalt and gravel surfaces together with hill climbs and descents was driven autonomously. In addition, fuel consumption was determined using an online measurement system. This set-up ensured both reliable and repeatable results that enabled indicating situations where, for example, improvements were the largest. In the conducted experiments, the fuel economy was 16.6% and 12.4% higher without and with an additional 1,000-kg load, respectively. Here, the FOC was compared with a rule-based solution inspired by a commercial control algorithm.

In **P.IV**, an NMPC scheme was developed to serve as a benchmark for non-hybrid controllers that do not require information about the future. The simulated responses of the FOC were compared with those obtained with the NMPC. The results proved the efficacy of the NMPC, as improved velocity-tracking could be achieved without decreasing the fuel economy. In addition, it enables increased versatility with easily balanced trade-off between these two measures of performance.

### **High Performance (F2)**

*The response of the system should not be significantly impaired in order to increase fuel economy.*

As discussed in Section 2.2.3, several variables can be considered when evaluating the achieved success. However, stressing the energy efficiency in the controller might result in decreased velocity-tracking. As the approach applied in this thesis is not based on tasks but tracking a pre-determined velocity trajectory, the results are easily affected by the chosen cost coefficients. Then again, this increases the versatility of the controller.

To show that the improvements of fuel economy have not impaired the functionality of the machine, a set of extreme tests was performed during the field experiments of **P.II**. In these tests, the machine was driven into such a steep hill that it could not climb to the top if stopped in the middle. Due to the higher engine speed in steady-state drive, the fuel economy of the commercial baseline controller was 8.4% higher in one test while in the others the difference was less than 1%. Nevertheless, these experiments proved that the achieved benefits are not based on impaired functionality.

In the simulations of **P.IV**, the designed NMPC exceeded the performance of the FOC and commercial baseline controller both in terms of velocity-tracking and energy efficiency. This is expected, as the utilized scheme

optimizes the response based on the dynamic model of the system, whereas the FOC, for example, is based on steady-state equations.

## 5.2 Practical importance (RQ2)

*How to demonstrate that the control solutions developed for **RQ1** have also practical worth?*

The most essential part of proving the practical worth of theoretically good controller is to implement it into a real HWM and conduct field experiments. Only this way can the effect of unmodeled factors (e.g., disturbances and features) be evaluated. This requires the controller to be real-time capable. In addition, there should be as few estimated values as possible (e.g., fuel consumption should be measured instead of calculating it based on other variables).

The obtained performance has to be compared with credible baselines that are preferably utilized in real HWMs of similar type. This is a challenge as the available data about these solutions is extremely scarce.

This answer is justified by discussing the features **F3**, **F4** and **F5**.

### Experimentally Verified (F3)

*Field tests are essential in the evaluation of the benefits of the developed controllers. Moreover, as the focus is on improving the fuel economy of HSDs, fuel consumption should be measured instead of predicting it with a model. Successful experimental testing also guarantees a certain level of robustness, as the utilized models are never perfectly consistent with the reality.*

Both the FOC of **P.II** and the velocity-tracking controller of **P.III** were evaluated in field tests. The results verified the applicability and performance of these controllers under modelling uncertainties in a variety of different tests.

The success was demonstrated in **P.II** with the online fuel consumption measurement system described in Section 3.1.3. By measuring this variable, the effects of all the possible modelling errors (e.g., utilization of steady-state BSFC maps of the engine) are removed from the data. The uncertainties related to human operators were lifted in the fuel economy tests with the autonomous drive algorithm originally presented in [5].

### Credible Comparison (F4)

*The performance of the developed controllers should be assessed by comparing both of them with feasible textbook solutions and state-of-the-art commercial algorithms of similar applications when viable.*

When evaluating the performance of the designed controller, it is a common practice to compare the obtained responses with those of other controllers. However, the lack of standardized methods together with the limited information available about the commercial control solutions of HWMs has induced a situation where the

controllers utilized as baselines are practically always devised by the researchers conducting the study. This is not that problematic if the reader knows the field well enough to assess whether the choices made are justified. Ideally, a globally optimal solution can be derived for the tested cycles.

The comparative controller utilized in the EM part of this research is devised based on a commercial algorithm (see Section 2.2.1.2 for details). However, the HSD motors with two discrete displacement settings are very rare in commercial machines. Therefore, the baseline does not exactly correspond to the commercial solution in terms of the control command of HSD motors. In addition, the minimum engine speed in **P.I** was set to 1,500 r/min, but in **P.II** and **P.IV**, it was 1,000 r/min. This resulted in improved energy efficiency of the baseline. In **P.III**, both classical state feedback and a PID controller were utilized in the experiments for comparison purposes.

One easily interpretable baseline for EM controllers can be obtained with DP, which enables determining global optima for a specific test cycle. Nevertheless, this requires accurate information, for example about the disturbances during the cycle, which in practice prevents utilizing the method in the field experiments of **P.II**, as collecting such data is not a trivial matter. However, DP suffers severely from “the curse of dimensionality,” meaning that the calculation time increases substantially if the model has several states. For this reason, comparisons against global optima were not performed in **P.IV**, in which the system model includes eight states and two control inputs.

### **Real-Time Implementable (F5)**

*The primary requirement for the controllers is that the information about the future should not be mandatory. This enables real-time implementation that is necessary for F3.*

In order to be real-time implementable, a control algorithm has to be executable in terms of available information and computational resources. The former is usually achieved if accurate information about the future is not required. The latter depends solely on the unit in which the calculations are performed. One solution for broadening the scope of applicable units is to decrease the search space of the algorithm for faster execution. However, this will probably have an effect on the degree of optimality.

None of the controllers devised in this research require information about the future. In **P.IV**, predictions were made for a pre-determined time ahead, but they were always based on the current state of the system and assumed a constant velocity reference. This enabled utilizing them, for example, in human-operated machines in which the next reference value cannot be exactly known.

The controllers presented in **P.II** and **P.III** were implemented in the research platform machine described in Chapter 3. In addition, simulations of **P.I** were performed in real-time. Furthermore, the execution time of the FOC, discussed in **P.I** and **P.II**, can be made faster by decreasing the number of CCCs included in the search space.

The NMPC presented in **P.IV** is not optimized in terms of calculation time. Even with modern processing units, the current implementation is not real-time capable. However, the presented algorithm is intended for a benchmark to which, for example, implementations including less states or state-dependent linear models can be compared.

### 5.3 Adaptability and flexibility (RQ3)

*Can the controllers of drive-by-wire machines be designed in way that enables reduction of costs via faster control design and commissioning of HWMs?*

Model-based approach enables designing the controllers in a cost-efficient way as the higher level of accuracy of the utilized model decreases the amount of tunable parameters. This is because the required values are usually related to components specifications and, therefore, easily available. In addition, the model forms a separate part of the controller that can be replaced with relatively small effort. Thus, the structure is utilizable in several types of HWMs.

This answer is justified by discussing the feature **F6**.

#### Generality and Modularity (F6)

*Structures of the devised controllers should be applicable to multiple system layouts of HSDs, and the number of tunable parameters should be kept to a minimum. In addition, the design has to enable the controller of an individual system to be integrated into the upper level EM of the machine.*

In order to achieve as general a controller structure as possible, all the devised controllers are based on the model of the HSD system. In **P.I** and **P.II**, steady-state equations were utilized in the calculations of machine velocity and engine torque as a function of control commands. The solutions of **P.III** and **P.IV** are based on the dynamic system model that includes, for example, the efficiencies of hydraulic components. Still, though the aspects of generality were considered in the control design, experiments were only conducted with the research platform machine presented in Section 3.

These approaches guarantee a high level of generality as long as the described equations can be derived for the controlled system. In addition, a model-based approach significantly decreases the number of parameters required to tune the controller when compared to rule-based solutions with similar performances. Firstly, the NMPC of **P.IV** enables changing the response of the HSD system only by tuning a single parameter in the cost function. This is because the dynamics of the system are easily considered with the utilized model and constraints. Secondly, there are five tunable parameters in the velocity-tracking controller of **P.III**. This number also includes the two parameters related to the signal processing. When compared with the presented classical PID tracking, the additional two parameters enable a substantial performance increase.



As this research covers only the control design of HSD systems, instead of the EM of the entire machine, another system is required that divides the available engine power among all the systems of the machine, namely HSD, work functions and steering. In the controllers presented in **P.I**, **P.II** and **P.IV**, this interface with the upper level is implemented with the maximum allowed power that cannot be exceeded. However, in the conducted tests, this value was set to the maximum power of the engine.

## 6 Conclusion and Future Work

In this compendium thesis, we proposed controllers for both the EM and velocity-tracking of HSDs. The presented EM solutions improved the energy efficiency of these systems only by means of control algorithms. The scope of the thesis was limited to non-hybrid HSDs as hydraulic hybrid traction drives of HWMs are still merely concepts rather than commercial products. The devised controllers also offer credible benchmarks for the evaluation of the benefits of hybridization.

The contributions of this research are listed in Section 1.2, and the results are discussed in detail, for example, in Chapter 4. For a brief overview of the conducted research, the reader is referred to Table 2 (in Chapter 4).

The following can be regarded as the most important merits of the thesis:

- 1) The design, experimental verification, and the proven practical worth of the quasi-static FOC tested with simulations in **P.I** and the field tests in **P.II**.
- 2) Devising the NMPC scheme for the EM and velocity tracking of HSDs in **P.IV**. To the best of the author's knowledge, such detailed designs have not been presented in the literature for similar applications.

In addition, a GSVC approach was devised in **P.III**. This controller offers a solution for the shortcoming of the FOC that suffers from inadequate velocity-tracking under high-load situations. However, the integration of these two controllers remains to be completed in the future.

As the control methods developed in this thesis are model-based and designed to be as general as possible, they can also be utilized to control the other hydraulic systems of HWMs. Especially, extending the NMPC scheme for the control of work functions of the machine should theoretically be relatively simple. The FOC of **P.I** and **P.II** would require at least additional features that consider the different kinds of dynamics of linear hydraulic actuators.

For the NMPC framework, the future road map includes improvements that enable the utilization of non-derivative variables both for control commands and in the modelling of the system. Furthermore, the computational burden of the algorithm should be decreased for efficient testing. The methods to achieve this could involve, for example, surrogate models for faster predictions or modifying the algorithm to enable efficient utilization of different parallel computing techniques.

## Bibliography

- [1] Still, "Hybrid trucks in series production," 2018. [Online]. Available: <https://www.still.co.uk/hybrid-trucks-series-production.0.0.html>. [accessed 28 June 2018].
- [2] Liebherr, "Hybrid Power Booster Liebherr Pactronic," 3 2018. [Online]. Available: <https://www.liebherr.com/shared/media/maritime-cranes/downloads-and-brochures/brochures/liebherr-lhm-mobile-harbour-crane-pactronic-brochure.pdf>. [accessed 28 June 2018].
- [3] Jähne, H., "Struktursystematik & Effizienzpotential hydraulischer Fahrtriebe unter Berücksichtigung der Applikation," Ph.D. dissertation, Aachen: Shaker Verlag, 2012.
- [4] I. Kammer, A. M. Pascoal, P. P. Kahrgonekar and E. E. Coleman, "A Velocity Algorithm for the Implementation of Gain-scheduled Controllers," *Automatica*, vol. 31, no. 8, pp. 1185-1191, 1995.
- [5] R. Ghabcheloo, M. Hyvönen, J. Uusisalo, O. Karhu, J. Järä and K. Huhtala, "Autonomous Motion Control of a Wheel Loader," *ASME Dynamic Systems and Control Conf. and Bath/ASME Symposium on Fluid Power & Motion Control*, Hollywood, CA, USA, 2009.
- [6] L. Grüne and J. Pannek, *Nonlinear Model Predictive Control - Theory and Algorithms*, London, UK: Springer-Verlag London, 2011.
- [7] M. Lindgren and P.-A. Hansson, "A Transient Fuel Consumption Model for Non-road Mobile Machinery," *Biosystems Engineering*, vol. 87, no. 1, pp. 57-66, 2004.
- [8] M. Ahopelto, J. Backas and K. Huhtala, "Power management in a mobile work machine: reduced diesel rpm for better energy efficiency," *7th FPNI PhD Symposium on Fluid Power*, Reggio Emilia, Italy, 2012.
- [9] A. Sciarretta, M. Back and L. Guzzella, "Optimal Control of Parallel Hybrid Electric Vehicles," *IEEE Transactions on Control Systems Technology*, vol. 12, no. 3, pp. 352-363, 2004.
- [10] T.-V. Vu, C.-K. Chen and C.-W. Hung, "A Model Predictive Control Approach for Fuel Economy Improvement of a Series Hydraulic Hybrid Vehicle," *Energies*, vol. 7, pp. 7017-7040, 2014.
- [11] R. Langari and J.-S. Won, "Intelligent energy management agent for a parallel hybrid vehicle - Part I: System architecture and design of the driving situation identification process," *IEEE Transactions on Vehicular Technology*, vol. 54, no. 3, pp. 925-934, 2005.

- [12] C.-C. Lin, H. Peng, J. W. Grizzle and J.-m. Kang, "Power Management Strategy for a Parallel Hybrid Electric Truck," *IEEE Transactions on Control Systems Technology*, vol. 11, no. 6, pp. 839-849, 2003.
- [13] H. Jähne, S. Helduser, T. Kohmäscher, H. Murrenhoff, H. Deiters, H.-H. Harms, M. Bliesener and M. Geimer, "Drive Line Simulation for Increased Energy-Efficiency of Off-Highway-Machines," *6th International Fluid Power Conference, 6. IFK*, Dresden, Germany, 2008.
- [14] B. Vanwalleghem, C. Dousy and G. V. B. Pinte, "Optimization of the efficiency of hydrostatic drives," *8th International Fluid Power Conference, 8. IFK*, Dresden, Germany, 2012.
- [15] Bosch Rexroth AG, "Easy Machine Operation with Rexroth Automotive Drive and Anti Stall Control," Bosch Rexroth AG, Elchingen, Germany, 2003.
- [16] C.-W. Hung, T.-V. Vu and C.-K. Chen, "The Development of an Optimal Control Strategy for a Series Hydraulic Hybrid Vehicle," *Applied Sciences*, vol. 6, no. 4, p. 93, 2016.
- [17] X. Lin, A. Ivanco and Z. Filipi, "Optimization of Rule-Based Control Strategy for a Hydraulic-Electric Hybrid Light Urban Vehicle Based on Dynamic Programming," *SAE International Journal of Alternative Powertrains*, vol. 1, no. 1, pp. 249-259, 2012.
- [18] M. Omid, M. Lashgari, H. Mobli, R. Alimardani, S. Mohtasebi and R. Hesamifard, "Design of fuzzy logic control system incorporating human expert knowledge for combine harvester," *Expert Systems with Applications*, vol. 37, pp. 7080-7085, 2010.
- [19] J. Naranjo, F. Jimenez, O. Gómez and J. Zato, "Low Level Control Layer Definition for Autonomous Vehicles Based on Fuzzy Logic," *Intelligent Automation & Soft Computing*, vol. 18, no. 4, pp. 333-348, 2013.
- [20] J.-S. Won and R. Langari, "Intelligent energy management agent for a parallel hybrid vehicle - Part II: Torque distribution, charge sustenance strategies, and performance results," *IEEE Transactions on Vehicular Technology*, vol. 54, no. 3, pp. 935-953, 2005.
- [21] D. Wang, X. Lin and Y. Zhang, "Fuzzy logic control for a parallel hybrid hydraulic excavator using genetic algorithm," *Automation in Construction*, vol. 20, no. 5, pp. 581-587, 2011.
- [22] S. Hui, J. Ji-hai and W. Xin, "Torque control strategy for a parallel hydraulic hybrid vehicle," *Journal of Terramechanics*, vol. 46, no. 6, pp. 259-265, 2009.
- [23] R. Pfiffner, L. Guzzella and C. Onder, "Fuel-optimal control of CVT powertrains," *Control Engineering Practice*, vol. 11, no. 3, pp. 329-336, 2003.
- [24] S. Ahn, J. Choi, S. Kim, J. Lee, C. Choi and H. Kim, "Development of an integrated engine-hydro-mechanical transmission control algorithm for a tractor," *Advances in Mechanical Engineering*, vol. 7, no. 7, pp. 1-18, 2015.
- [25] N. Srivastava and I. Haque, "A review on belt and chain continuously variable transmissions (CVT): Dynamics and control," *Mechanism and Machine Theory*, vol. 44, no. 1, pp. 19-41, 2009.
- [26] S. Hui and J. Junqing, "Research on the system configuration and energy control strategy for parallel hydraulic hybrid loader," *Automation in Construction*, vol. 19, pp. 213-220, 2010.
- [27] F. A. Bender, M. Kaszynski and O. Sawodny, "Drive Cycle Prediction and Energy Management Optimization for Hybrid Hydraulic Vehicles," *IEEE Transactions on Vehicular Technology*, vol. 62, no. 8, pp. 3581-3592, 2013.

- [28] T. O. Deppen, A. G. Alleyne, K. A. Stelson and J. J. Meyer, "Optimal Energy Use in a Light Weight Hydraulic Hybrid Passenger Vehicle," *Journal of Dynamic Systems, Measurement, and Control*, vol. 134, no. 4, 2012.
- [29] C. Williamson and M. Ivantysynova, "Power Optimization for Multi-Actuator Pump-Controlled Systems," *7th International Fluid Power Conference, 7. IFK*, 22-24 March 2010, Aachen, Germany, 2010.
- [30] E. D. Tate, J. W. Grizzle and H. Peng, "SP-SDP for Fuel Consumption and Tailpipe Emissions Minimization in an EVT Hybrid," *IEEE Transactions on Control Systems Technology*, vol. 18, no. 3, pp. 673-687, 2010.
- [31] R. Kumar and M. Ivantysynova, "An Instantaneous Optimization Based Power Management Strategy to Reduce Fuel Consumption in Hydraulic Hybrids," *International Journal of Fluid Power*, vol. 12, no. 2, pp. 15-25, 2011.
- [32] J. Liu and H. Peng, "Control Optimization for a Power-Split Hybrid Vehicle," *Proceedings of the American Control Conference*, Minneapolis, Minnesota, USA, June 14-16, 2006, pp. 466-471, 2006.
- [33] C. Musardo, G. Rizzoni, Y. Guezennec and B. Staccia, "A-ECMS: An Adaptive Algorithm for Hybrid Electric Vehicle Energy Management," *European Journal of Control*, vol. 11, pp. 509-524, 2005.
- [34] G. Bo and G. Rizzoni, "An adaptive algorithm for hybrid electric vehicle energy management based on driving pattern recognition," *2006 ASME International Mechanical Engineering Congress and Exposition, IMECE2006*, November 5-10, 2006, Chicago, IL, United States, 2006.
- [35] B. Wu, C.-C. Lin, Z. Filipi, H. Peng and D. Assanis, "Optimal Power Management for a Hydraulic Hybrid Delivery Truck," *Vehicle System Dynamics*, vol. 42, no. 1-2, pp. 23-40, 2004.
- [36] T. Nilsson, A. Fröberg and J. Åslund, "Minimizing Fuel Use During Power Transients for Naturally Aspirated and Turbo Charged Diesel Engines," 9 December 2014. [Online]. Available: <http://www.diva-portal.org/smash/get/diva2:770141/FULLTEXT01.pdf>. [accessed 12 February 2018].
- [37] T. O. Deppen, A. G. Alleyne, K. A. Stelson and J. J. Meyer, "Model Predictive Control of an Electro-hydraulic Powertrain with Energy Storage," *ASME 2011 Dynamic Systems and Control Conference and Bath/ASME Symposium on Fluid Power and Motion Control, DSCC 2011*, October 31 - november 2, 2011, Arlington VA, USA, pp. 225-232, 2011.
- [38] H. Borhan, A. Vahidi, A. M. Phillips, M. L. Kuang, I. V. Kolmanovsky and S. Di Cairano, "MPC-based energy management of a power-split hybrid electric vehicle," *IEEE Transactions on Control Systems Technology*, vol. 20, no. 3, pp. 593-603, 2012.
- [39] R. T. Meyer, R. A. DeCarlo, N. M. Jali and K. B. Ariyur, "Behavioral Modeling and Optimal Control of a Vehicle Mechanical Drive System," *2015 American Control Conference*, July 1-3, 2015. Chicago, IL, USA, 2015.
- [40] R. Kumar, "A Power Management Strategy for Hybrid Output Coupled Power-Split Transmission to Minimize Fuel Consumption," Ph.D. dissertation, West Lafayette, Indiana, USA: Purdue University, 2010.
- [41] T. O. Deppen, A. G. Alleyne, J. J. Meyer and K. A. Stelson, "Comparative Study of Energy Management Strategies for Hydraulic Hybrids," *Journal of Dynamic Systems, Measurement, and Control*, vol. 137, no. 4, 2015.

- [42] T. Nilsson, A. Fröberg and J. Åslund, "Predictive control of a diesel electric wheel loader powertrain," *Control Engineering Practice*, vol. 41, pp. 47-56, 2015.
- [43] D. F. Opila, W. X. R. McGee, R. B. Gillespie, J. A. Cook and J. W. Grizzle, "An energy management controller to optimally trade off fuel economy and drivability for hybrid vehicles," *IEEE Transactions on Control Systems Technology*, vol. 20, no. 6, pp. 1490-1505, 2012.
- [44] T. Coen, B. Saeys, J. Missotten and J. DeBaerdemaeker, "Cruise control on a combine harvester using model-based predictive control," *Biosystems Engineering*, vol. 99, no. 1, pp. 47-55, 2008.
- [45] P. Shakouri, A. Ordys and M. R. Askari, "Adaptive cruise control with stop&go function using the state-dependent nonlinear model predictive control approach," *ISA Transactions*, vol. 51, pp. 622-631, 2012.
- [46] P. Shakouri and A. Ordys, "Nonlinear Model Predictive Control approach in design of Adaptive Cruise Control with automated switching to cruise control," *Control Engineering Practice*, vol. 26, pp. 160-177, 2014.
- [47] J. Lennevi and J.-O. Palmberg, "Application and implementation of LQ design method for the velocity control of hydrostatic transmissions," *Proceedings of the Institution of Mechanical Engineers. Part I, Journal of systems and control engineering*, vol. 209, no. 4, pp. 255-268, 1995.
- [48] S. Strano and M. Terzo, "A SDRE-based tracking control for a hydraulic actuation system," *Mechanical Systems and Signal Processing*, vol. 60-61, pp. 715-726, 2015.
- [49] J. C. Taylor and D. Robertson, "State-dependent control of a hydraulically actuated nuclear decommissioning robot," *Control Engineering Practice*, vol. 21, pp. 1716-1725, 2013.
- [50] D. Hu, S. Ding, H. Zhu, B. Xu and H. Yang, "Velocity-tracking Control of the Variable-speed Controlled Hydraulic System: Using Compound Algorithm of PD & Feed-forward-feedback Control," *2011 Third International Conference on Measuring Technology and Mechatronics Automation*, Shangshai, China, 2011.
- [51] Q. Zhang and B. Li, "Feedback Linearization PID Control for Electro-hydrostatic Actuator," *2011 2nd International Conference on Artificial Intelligence, Management Science and Electronic Commerce (AIMSEC)*, Dengleng, China, 2011.
- [52] Y. Wang, Z. Sun and K. Stelson, "Nonlinear tracking control of a transient hydrostatic dynamometer for hybrid powertrain research," *Proceedings of the ASME 2010 Dynamic Systems and Control Conference*, September 12-15, 2010, Cambridge, Massachusetts, USA, 2010.
- [53] X. Li, X. Wang and Y. Wang, "Mixed sensitivity  $H_\infty$  controller design for variable-speed pump-controlled motor system," *2014 IEEE International Conference on Mechatronics and Automation (ICMA)*, Tianjin, China, 2014.
- [54] N. Guo and J. Hu, "Velocity Control System with Variable Universe Adaptive Fuzzy-PD Method for Agricultural Vehicles," *Proceeding of the 11th World Congress on Intelligent Control and Automation*, Shenyang, China, 2014.
- [55] A. K. Yadav and P. Gaur, "Intelligent modified internal model control for speed control of nonlinear uncertain heavy duty vehicles," *ISA Transactions*, vol. 56, pp. 288-298, 2015.
- [56] H. T. Do, H. G. Park and K. K. Ahn, "Application of an adaptive fuzzy sliding mode controller in velocity control of a secondary controlled hydrostatic transmission system," *Mechatronics*, vol. 24, no. 8, pp. 1157-1165, 2014.

- [57] D. Bertsekas, *Dynamic Programming and Optimal Control Vol. I*, Belmont, Massachusetts: Athena Scientific, 2005.
- [58] S. Moura, "Dynamic Programming," 10 December 2014. [Online]. Available: <https://ecal.berkeley.edu/files/ce191/CH05-DynamicProgramming.pdf>. [accessed 5 February 2018].
- [59] Bosch Rexroth AG, "Axial Piston Variable Pump A4VG Data sheet RE 92004/06.12," June 2012. [Online]. Available: [https://md.boschrexroth.com/modules/BRMV2PDFDownload-internet.dll/re92004\\_2012-06.pdf?db=brmv2&lvid=1164753&mvid=12275&clid=1&sid=B2BD73BC58A081488FD4B3D9076A5704.borex-tc&sch=M&id=12275,1,1164753](https://md.boschrexroth.com/modules/BRMV2PDFDownload-internet.dll/re92004_2012-06.pdf?db=brmv2&lvid=1164753&mvid=12275&clid=1&sid=B2BD73BC58A081488FD4B3D9076A5704.borex-tc&sch=M&id=12275,1,1164753). [accessed 24 August 2016].
- [60] Eaton Corporation, "ETAC: Electronic Transmission Automotive Control User's Manual," Eaton Corporation, Eden Prairie, USA, 2007.
- [61] Bosch Rexroth, "Application software BODAS-drive DRC," August 2017. [Online]. Available: [https://md.boschrexroth.com/modules/BRMV2PDFDownload-internet.dll/re95323\\_2017-08.pdf?db=brmv2&lvid=1202620&mvid=13186&clid=20&sid=362AD729D0095F2BCC65CAA1C64B7DB.borex-tc&sch=M&id=13186,20,1202620](https://md.boschrexroth.com/modules/BRMV2PDFDownload-internet.dll/re95323_2017-08.pdf?db=brmv2&lvid=1202620&mvid=13186&clid=20&sid=362AD729D0095F2BCC65CAA1C64B7DB.borex-tc&sch=M&id=13186,20,1202620). [accessed 6 February 2018].
- [62] Danfoss, "Danfoss Best Point Control - Greater efficiency through intelligent engine speed control," 2015. [Online]. Available: [http://files.danfoss.com/documents/Best point control Brochure en-US.pdf](http://files.danfoss.com/documents/Best%20point%20control%20Brochure%20en-US.pdf). [accessed 29 November 2017].
- [63] M. Scheider, O. Koch, J. Weber, M. Bach and G. Jacobs, "Green Wheel Loader – Development of an energy efficient drive and control system," *9th International Fluid Power Conference, 9. IFK*, 24-26 March 2014. Aachen, Germany., 2014.
- [64] M. Kache, "Investigating an all-hydraulic hybrid system diesel-hydraulic rail cars," *European Transport Research Review*, vol. 6, no. 2, pp. 181-189, 2014.
- [65] S. Agarwal, M. Olson, T. Meehan and N. Wadwankar, "Fuel Economy Comparison Studies of Forklift Transmission Architecture," *SAE Commercial Vehicle Engineering Congress, COMVEC 2015*, 6-8 October, 2015. Rosemont, USA., 2015.
- [66] C.-K. Chen, T.-V. Vu and C.-W. Hung, "Control Strategy Development and Optimization for a Series Hydraulic Hybrid Vehicle," *Engineering Letters*, vol. 21, no. 2, pp. 101-107, 2013.
- [67] K. L. Cheong, Z. Du, P. Y. Li and T. R. Chase, "Hierarchical Control Strategy for a Hybrid Hydro-mechanical Transmission (HMT) Power-Train," *2014 American Control Conference, ACC 2014*. Portland, Oregon., 2014.
- [68] J.-C. Ossyra and M. Ivantysynova, "Drive Line Control for Off-Road Vehicles Helps to Save Fuel," *SAE Commercial Vehicle Engineering Congress and Exhibition, COMVEC 2004*, October 26-28, 2004. Chicago, IL, USA, 2004.
- [69] W. Wu, J. Hu, C. Jing, Z. Jiang and S. Yuan, "Investigation of energy efficient hydraulic hybrid propulsion system for automobiles," *Energy*, vol. 73, pp. 497-505, 2014.
- [70] D. Opila, X. Wang, R. McGee and J. Grizzle, "Real-time implementation and hardware testing of a hybrid vehicle energy management controller based on stochastic dynamic programming," *Journal of Dynamic Systems, Measurement and Control*, vol. 135, no. 2, 2013.



- [71] R. Hippalgaonkar and M. Ivantysynova, "Optimal Power Management for Hydraulic Hybrid Mobile Machines - Part II: Machine Implementation and Measurement," *Journal of Dynamic Systems, Measurement, and Control*, vol. 138, p. 051003, 2016.
- [72] N. Daher and M. Ivantysynova, "Energy analysis of an original steering technology that saves fuel and boosts efficiency," *Energy Conversion and Management*, vol. 86, pp. 1059-1068, 2014.
- [73] M. Sprengel, T. Bleazard, H. Haria and M. Ivantysynova, "Implementation of a novel hydraulic hybrid powertrain in a sports utility vehicle," *4th IFAC Workshop on Engine and Powertrain Control, Simulation and Modeling, E-COSM 2015*, August 23-26, 2015. Rueil-Malmaison, Columbus, United States, 2015.
- [74] D. Padovani and M. Ivantysynova, "Investigation of an Energy Efficient Hydraulic Propulsion System for a Railway Machine," *Journal of Dynamic Systems, Measurement, and Control*, vol. 138, p. 031009, 2016.
- [75] V. Nezhadali, B. Frank and L. Eriksson, "Wheel loader operation—Optimal control compared to real drive experience," *Control Engineering Practice*, vol. 48, pp. 1-9, 2016.
- [76] J. Backas, M. Ahopelto, M. Huova, A. Vuohijoki, O. Karhu, R. Ghabcheloo and K. Huhtala, "IHA-machine: A Future Mobile Machine," *The Proceedings of the Twelfth Scandinavian International Conference on Fluid Power*, Tampere, May 18-20, 2011.
- [77] R. Filla, "Representative Testing of Emissions and Fuel Consumption of Working Machines in Reality and Simulation," *SAE Technical Paper 2012-01-1946*, p. 9, 2012.
- [78] G. Stein, A. Fröberg, J. Martinsson, B. Brattberg, R. Filla and J. Unneback, "Fuel efficiency in construction equipment – optimize the machine as one system," *AVL International Commercial Powertrain Conference*, May 22, 2013.
- [79] Japan Construction Mechanization Association, "Earth-moving machinery - Fuel consumption on hydraulic excavator - Test procedures," *JCMA Standard H 020*, 2007.
- [80] Japan Construction Mechanization Association, "Earth-moving machinery – Fuel consumption on wheel loader - Test procedures," *JCMAS standard H 022*, 2007.
- [81] B. Frank, L. Skogh, R. Filla and M. Alaküla, "On increasing fuel efficiency by operator assistant systems in a wheel loader," *The 2012 International Conference on Advanced Technologies and Integration (VTI 2012)*, 16-19 July 2012. Changchun, China, 2012.
- [82] United States Environmental Protection Agency, "EPA Nonregulatory Nono.ad Duty Cycles," 1 August 1999. [Online]. Available: <https://www.epa.gov/moves/epa-nonregulatory-nono.ad-duty-cycles>. [accessed 17 January 2018].
- [83] C. Williamson and M. Ivantysynova, "The Effect of Pump Efficiency on Displacement-controlled Actuator Systems," *The Tenth Scandinavian International Conference on Fluid Power*, May 21-23, 2007. Tampere, Finland., 2007.
- [84] H. H. Triet and K. K. Ahn, "Comparison and assessment of a hydraulic energy-saving system for hydrostatic drives," *Proceedings of the Institution of Mechanical Engineers, Part I: Journal of Systems and Control Engineering*, vol. 225, pp. 21-34, 2011.
- [85] C. A. Williamson, "Power Management for Multi-Actuator Mobile Machines with Displacement Controlled Hydraulic Actuators," Ph.D. dissertation, West Lafayette, IN: Purdue University, 2010.

- [86] G. Paganelli, G. Ercole, A. Brahma, Y. Guezennec and G. Rizzoni, "General supervisory control policy for the energy optimization of charge-sustaining hybrid electric vehicles," *JSAE Review*, vol. 22, no. 4, pp. 511-518, 2001.
- [87] M. Ahopelto, J. Backas, R. Ghabcheloo and K. Huhtala, "Improved Energy Efficiency and Controllability of Mobile Work Machines by Reduced Engine Rotational Speed," *Proceedings of the ASME 2013 International Mechanical Engineering Congress & Exposition, IMECE2013*, San Diego, California, USA, 2013.
- [88] Y. Wang, H. Zhang and Z. Sun, "Optimal control of the transient emissions and the fuel efficiency of a diesel hybrid electric vehicle," *Proc IMechE Part D: J Automobile Engineering*, vol. 227, no. 11, pp. 1546-1561, 2013.
- [89] R. Hippalgaonkar and M. Ivantysynova, "Optimal Power Management for Hydraulic Hybrid Mobile Machines - part I: Theoretical studies, modeling and simulation," *Journal of Dynamic Systems, Measurement, and Control*, vol. 138, pp. 051002-23, 2016.
- [90] T. Krogerus, M. Hyvönen, J. Backas and K. Huhtala, "Anomaly Detection and Diagnostics of a Wheel Loader Using Dynamic Mathematical Model and Joint Probability Distributions," *Proceedings of the 14th Scandinavian International Conference on Fluid Power*, Tampere, Finland, 2015.
- [91] Xingjian, W., Siru, L., Shaoping, W., Zhaomin, H. and Chao, Z., "Remaining useful life prediction based on the Wiener process for an aviation axial piston pump," *Chinese Journal of Aeronautics*, vol. 29, no. 3, pp. 779-788, 2016
- [92] M. Huova, M. Karvonen, V. Ahola, M. Linjama and M. Vilenius, "Energy Efficient Control of Multiactuator Digital Hydraulic Mobile Machine," *7th International Fluid Power Conference, 7. IFK*, Aachen, Germany, 2010.
- [93] AVL, "AVL product description KMA Mobile," 29 May 2009. [Online]. Available: [https://www.avl.com/c/document\\_library/get\\_file?uuid=168caf92-827a-44ab-9dd2-33281cb4eb3d&groupId=10138&download](https://www.avl.com/c/document_library/get_file?uuid=168caf92-827a-44ab-9dd2-33281cb4eb3d&groupId=10138&download). [accessed 22 January 2018].

## **Publication P.I**

Backas, J., Ghabcheloo, R., Hyvönen, M. & Huhtala, K. 2014. Fuel Optimal Controller for Hydrostatic Drives – A Simulation Study and Model Validation. Proceedings of the Bath/ASME 2014 Symposium on Fluid Power & Motion Control, FPMC2014. September 10-12, 2014, Bath, United Kingdom.

© ASME. Reprinted with permission.

**FPMC2014-7808**

**FUEL OPTIMAL CONTROLLER FOR HYDROSTATIC DRIVES – A SIMULATION  
 STUDY AND MODEL VALIDATION**

**Joni Backas**

Tampere University of Technology,  
 Department of Intelligent Hydraulics and Automation  
 Tampere, Finland

**Reza Ghabcheloo**

Tampere University of Technology,  
 Department of Intelligent Hydraulics and Automation  
 Tampere, Finland

**Mika Hyvönen**

Tampere University of Technology,  
 Department of Intelligent Hydraulics and Automation  
 Tampere, Finland

**Kalevi Huhtala**

Tampere University of Technology,  
 Department of Intelligent Hydraulics and Automation  
 Tampere, Finland

**ABSTRACT**

This paper presents an optimal controller for fuel efficiency of a hydraulic mobile machine with hydrostatic drive (HSD). The solution is validated using a semi-empirical simulated research platform. The drive transmission of the machine includes one variable displacement hydraulic pump and four two-speed hub motors. There is no energy storage installed. Thus, the structure of the HSD and presented improvements in fuel economy are comparable to traditional machines.

The optimal controller is compared to a baseline controller that intuitively keeps the components at their high efficiency regions. In simulated hill tests, fuel economy was improved by up to 25.9 % depending on the slope of the hill and velocity reference.

**NOMENCLATURE**

|          |  |
|----------|--|
| BSFC     | Brake specific fuel consumption                |
| F        | Force  |
| K        | Gain   |
| P        | Power  |
| Q        | Volumetric flow                                |
| <b>Q</b> | Vector of state variable cost coefficients     |
| <b>R</b> | Vector of reference variable cost coefficients |
| T        | Torque (estimated)                             |
| V        | Geometric displacement                         |
| d        | Diameter                                       |
| n        | Rotational speed                               |

|                      |                               |
|----------------------|-------------------------------|
| $\dot{m}$            | Mass flow                     |
| v                    | Velocity                      |
| $\Delta p$           | Pressure difference           |
| $\Delta n$           | Control error of engine speed |
| $\varepsilon$        | Relative displacement         |
| $\eta$               | Efficiency                    |
| ( ) <sub>L</sub>     | Load                          |
| ( ) <sub>LL</sub>    | Load limited                  |
| ( ) <sub>FF</sub>    | Feedforward                   |
| ( ) <sub>aux</sub>   | Auxiliary                     |
| ( ) <sub>cur</sub>   | Current                       |
| ( ) <sub>droop</sub> | Droop percent                 |
| ( ) <sub>e</sub>     | Engine                        |
| ( ) <sub>est</sub>   | Estimated                     |
| ( ) <sub>ext</sub>   | External                      |
| ( ) <sub>f</sub>     | Fuel                          |
| ( ) <sub>hm</sub>    | Hydromechanical               |
| ( ) <sub>m</sub>     | Motor (hydraulic)             |
| ( ) <sub>mach</sub>  | Machine                       |
| ( ) <sub>max</sub>   | Maximum                       |
| ( ) <sub>p</sub>     | Pump                          |
| ( ) <sub>ref</sub>   | Reference                     |
| ( ) <sub>req</sub>   | Required                      |
| ( ) <sub>t</sub>     | Tyre                          |
| ( ) <sub>vol</sub>   | Volumetric                    |

## INTRODUCTION

Energy management is one of the most researched topics of fluid power community at both academia and industry. Mobile work machines consume large amount of energy, their energy efficiency is generally low, and their emissions produce significant burden on the environment. The ever increasing limitation on emissions set by legislation requires better fuel economy in the future [1]. This is particularly important for fluid power because of high energy losses of hydraulic systems compared to their electric alternatives.

Improved system efficiency does not necessarily require new components and systems. As shown in this paper, considerable fuel savings can be achieved by improved control strategy of electronically controlled actuators.

However, currently majority of the machines operating in public roads and fields are not driven-by-wire, mostly for safety regulation and price. In addition, machine building industry is traditionally seen as very rigid and sceptical towards new technologies. For improved fuel economy, operating points of the controllable components of the power transmission must be adjusted according to load and velocity. But because the loading conditions of these machines constantly change, it is not possible for the driver to operate the machine optimally without the assistance of computer. This requires a drive-by-wire machine.

Even though there are semi-autonomous machines with computerized control systems in closed areas such as mines [2] and harbours [3], one can argue that there is a huge gap between academic research platforms and commercial machines. For example, a lot of academic research has been conducted by controlling hydraulic systems with novel system layouts [4] or installing energy storage components [5]. These are usually done with novel control methods ranging from rule-based [6] to optimization approaches [5]. In addition, demand-adapting [7] and minimized [8] engine speed control has been studied. In on-road vehicles, the fuel optimal control of continuously variable transmissions (CVT) has been active for a long time [9] and this type of powertrains are becoming more common also in off-road machines [10].

In this paper, the improvements of fuel economy are based on optimal control methods, where the operating points of the diesel engine, variable displacement pump and hydraulic motors are calculated based on velocity reference, demanded load and efficiency curves. Moreover, the components of the research platform (a 3.5-ton wheel loader) are commercially available and there are no energy storage components in the hydrostatic drive (HSD). Therefore, the results are also applicable to the current machines that are equipped by such components that are controlled over CAN bus and they do not require changes in their mechanical design. The improved fuel economy shows that drive-by-wire components have more to offer than just reduced number of hoses and more user-friendly interfaces.

The proof of concept developed in this paper is validated using a real-time simulator that includes empirically validated models of hydraulic components and diesel engine, machine mechanics and tyre-terrain interaction (improved version of

[11]). Optimal control strategies developed in this paper are also implemented in real time environment, so the real machine experiments will be done with minimum effort. Only the input/output (I/O) interface of the model has to be changed when implemented to the research platform. This will increase reliability of the implementation, since most of the software bugs can be solved during simulation, and also prevent human mistakes in translating the control algorithms to a different software environment.

A baseline controller was developed and used as a reference. In the baseline controller, the operating points of the actuators are selected only based on velocity reference. It is devised based on the facts that the pump and motors have higher efficiency at higher displacement.

We will show that it is possible to achieve fuel consumption reduction up to 25 % when optimal controller is compared to this baseline controller. The controllability and performance of the system is also preserved. Simulation tests clearly show that especially at low velocities the improvements of fuel economy are high. In the simulations, it was observed that the main factor that reduces fuel consumption is the active control of the rotational speed of diesel engine.

Next section presents the modelled research platform and related equations. This is followed by sections covering the optimal controller and the validation of the real-time simulator. The last part of the paper presents the results of hill climbing simulations with the two controllers.

## SYSTEM DESCRIPTION

### Research Platform Machine

The research platform, called IHA-machine, is engineered at the Department of Intelligent Hydraulics and Automation (IHA) in Tampere University of Technology (TUT). The machine is presented in Fig. 1.



Figure 1. Research platform (IHA-machine).

The HSD of IHA-machine includes variable displacement closed circuit hydraulic pump ( $110 \text{ cm}^3$ ) and four hub motors connected to each wheel. A simplified hydraulic diagram is presented in Fig. 2. Required power for the systems of the machine is produced with a 100-kW diesel engine. Lift and tilt functions are implemented with digital hydraulics [12]. This paper will concentrate on the optimization of prime mover and HSD, and digital hydraulics is out of the scope of this paper. For more detailed description of the systems of the machine, an interested reader is referred to [13].

The displacement of the hydraulic motors can only be changed between two discrete states (470/282 cm<sup>3</sup>). When the pressure of boost pump is connected to the port X of the motors (see Fig. 2), the displacement is reduced to 60 % of the maximum. In theory, this reduces both maximum torque and required volumetric flow by 40 % (see Eq. (3) and (2)).

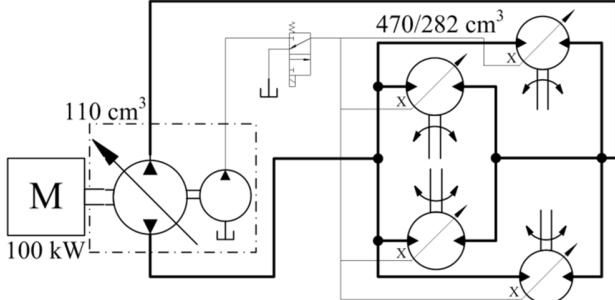


Figure 2. Hydraulic diagram of hydrostatic drive.

### Mathematical Models

The steady-state models of the machine required for control design are presented in this section. Fig. 3 illustrates interactions among the components of HSD.

The control signals of the system are relative displacements of the HSD pump ( $\epsilon_{p,ref}$ ) and those of the motors ( $\epsilon_{m,ref}$ ) together with the rotational speed of the engine ( $n_{e,ref}$ ). The loading conditions of the machine are defined by external forces ( $F_{ext}$ ). These include all resistive forces such as frictions, air resistance etc., which eventually define the torque of HSD pump ( $T_p$ ) exerted on the engine. Pressure differences of the HSD pump and that of the motors are assumed equal ( $\Delta p$ ) i.e. the pressure loss of hoses is assumed insignificant.

The volumetric flow of the HSD pump ( $Q_p$ ) and the speed of the machine ( $v_{mach}$ ) are calculated with Eq. (1) and (2), respectively. In deriving Eq. (2), the fact that the rotational speeds of the hydraulic motors ( $n_m$ ) are directly proportional to  $Q_p$  was used, and thus is also the velocity of the machine. It is also assumed that  $Q_p$  is evenly distributed between the hub motors in every situation.

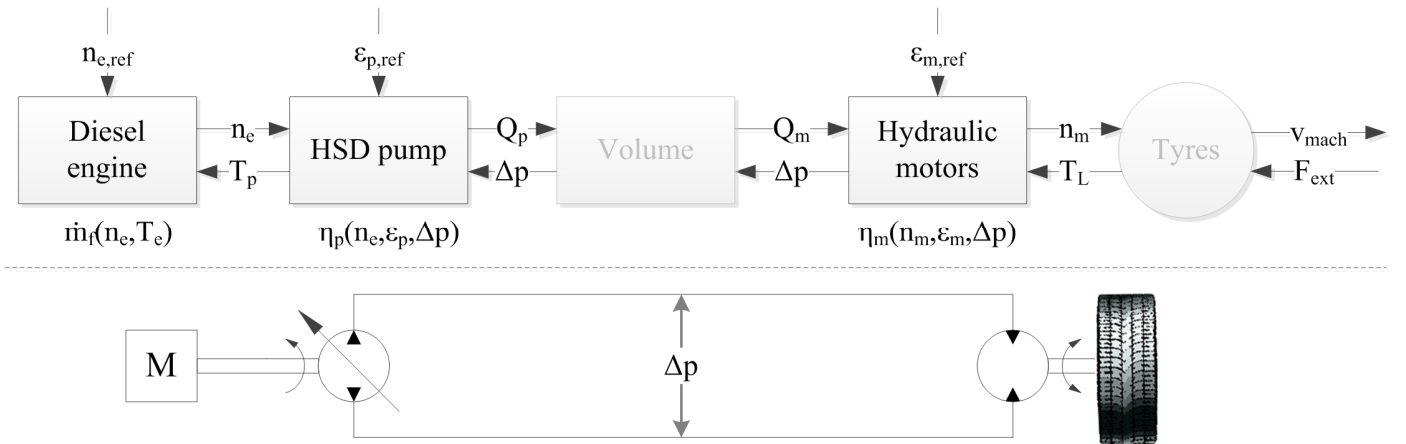


Figure 3. Connections of the components of hydrostatic drive.

$$Q_p = \epsilon_p V_p n_e \eta_{vol,p} \quad (1)$$

$$v_{mach} = \pi d_t n_m = \pi d_t \frac{Q_p \eta_{vol,m}}{4 \epsilon_m V_m} \quad (2)$$

$$= \pi d_t \frac{n_e \epsilon_p V_p \eta_{vol,p}}{4 \epsilon_m V_m} \eta_{vol,m}$$

where

- $\epsilon_{p/m}$  is the relative displacement of HSD pump/motor [-]
- $V_{p/m}$  is the displacement of HSD pump/motor [m<sup>3</sup>]
- $n_e$  is the rotational speed of the engine [1/s]
- $\eta_{vol,p/m}$  is the volumetric efficiency of HSD pump/motor [-]
- $d_t$  is the diameter of the tyre [m]
- $n_m$  is the rotational speed of the motor [1/s]

In steady-state conditions, the torque of hydraulic motors ( $T_m$ ) is equal to loading torque ( $T_L$ ) as in Eq. (3).

$$T_m \stackrel{v=0}{\cong} T_L \Leftrightarrow \epsilon_m \frac{V_{g,m}}{2\pi} \Delta p \eta_{hm,m} = F_{ext} \frac{d_t}{2} \quad (3)$$

where

- $\eta_{hm,m}$  is the hydromechanical efficiency of HSD motors [-]
- $\Delta p$  is the pressure difference of HSD pump (and motors)

Based on Eq. (3), the HSD pump has to provide high enough  $\Delta p$  in order to keep the machine moving in all loading conditions. For this, the pump requires torque ( $T_p$ ) from the engine. This can be calculated with Eq. (4).

$$T_p = \epsilon_p \frac{V_p}{2\pi} \frac{\Delta p}{\eta_{hm,p}} \quad (4)$$

where

- $\eta_{hm,p}$  is the hydromechanical efficiency of HSD pump [-]

In addition, a constant amount of torque is reserved for auxiliary devices ( $T_{aux}$ ) such as the boost pump, battery charger etc. The engine has to generate enough torque ( $T_e$ ) for all the considered systems; this is the sum of the torques of individual systems and is here calculated with Eq. (5).

$$T_e = T_p + T_{aux} \quad (5)$$

The efficiency of diesel engines is commonly described with brake specific fuel consumption (BSFC) that defines the amount of fuel required for a unit of energy ( $[BSFC_e] = \text{g/kWh}$ ) at different rotational speeds and torques. Observing the BSFC-maps of engines, one can conclude that in most situations BSFC-values are lower at higher torques. However, the mass flow of consumed fuel ( $[\dot{m}_f] = \text{g/h}$ ) increases together with the output power of the engine ( $P_e$ ) as shown in Eq. (6).

$$\begin{aligned} \dot{m}_f &= BSFC_e P_e = BSFC_e T_e * 2\pi n_e \\ &= BSFC_e (T_p + T_{aux}) * 2\pi n_e \end{aligned} \quad (6)$$

### OPTIMAL CONTROLLER

The optimal controller will generate a combination of control signals (rotational speed of the engine ( $n_{e,ref}$ ), the displacement of HSD pump ( $\varepsilon_{p,ref}$ ) and the displacement of HSD motors ( $\varepsilon_{m,ref}$ )), to minimize fuel consumption, and track the desired velocity, while keeping the controllability.

Maximum available torque of a diesel engine is a function of rotational speed and reaches to a maximum in the middle of the operation region. Optimal solution will generate operating profiles for the diesel engine that may fall at the rising part of the torque curve of the engine. In this region, the engine generates less torque for lower speed, thus the speed will drop even more and eventually stall, if the load of the engine is not reduced accordingly. In order to address this issue, firstly the power of HSD has to be estimated based on a model of the machine and the efficiencies of components in different loading conditions. Obviously, the optimization is as accurate as the accuracy of the models allows.

### Structure of Controller

Optimal controller employs a cost function. In this cost function, to be described in detail below, penalized variables are consumed fuel for travelled distance ( $[\text{g/m}]$ ), estimated velocity error, and the changes of control references. Operational space of the reference values is discretized to improve calculation efficiency and match the CAN interface resolution. They are chosen from following sets:

- $n_{e,ref} \in \{1000, 1010, \dots, 2200\} \text{ r/min}$
- $\varepsilon_{p,ref} \in \{0, 0.01, \dots, 1\}$
- $\varepsilon_{m,ref} \in \{0.6, 1\}$

The block diagram of the main parts of the controller is presented in Fig. 4. The inputs of the controller are velocity reference ( $v_{ref}$ ),  $\Delta p$ ,  $\varepsilon_p$ ,  $\varepsilon_m$  and  $n_e$ . At first, the loading condition is estimated. Based on that it is possible to estimate machine velocities and required engine torques with every control combination (with the discretization choices above  $121 \times 101 \times 2$  combinations in total). Finally, control combination that results in minimum cost (see Eq. (10)) is transmitted to actuators. Obviously, optimization is as accurate as the accuracy of the models allows. The cycle time of the optimization (Fig. 4, blocks 1 – 5) is 50 ms. In the next few sections, each block is presented in detail.

### Load Estimation

This section describes Fig. 4, block 1. The required  $T_m$  (see Eq. (3)) is estimated based on  $\Delta p$ . This is expressed in Eq. (7).

$$\begin{aligned} T_{m,cur} = T_{m,req} &\Leftrightarrow \Delta p_{req} = \frac{T_{m,cur}}{\eta_{hm,m,req} \varepsilon_{m,req}} \\ &= \frac{\Delta p \eta_{hm,m,cur}(n_m, \varepsilon_{m,cur}, \Delta p) \varepsilon_{m,cur}}{\eta_{hm,m,req}(n_m, \varepsilon_{m,req}, \frac{\varepsilon_{m,cur}}{\varepsilon_{m,req}} \Delta p) \varepsilon_{m,req}} \end{aligned} \quad (7)$$

where

- $T_{m,cur}$  is the torque generated by hydraulic motors with current pressure difference and displacement [Nm]
- $n_{m,ref}$  is the rotational speed of hydraulic motor with the velocity reference of the machine [r/s]
- $\varepsilon_{m,cur}$  is the current displacement setting of hydraulic motor [-]
- $\varepsilon_{m,req}$  is the alternative displacement setting of hydraulic motor [-]

Here measured values of pressure signals  $\Delta p$  are used. To reduce high frequency components of  $\Delta p$ , a modified version of the filter engineered by Luomaranta [14] is used. With Eq. (7), the hydromechanical efficiency of HSD motors is included in the model as a function of rotational speed, displacement and

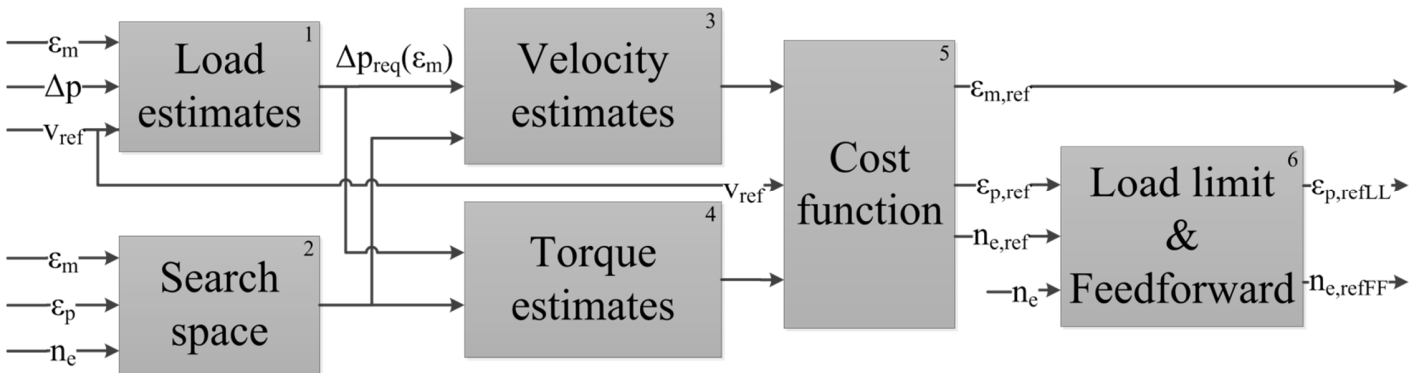


Figure 4. Structure of the optimal controller.

pressure difference. Notice that only pressures related to the current motor displacement are available. Therefore, when calculating this efficiency for alternative displacement, it is assumed that pressure difference is directly proportional to the change of  $\varepsilon_m$ , that is,  $\frac{\varepsilon_{m,cur}}{\varepsilon_{m,req}}\Delta p$ .

### Steady-state Velocity and Torque Estimates

The controller is based on the Eq. (1) – (6) and the steady-state models (based on measurements) of the components. The required pressure difference for all the displacement settings of HSD motors can be estimated with Eq. (7). Therefore, it is possible to calculate the velocity of the machine and the required output torque of engine for every control combination. This section describes how these calculations are made in the controller.

**Machine Velocity Estimates** This section describes Fig. 4, block 3. Eq. (2) determines the velocity of the machine as a function of the volumetric efficiency of HSD pump and motors. This is restated in Eq. (8).

$$v_{est} = \pi d_t \frac{V_p}{V_m} \frac{n_e \varepsilon_p}{\varepsilon_m} \eta_{vol,p}(n_e, \varepsilon_p) \eta_{vol,m}(n_m, \varepsilon_m) \quad (8)$$

To reduce computational costs, tabulated velocity estimates ( $v_{est}$ ) are used instead of calculating them again for every execution cycle. As seen from Eq. (8), effect of  $\Delta p$  on volumetric efficiency is not considered even though pressure is known to have a strong effect on the leakages. Otherwise, when  $\Delta p$  increases so would do the leakages, which had to be compensated by increasing  $Q_p$ . This would raise pressure even more and cause oscillations that also decrease the fuel economy of the machine. This implementation was chosen to reduce oscillations during the acceleration of the machine. However, it increases velocity reference tracking error.

**Engine Output Torque Estimates** This section describes Fig. 4, block 4. Required  $T_e$  for every control combination is calculated with Eq. (4) and (5). The final estimate value ( $T_{e,est}$ ) is determined with Eq. (9).

$$T_{e,est} = \begin{cases} \infty & , T_{e,est} > T_{e,max}(n_{e,ref}) \\ \varepsilon_p \frac{V_{g,p}}{2\pi} \frac{\Delta p}{\eta_{hm,p}(n_{e,ref}, \varepsilon_{p,ref}, \Delta p)} + T_{aux} & , otherwise \end{cases} \quad (9)$$

Eq. (9) is used only if a certain control combination is feasible i.e. the maximum torque curve of the engine ( $T_{e,max}(n_e)$ ) is not exceeded. For unfeasible combination, the required torque is set to infinity, which results in infinite cost.

Exceeding the maximum torque curve should especially be avoided when  $n_e$  is below the speed of maximum torque (usually in the middle of its operation region). In this rising part of the torque curve, high load can easily stall the engine. This originates from the basic operation of diesel engines, because their rotational speed decreases when load increases. If the engine operates at this region, it can generate less torque for

lower speed, thus the speed will drop even more. Eventually, this results in the stall of the engine, if the load is not reduced accordingly.

### Cost Function

After all the relevant steady-state values of the machine are estimated, the control combination that results in the lowest value of Eq. (10) is selected as the output of the optimal controller (see Fig. 4, block 5). Penalized variables are consumed fuel for travelled distance ([g/m]), estimated velocity error and the changes of control references. Vectors  $\mathbf{Q}$  and  $\mathbf{R}$  contain cost coefficients for state and reference variables, respectively.

$$J(t) = \mathbf{Q} \begin{bmatrix} \frac{\dot{m}_f(t)}{v_{est}(t)} \\ |v_{ref}(t) - v_{est}(t)| \end{bmatrix} + \mathbf{R} \begin{bmatrix} \sum_{i=1}^3 |\varepsilon_{m,ref}(t) - \varepsilon_{m,ref}(t-i)| \\ \sum_{i=1}^3 |\varepsilon_{p,ref}(t) - \varepsilon_{p,ref}(t-i)| \\ \sum_{i=1}^3 |n_{e,ref}(t) - n_{e,ref}(t-i)| \end{bmatrix} \quad (10)$$

Consumption for travelled distance is penalized, because the controller optimizes the cost for one sample interval at a time. Therefore, the optimization has to be power type, instead of energy. This makes the cost independent of time.

Penalties for the changes of control references are placed for the last 3 intervals to avoid frequent changes. This reduces e.g. pressure variations and the wear of the actuators as the changing frequency is lower. In addition, experiments show that this also improves fuel economy. This might originate from the fact that every time the  $n_e$  is increased, some amount of energy cannot be recuperated back from rotational energy.

### Search Space

This section describes Fig. 4, block 2. This block enables the reduction of computational effort by reducing the number of investigated control combinations. The size of this search space can be freely defined in advance and separately for  $n_{e,ref}$ ,  $\varepsilon_{p,ref}$  and  $\varepsilon_{m,ref}$ . This facilitates successful real-time implementation. A graphical illustration is presented in Fig. 5.

The following choices have been made. If the search space does not cover all the possible control combinations, evaluated combinations depend on the current operation point. The number of feasible reference values above and below the measured value of a control variable is independent, but their sum is always constant. For example, if  $\varepsilon_p$  is at maximum, the number of feasible references below the measured value is increased correspondingly.



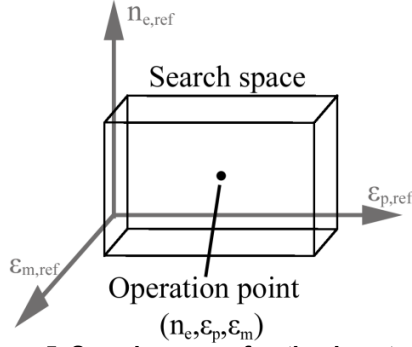


Figure 5. Search space of optimal controller.

Another purpose of the search space is to limit the maximum rate of change of the control variables for one evaluation cycle of the controller. This influences in the functionality of the machine in a similar way as the costs of the reference changes in Eq. (10). In practice, a control combination outside the search space is made unfeasible by setting corresponding  $T_{e,est}$  to infinity similar to the case where maximum torque value is exceeded as in Eq. (9).

#### Additional Parts of the Controller for Improved Functionality

Because the optimal controller utilizes only the steady-state model of the machine, some additional strategies are implemented to improve functionality (see Fig. 4). Firstly, engine droop is compensated by increasing the  $n_{e,ref}$  according to the estimated load. Secondly, the load of the engine is limited by limiting the changing rate of  $\varepsilon_{p,ref}$ . Both are evaluated every time the inputs of the controller are acquired, i.e. at 5 ms cycle. The faster cycle time (compared to optimization) enables more rapid reactions for the changes of load. See Fig. 4, block 6.

**Feedforward to Compensate Engine Droop** The electronic control units (ECU) of diesel engines have closed loop control for rotational speed. However, usually a certain amount of error is allowed. This is called engine droop and it is proportional to the load of the engine. Droop dampens the response and stabilizes the engine controller.

When the optimal control combination is determined based on the machine model, rotational speed reference (i.e. the optimal point) cannot be reached without compensating the engine droop. This is done with a feedforward compensator that implements Eq. (11).

$$n_{e,refFF} = \left( 1 + K_{droop} \frac{T_{e,est}}{T_{e,max}(n_{e,ref})} \right) n_{e,ref} \quad (11)$$

where

$K_{droop}$  is the maximum droop value of engine ECU [%]

The compensator increases  $n_{e,ref}$  based on estimated load torque ( $T_e$ ) and the droop parameter of engine ECU. As a result, the compensated reference ( $n_{e,refFF}$ ) should decrease the error between the measured  $n_e$  and the optimal reference  $n_{e,ref}$ .

**Faster Load Limiting** The optimal controller is only valid for quasi-static situations, because of the models used.

The bandwidth of the controller is also limited by low-pass filtering of measured  $\Delta p$ . To address dynamic situations, e.g. when the machine is driven to a hill or accelerated rapidly, the maximum displacement of the HSD pump is limited to restrict load on the engine. Otherwise, fast load increase might stall the engine. Equation (12) describes how this is done.

$$\varepsilon_{p,refLL} = \begin{cases} \varepsilon_{p,ref} & , n_{e,ref} - n_e \leq K_{droop} n_{e,ref} \\ \min \left( \frac{\min(n_{e,ref} - n_e, \Delta n_{e,max})}{\Delta n_{e,max}}, \varepsilon_{p,ref} \right) & , otherwise \end{cases} \quad (12)$$

where

$\Delta n_{e,max}$  is the upper limit for the error of rotational speed [r/min]

The limiter is not active if the rotational speed error can be explained by engine droop ( $n_{e,ref} - n_e > K_{droop} n_{e,ref}$ ). Otherwise,  $\varepsilon_{p,ref}$  is limited directly proportional to the error. Additionally, this feature facilitates accelerating the rotational speed of the engine more rapidly, because of increased available torque and the engine operating in regions with better dynamic characteristics.

## REAL-TIME SIMULATOR OF THE RESEARCH PLATFORM

### Fuel Consumption of Diesel Engine

The steady-state characteristics of HSD are described with Eq. (1) - (6). Almost all of them include at least one term related to the efficiency of a hydraulic component or the brake specific fuel consumption of diesel engine. All of these are measured in steady-state conditions and the data covers operating regions comprehensively. The efficiencies of HSD pump were measured at the laboratory of IHA, but the BSFC of the diesel engine and efficiencies of hydraulic motors were provided by their manufacturers.

Both the optimal controller and the simulation model of the machine use the same data. However, due to divergent model types there can be minor differences. For example, the brake specific fuel consumption map is converted into a table that outputs torque as a function of rotational speed and injection rate of the engine.

In the simulation model, the volumetric and hydromechanical efficiencies of HSD pump and motors are modelled as leakages and frictions, respectively. On the other hand, in the optimal controller the hydraulic losses are included as efficiencies. Therefore, it is evident that differences exist, even though both the models are fitted to the measured data.

### Dynamic Models

The diesel engine of the research platform has common rail injection system. Because of this, the dynamics of fuel injection are modelled with very fast 1<sup>st</sup> order system and a PID-controller. The more significant part of the engine dynamics originate from torque generation. This is also a first order system that is scaled according to the rotational speed of the

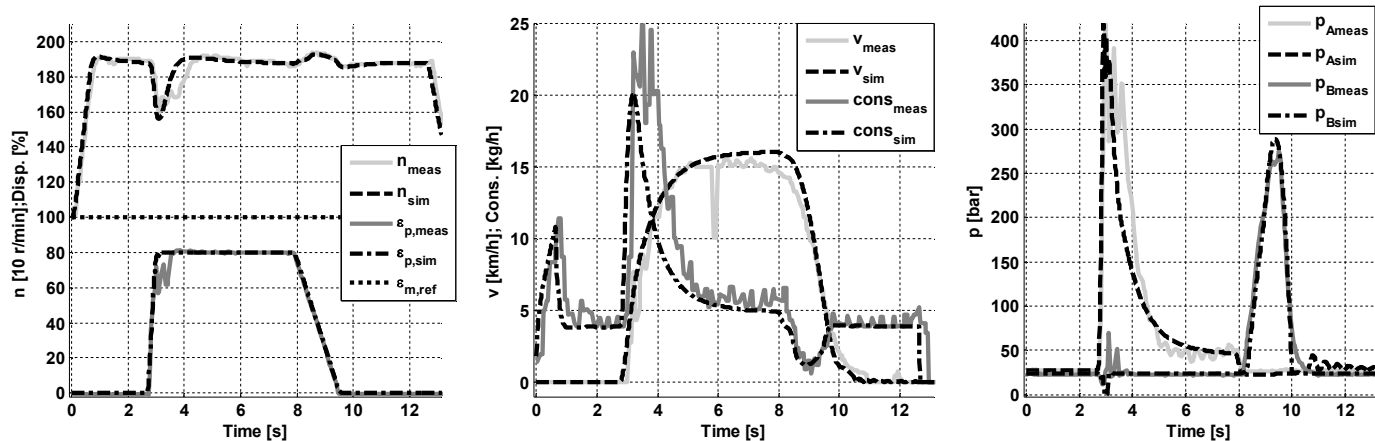


Figure 6. Comparison of measured and simulated data.

engine. However, not all the features of the engine ECU are included. The dynamics of the engine is validated with separate measurement data. Detailed description of the structure of the engine model is presented in [15].

The dynamics of the displacement of the HSD pump are modelled with first order transfer function and rate limiter. Transfer function is different for increasing and decreasing displacement. This model is also validated based on separate step and ramp response measurements.

Parameters of the HSD motors are based on the manufacturer's catalogue and provided measurement data. The dynamics of the displacement change of all four HSD motors is validated using the measurement data of the entire machine, because there is no direct measurement available related to this. The dynamic models of additional components, e.g. pressure relief and flush valve, are modelled based on the catalogue data of their manufacturers.

### Validation of the Simulation Model

The simulation model was validated with the data measured from the CAN-buses of the machine. The conducted measurements included several (50) acceleration/deceleration tests with different steady-state velocities. In some tests, the displacement of hydraulic motors was also changed on the fly.

While validating the simulation model, it was noticed that the hydrostatic drive was not as stiff during deceleration as assumed. It was evident that there was a leakage that was not similar for both ports of the HSD pump. After jamming the simulated flush valve to a position where all the flushed flow comes from the A-port side of the pump, both the shapes and levels of simulated pressures started to correspond to the measured values. However, in the conducted controller comparison simulations, the flush valve is operating normally.

Fig. 6 presents an example of validation measurement where the engine is operating at 1900 r/min and the reference of the pump is changed stepwise from 0 to 80 %. Motors are at full displacement. The measurements were not made on a completely flat surface and actually there is a mild uphill after the beginning of the acceleration. However, there is no slope in the simulated terrain. This is also true for Fig. 7.

It can be seen from the Fig. 6 that simulation model data corresponds well to measured data. However, there is a difference between the real machine and simulation model in how the displacement of the pump ( $\epsilon_p$ ) is changing at time around 3 seconds. This might originate from the controller of the pump that reduces the reference of  $\epsilon_p$  (to prevent cavitation) when the lower pressure decreases below some pre-determined value. This can occur if the boost pump is not able to produce

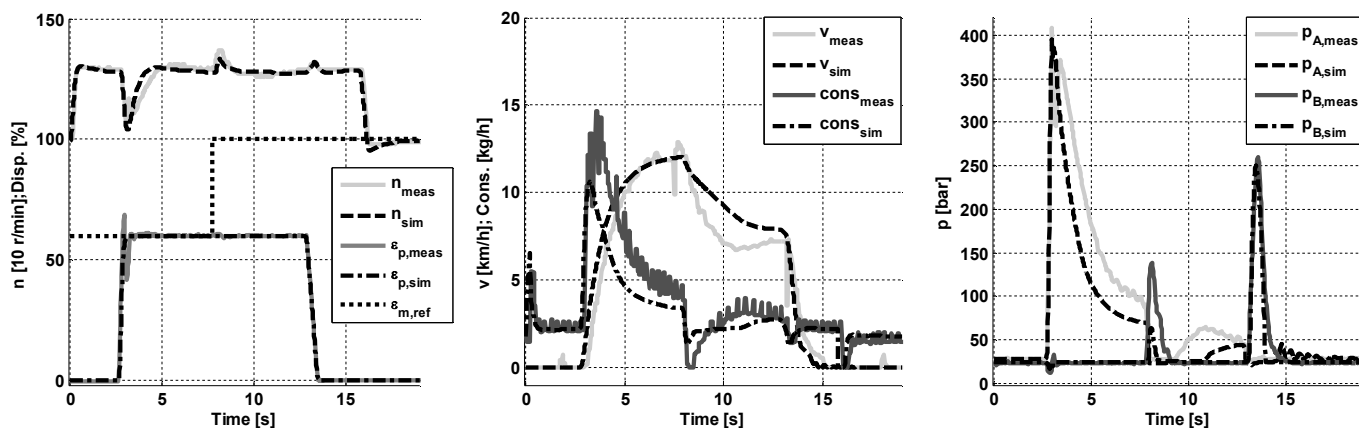


Figure 7. Comparison of measured and simulated data during  $\epsilon_{m,ref}$  increase.

enough flow to the lower pressure side volume. This phenomenon is not included in the pump model.

It was also noticed that the model of the diesel engine seems to generate torque a bit differently than the real engine, especially at lower rotational speeds with high loads. It is possible that there are some parameters in the engine ECU that are not considered in the simulation model, for example related to the stall prevention of the engine.

Fig. 7 presents a test where the displacements of the motors are increased during driving. The most significant issue is related to the pressures. The pressure level of the model is too low at steady-state situations with reduced displacement of the motors. This has a direct effect on the consumption values. However, when the displacement is increased, the model is more accurate. The error between measured and modelled pressures at reduced displacement is most likely related to the friction and leakage flow models of the HSD motors which were tuned based on manufacturer data.

However, the validation clearly shows that the phenomena are modelled correctly, which is seen from the corresponding shapes of the curves. Validation results of the other operation points were similar to the ones discussed above i.e. the only significant difference was found in the steady-state pressures at reduced  $\epsilon_m$ .

We utilize the model to compare the fuel consumption and functionality of the machine with different controllers. In this kind of model to model comparison (cp. not model to machine), the shapes of the curves are more important than precisely accurate absolute values. Therefore, it can be concluded that the simulation model is applicable for comparative tests of control algorithms. After all, any simulation model that assumes e.g. constant temperature represents a mobile work machine in only one situation. Analysing the robustness of the optimal controller has to be done separately.

## SIMULATION RESULTS

### Baseline Controller

The operation of the machine with optimal controller is compared to a non-optimal controller. The functionality of this baseline controller is presented by illustrating the control references in Fig. 8.

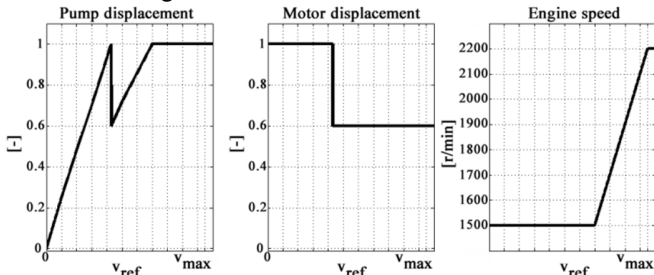


Figure 8. Control references of the baseline controller.

As seen in Fig. 8, control references are generated based only on velocity reference. There are three main stages in the controller. In the first stage,  $\epsilon_{p,ref}$  is increased with  $v_{ref}$ ,  $\epsilon_{m,ref}$  is

held at maximum and  $n_{e,ref}$  in pre-defined minimum value. At the beginning of second stage,  $\epsilon_{m,ref}$  are reduced stepwise to 0.6. In order to maintain the same velocity,  $\epsilon_{p,ref}$  has to change accordingly (see Eq. (8)). With higher velocity references  $\epsilon_{p,ref}$  is again directly proportional to  $v_{ref}$ . In the last stage, only  $n_{e,ref}$  increases linearly with  $v_{ref}$  ( $\epsilon_{p,ref} = 1$  and  $\epsilon_{m,ref} = 0.6$ ). The parameters of the baseline controller were tuned for the velocity to match the reference in steady-state conditions. Intuitively, this strategy will keep the pump, the motors and the engine in their high efficiency regions. It will be clear from the consumption figures in the next section that using the baseline controller the consumption closely follows that of the optimal controller in most of the situations.

### Comparison of the Controllers

The fuel consumptions of optimal and baseline controllers are compared in a drive cycle which includes a hill. The simulated hill is presented in Fig. 9. In the tests, the starting point of the machine is 65 m from the hill. From this point it accelerates to a reference velocity and climbs the hill. At the top of hill, the reference is changed to a lower value and machine drives downhill. When the machine has returned to the level ground, the velocity reference is set to 0 m/s. The tests are conducted with hills of different height ( $h$ ) and the slopes at both side of the hill are kept the same. Used velocity references and hill heights are presented in Table 1.

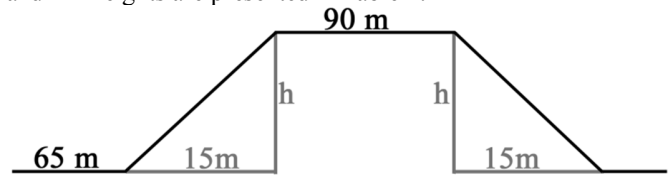


Figure 9. Hill of controller comparison tests  $h = \{1,2,3,4\}$ .

Fig. 10 presents control variables, velocities and fuel consumptions of a test with 2-m hill and velocity reference changing from 4.3 to 2.5 m/s. All the variables are presented as a function of travelled distance instead of time. This choice was made to ease the comparison between the controllers, because now the changes occur at the same point of the horizontal axis. Recall that the penalized variable in the cost function of the optimal controller was consumption per travelled distance. Therefore, the total amount of consumed fuel is the area under consumption curves.

As seen from Fig. 10, the optimal controller accelerates the machine at the beginning with full motor displacement. The rotational speed of the engine is also increased from the minimum value. Shortly after this, both of these are reduced in order to reduce the fuel consumption.

The velocity of the machine does not reach the reference exactly. This originates both from the difference between the model of the controller and simulator, but also from the fact that e.g. consumption is considered at the cost function. The parameters of the baseline controller were tuned to generate velocities that match the reference values in steady-state conditions. There is not closed-loop velocity control.

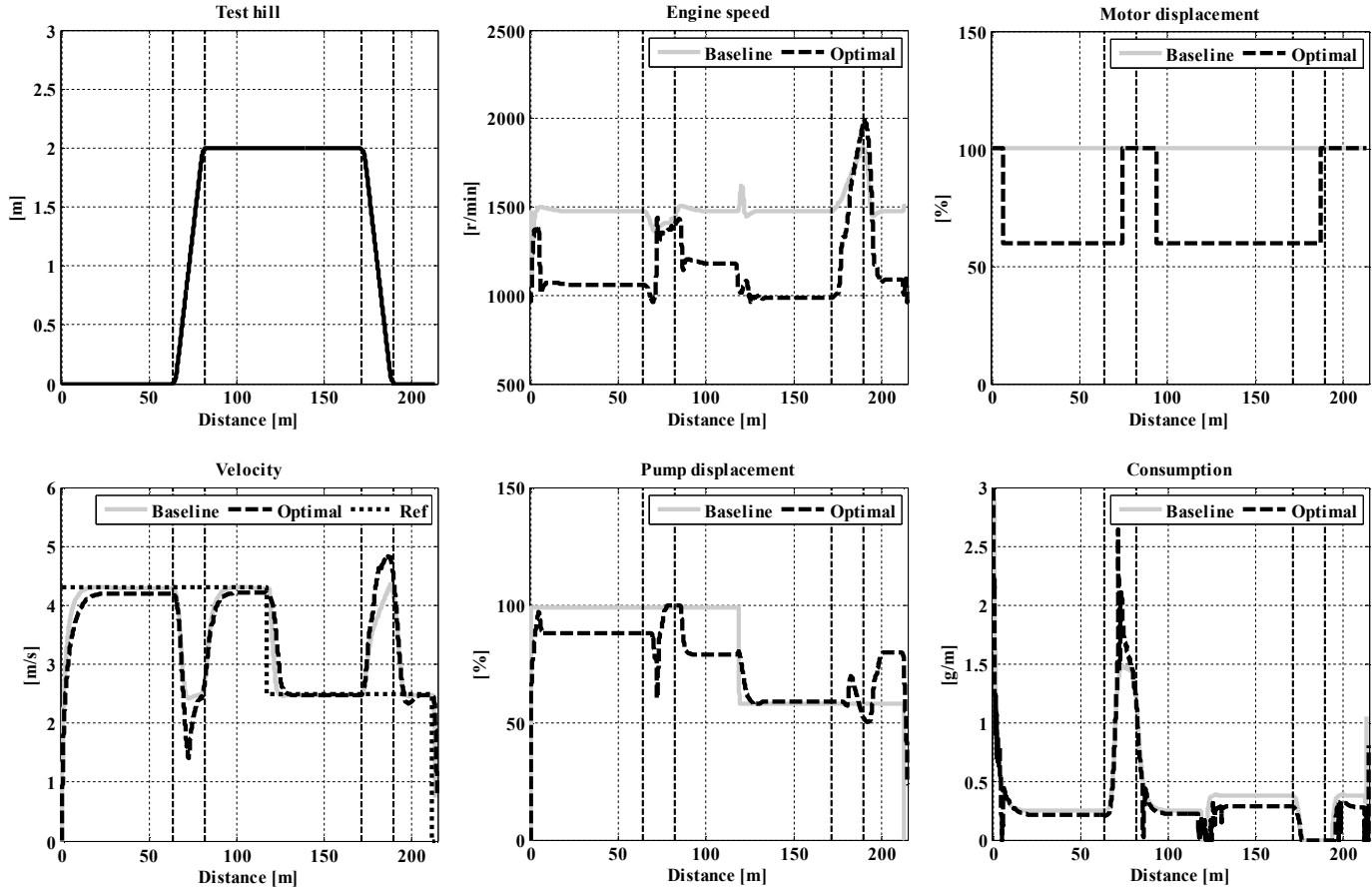


Figure 10. Test with 2-m hill and velocity reference 4.3 - 2.5 m/s.

When the uphill starts (at distance = 65 m), the  $\Delta p$  increases and due to this rapid load peak, the rotational speed of the engine begins to drop. At this point, all the references of the optimal controller are increased, which places a heavy burden to the engine. To prevent stalling the engine, for short time,  $\varepsilon_p$  is reduced with the load limiting function (see Eq. (12)). For this reason, at this point the consumption with the optimal controller is higher than that with the baseline controller. At the hill top, all the control variables are decreased again. Large velocity error originates from the fact that  $\Delta p$  is not considered in the velocity estimate of the optimal controller (see Eq. (8)).

When the velocity reference is reduced at distance 117m, the  $\varepsilon_p$  and  $n_c$  are decreased further down by the optimal controller. At this part, the consumption difference of the controllers increases, because the baseline controller does not reduce the displacement of the hydraulic motors. The required additional flow is produced with higher  $n_c$  as the displacements of the pump are almost the same. At the downhill, velocities increase rapidly, because there is neither closed-loop velocity control nor a mode for negative  $\Delta p$  in the optimal controller.

Table 1 summarizes all the conducted simulations with different hill heights and velocity references. Fig. 11 presents

the integrated fuel consumptions of all the simulations with both controllers. The optimal controller is able to reduce the fuel consumption in every test where comparison is possible. In some tests, the baseline controller operated machine could not complete the task. This was due to the lack of load limiting functions that resulted in the stall of the engine. These tests are labelled as dnf (did not finish). The amount of consumed fuel increases together with the height of the hill. Also lower velocities have similar effect, because longer time is required to complete the same task when the machine is moving slower. Only exception is the test with  $h = 4$  m and  $v_{ref} = 4.3 \rightarrow 2.5$  m/s, in which the engine almost stalls even with the optimal controller. This results in higher total fuel consumption.

Based on Table 1 (and Fig. 11), it can be stated that the relative amount of saved fuel ( $\Delta cons.$  [%]) increases as the velocity and the loading of the machine (hill height) decrease.

This is due to the fact that with higher velocities and loads the rotational speed of the engine has to be increased. In these situations, the optimal controller needs to accelerate the engine to meet the required volumetric flow or power demand, while the baseline controller is already close to the optimal points.

Table 1. Simulation results of hill tests with the two controllers.

| Hill tests |                     | Optimal controller |              |             |                    | Baseline controller |              |             |
|------------|---------------------|--------------------|--------------|-------------|--------------------|---------------------|--------------|-------------|
| h [m]      | Velocity ref. [m/s] | mf                 | Distance [m] | Cons. [g/m] | $\Delta$ cons. [%] | mf                  | Distance [m] | Cons. [g/m] |
|            |                     | [g]                |              |             |                    | [g]                 |              |             |
| 4          | 3 → 1.5             | 141.23             | 213.99       | 0.66        | -15.4              | 165.85              | 212.69       | 0.78        |
|            | 4.3 → 2.5           | 148.2              | 216.23       | 0.69        | NA                 | dnf                 | dnf          | dnf         |
|            | 7.5 → 4             | 113.57             | 218.65       | 0.52        | NA                 | dnf                 | dnf          | dnf         |
|            | 9 → 6               | 108.74             | 228.08       | 0.48        | NA                 | dnf                 | dnf          | dnf         |
| 3          | 3 → 1.5             | 98.91              | 214.01       | 0.46        | -19.4              | 121.93              | 212.7        | 0.57        |
|            | 4.3 → 2.5           | 83.45              | 215.09       | 0.39        | -7.6               | 89.68               | 213.52       | 0.42        |
|            | 7.5 → 4             | 79.83              | 218.32       | 0.37        | NA                 | dnf                 | dnf          | dnf         |
|            | 9 → 6               | 76.56              | 224.86       | 0.34        | -5                 | 79.61               | 222.19       | 0.36        |
| 2          | 3 → 1.5             | 82.24              | 213.95       | 0.38        | -23.9              | 107.41              | 212.69       | 0.51        |
|            | 4.3 → 2.5           | 69.55              | 215.05       | 0.32        | -13                | 79.37               | 213.53       | 0.37        |
|            | 7.5 → 4             | 64.81              | 217.51       | 0.3         | -7.6               | 69.4                | 215.21       | 0.32        |
|            | 9 → 6               | 65.03              | 223.29       | 0.29        | -7.9               | 69.38               | 219.44       | 0.32        |
| 1          | 3 → 1.5             | 73.21              | 214.08       | 0.34        | -25.9              | 98.16               | 212.69       | 0.46        |
|            | 4.3 → 2.5           | 59.14              | 214.86       | 0.28        | -18.7              | 72.33               | 213.54       | 0.34        |
|            | 7.5 → 4             | 57.13              | 217.54       | 0.26        | -10.7              | 63.32               | 215.21       | 0.29        |
|            | 9 → 6               | 59.04              | 222.28       | 0.27        | -9.5               | 64.22               | 218.89       | 0.29        |

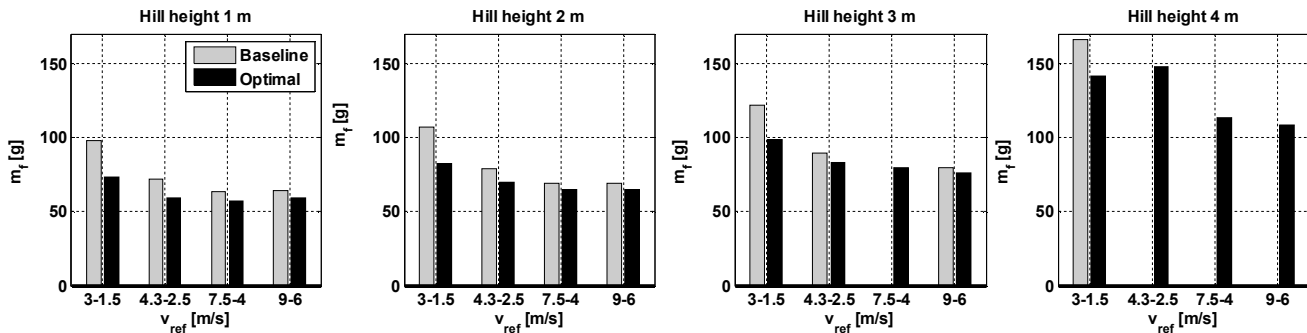


Figure 11. Consumed fuels of Table 1.

## SUMMARY AND CONCLUSION

In this paper, an optimal fuel control strategy was presented for hydrostatic drive systems and efficacy of the controller was evaluated on a wheel loader in simulated hill tests. The controller was compared to a baseline controller that keeps the components of HSD at their high efficiency regions. The simulations were conducted with a semi-empirical real-time simulator. Some results were also presented to verify both static and dynamic behaviour of the simulated machine and the environment compared to the real machine scenario.

The optimal control output is determined with a cost function which is only evaluated at pre-determined number of combinations around the current operating point by considering available calculation power.

The results show the potential of presented control strategy, as the amount of consumed fuel per travelled distance was up to 25.9 % lower with the optimal controller. Moreover, the

addition of the load limiting function improved the applicability of the optimal controller in real scenarios.

Control calculations were based on the steady-state values, both for efficiency curves of the hydraulic components and brake specific fuel consumption curves of the engine. Thus, the optimality of this strategy can only be ensured for steady-state situations. However, to address dynamic situations, addition of costs was proposed on control signal variations and employment of load limiting functions. Simulations proved the concept. The final assessment of success can only be done with a real machine. These tests are going to be conducted during summer 2014.

## REFERENCES

- [1] Langer, T. and Khan, S., 2013, "International Alignment of Fuel Efficiency Standards for Heavy-

- Duty Vehicles”, The International Council on Clean Transportation, ICCT, 2013.
- [2] Bills, K. and Cherrington, M., 2013, ”The mining factory”, *Solid Ground*, 1/2013.
- [3] Freundlich, T., 2013, ”Straddling the world”, *Kalmar Global*, 1/2013.
- [4] Zimmermann, J. and Ivantysynova, M., “Effect of Installed Hydraulic Corner Power on The Energy Consumption and Performance of Multi-Actuator Displacement Controlled Mobile Machines,” *Proceedings of the ASME 2009 Dynamic Systems and Control Conference, DSCC2009*, Hollywood, California, USA, 2009.
- [5] Kumar, R. and Ivantysynova, M., 2011, ”An Instantaneous Optimization Based Power Management Strategy to Reduce Fuel Consumption in Hydraulic Hybrids”, *International Journal of Fluid Power*, (12)2, pp. 15 – 25.
- [6] Jaewoong, C., Hakgu, K., Seungjin, Y. and Kyongsu, Y., 2011, ”Development of integrated controller for a compound hybrid excavator”, *Journal of Mechanical Science and Technology*, (25)6, pp. 1557-1563.
- [7] Jähne, H., Kohmäscher, T., Deiters, H. and Bliesener, M. “Drive Line Simulation for Increased Energy-Efficiency of Off-Highway-Machines,” *6<sup>th</sup> International Fluid Power Conference, 6. IFK*, Dresden, Germany, 2008.
- [8] Ahopelto, M., Backas, J. and Huhtala, K. , 2012, “Power management in a mobile work machine: reduced diesel rpm for better energy efficiency”, *7<sup>th</sup> FPNI PhD Symposium on Fluid Power*, Reggio Emilia, Italy.
- [9] Pfiffner, R., Guzzella, L. and Onder, C.H., 2003, “Fuel-optimal control of CVT powertrains”, *Control Engineering Practice*, (11)3, pp. 329-336.
- [10] Aitzetmüller, H., “Hydrostatic- mechanical power split transmission for locomotives”, *International Conference on Gears*, Munich, Germany, 2010.
- [11] Hyvönen M., Vilenius J., Vuohijoki A., and Huhtala K., 2006, “Mathematical Model of the Valve Controlled Skid Steered Mobile Machine”, *2<sup>nd</sup> International Conference on Computational Methods in Fluid Power*, August 2006, Aalborg, Denmark
- [12] Huova, M., Karvonen, M., Ahola, V., Linjama, M. and Vilenius, M., 2010, ”Energy Efficient Control of Multiactuator Digital Hydraulic Mobile Machine”, *7<sup>th</sup> International Fluid Power Conference, 7. IFK*, Aachen, Germany.
- [13] Backas, J., Ahopelto, M., Huova, M., Vuohijoki, A., Karhu, O., Ghabcheloo, R. & Huhtala, K., 2011, ”IHA-machine: A Future Mobile Machine”, *The Proceedings of the Twelfth Scandinavian International Conference on Fluid Power*, Tampere, May 18-20.
- [14] Luomaranta, M., 1999, ”A Stable Electrohydraulic Load Sensing System Based on a Microcontroller”, *The Proceedings of the Sixth Scandinavian International Conference on Fluid Power*, Tampere, May 26-28, 1999.
- [15] Erkkilä, M., 2007, “Dynamic Model of CVT Power Train”, *The Proceedings of the Tenth Scandinavian International Conference on Fluid Power*, Tampere, Finland, May 21-23, 2007.

## **Publication P.II**

Backas, J., Ghabcheloo, R., Tikkanen, S. & Huhtala, K. 2016. Fuel Optimal Controller for Hydrostatic Drives and Real-World Experiments on a Wheel Loader. *International Journal of Fluid Power*, 17 (3). DOI: 10.1080/14399776.2016.1202081. pp. 187-201.

© Taylor and Francis. Reprinted with permission.

The color print of this publication is available online (DOI: 10.1080/14399776.2016.1202081)

# Fuel optimal controller for hydrostatic drives and real-world experiments on a wheel loader

Joni Backas , Reza Ghabcheloo , Seppo Tikkanen  and Kalevi Huhtala 

Department of Intelligent Hydraulics and Automation, Tampere University of Technology, Tampere, Finland

## ABSTRACT

In this study, we design a fuel optimal controller for hydrostatic drive transmissions (HSD) that significantly improves their fuel economy. Contrary to great proportion of the literature, efficacy of the controller is demonstrated by real machine implementation equipped with online fuel consumption measurement system. The main control objective of the devised controller is to minimise consumed fuel per travelled distance. Control commands are determined utilizing steady-state equations of the system, which facilitates real-time implementation. Dynamic situations are addressed with auxiliary functions running at higher frequency than the fuel economy part of the controller. The machine is a 5-ton wheel loader with pure HSD and no energy storage devices installed. In addition, all the components are commercially available. Thus, structure of the HSD and presented improvements in fuel economy are comparable to commercial machines and retrofitting existing drive-by-wire machinery with proposed controller will require little cost. The optimal controller is compared to a rule-based alternative that is based on a control method utilized in commercial wheel loaders. In autonomously driven drive cycles, measured total fuel consumption reduced up to 16.6% with the devised controller. In addition, the functionality of the controller is proven in extreme hill climbing tests.

## ARTICLE HISTORY

Received 25 January 2016  
Accepted 13 June 2016

## KEYWORDS

Fuel economy; power management; energy efficiency; power transmission; non-road mobile machinery

## 1. Introduction

Invariably decreasing oil resources and the growing number of machines operated by fossil fuels increase the demand for energy efficient solutions in the different fields of industry and transportation. Investigations in fuel economical technologies for passenger cars have been a very active field of research already for a long time. In 1997, Toyota Prius, the first mass produced hybrid vehicle, was introduced. However, the same statement cannot be made for machines utilized in construction industry, even though their estimated annual fuel consumption in European Union was 18.6 million tons (Arcadis 2010) and their emissions produce a significant burden on the environment. These machines generally use hydraulic power transmissions due to high power density requirement. However, due to utilized system configurations and control methods in commercial machines, hydraulic systems exhibit higher energy losses compared to their electric alternatives.

In recent years, some hydraulic hybrid concept machines have been presented at exhibitions by e.g. John Deere (The Lubrizol Corporation 2013) and Kawasaki (KCMA Corporation 2011), but due to their cost, their widespread use is limited. However, improving the energy efficiency of non-road mobile machines

(NRMM) does not necessarily require additional components or systems such as energy storages. We show in this paper that considerable fuel savings can be achieved by improved control strategy of electronically controlled hydraulic actuators. Thus, mechanical complexity, initial investment and maintenance costs are kept low. Still, the proportion of these drive-by-wire machines in non-road applications is quite low. This is mostly due to the fact that the field is very cost-conscious and the payback time of new systems should be short. We believe the application of fuel optimal strategies presented in this paper will reduce the consumption to a level that the increased price of drive-by-wire machines is justified.

The key factor for higher fuel economy is adjusting the operation points of the control components of the machine according to load and velocity. But because loading conditions constantly change, it is not possible for the driver to operate the machine optimally without the assistance of computer. This requires a drive-by-wire machine and intelligent control strategy.

In automotive industry, electronically controlled actuators have been utilized widely for a long time. Different power management strategies are still actively researched both by the academia and industry. Continuously variable transmissions offer significant improvements of



fuel economy for non-hybrid passenger cars with the cost of increased control complexity (Piffner *et al.* 2003, Srivastava and Haque 2009). During the recent years, especially control of hybrid electric vehicles (HEV) and hydraulic hybrid vehicles (HHV) have been investigated extensively. Power management solutions of HEVs include a number of different methods reviewed e.g. in Sciarretta and Guzzella (2007). Even though HHVs are not as widely researched as HEVs, similar approaches are used in their power management as well. The most utilized strategies, suitable also for real-time implementation, are rule-based (Filipi *et al.* 2004, Kum *et al.* 2011, Hippalgaonkar and Ivantysynova 2012) equivalent consumption minimisation strategy (Paganelli *et al.* 2001, Sciarretta *et al.* 2004, Serrao *et al.* 2011), model predictive control (MPC) (Feng *et al.* 2011, Kermani *et al.* 2011, Deppen *et al.* 2012) and stochastic dynamic programming (SDP) (Meyer *et al.* 2010, Opila *et al.* 2013).

Usually NRMMs have at least partially hydraulic drive transmissions, and there are no commercial hybrid drive transmissions available for them. Nevertheless, there is a growing interest towards improving the inherently low efficiency of fluid power systems and several academic departments are focusing on this kind of machines. Rule-based, MPC and SDP strategies were compared in laboratory experiments for HHV transmission by Deppen *et al.* (2015). They emulated diesel engine with an electric motor, and load with a hydraulic motor both controlled with appropriate simulation models. The improvements of fuel economy were determined with brake specific fuel consumption (BSFC) maps of the modelled engine. Their main conclusion was that no control method can be considered superior in all applications and choosing the most appropriate one has to be made based on assumed system and drive cycle. Kumar and Ivantysynova (2011) used similar test set-up, but their transmission had also mechanical path between the load and the emulated gasoline engine of Toyota Prius. The system was controlled with instantaneous optimisation based algorithm. Also the control of non-hybrid drive transmission has been investigated by Jähne *et al.* (2008). They compared demand-adapting engine speed with two other control concepts in their simulation study. In the research of Ahopelto *et al.* (2013), similar approach was utilized in the field tests of a wheel loader. In addition, the energy efficiency improvements of other subsystems of NRMM have been investigated, e.g. steering by Daher and Ivantysynova (2014), implement hydraulics by Huova *et al.* (2010) and the swing motion of excavator by Caterpillar Inc. (2013).

Despite the numerous published results about novel controllers for HEVs, HHVs and NRMMs, there seems to be a significant gap between simulation studies and reported hardware tests. Even more noteworthy is the lack of research in which the success is evaluated with real fuel consumption instead of e.g. modelled

steady–steady efficiencies. However, some exceptions with measured improvement can be found. Wang *et al.* measured fuel consumption of HEV powertrain in laboratory test bench with similar equipment that is used in this paper (Wang *et al.* 2013). Paganelli *et al.* determined consumed fuel volume and corrected the number with the difference of battery state of charge (Paganelli *et al.* 2001). Williamson weighted external fuel tank (Williamson 2010) and Ahopelto *et al.* presented the fuel consumption data provided by the electronic control unit of the engine (Ahopelto *et al.* 2013).

In this paper, we utilize optimal control methods to define control commands for the components of hydrostatic drive transmission (HSD), namely diesel engine, variable displacement hydraulic pump and hydraulic motors. This optimal control combination is solved on given velocity reference, demanded load and efficiency curves. The algorithm does not utilize information about the complete cycle. Therefore, the results differ from global optima. It is important to note that in our test setup all the components of HSD are commercially available and there are no energy storage components installed. Moreover, the developed algorithm can be executed in commercial programmable logic controllers (PLC) due to its relative simplicity and adjustability. This makes our results applicable to current machines equipped with CAN bus controlled components without any changes in their mechanical design. In this study, we use a 5-ton wheel loader as research platform. The consumed fuel is measured on-line and the collected data proves that drive-by-wire operation has even more to offer than just reduced number of hoses and more user-friendly interfaces.

The empirical tests were conducted in the test area of the Department of Intelligent Hydraulics and Automation (IHA) of Tampere University of Technology (TUT). The area includes both asphalt and gravel surfaces, and slopes up to 20 degrees. Unlike the majority of energy management studies, we present online measured fuel consumption data to show the efficacy of our control strategy. The repeatability of the experiments is guaranteed by generating the references with computers instead of human operators.

For comparison purposes, a rule-based controller was devised. This controller is very similar to the way some machine manufacturers control their HSD systems. In this rule-based control, the engine command is proportional to velocity reference, and hydraulic displacement ratio is varied depending on the measured engine speed. Similar baseline controllers are also utilized in Jähne *et al.* (2008).

We will show that fuel economy can be improved up to 16.6%, when the optimal controller is compared to the rule-based controller. Moreover, the controllability and performance of the system is also preserved. The field tests agree with the simulation results the authors

reported in Backas *et al.* (2014). Based on the test results, we can confidently state that the main factor for reduced fuel consumption is the active control of the rotational speed of diesel engine. This may cause the loss of controllability, which is addressed in this paper.

Next section presents the research platform and related equations. This is followed by sections covering the optimal controller and the control architecture of the machine. The last part of the paper presents the results of empirical tests with the two controllers.

## 2. System description

In this section, we introduce the research platform machine, namely its HSD and the control systems. For more detailed description of the systems of the machine, an interested reader is referred to Backas *et al.* (2011). Moreover, we describe and derive the steady-state equations of translational motion of the machine to be used by the optimal controller.

### 2.1. Research platform machine

The research platform, called IHA-machine, is engineered at the Department of IHA in TUT. The machine is presented in Figure 1.

#### 2.1.1. Hydraulic system

The HSD of the machine is a closed hydraulic circuit. This means that the fluid utilized in the transfer of power is fed back to the pump from the motors, instead of being circulated through a tank. A simplified diagram of HSD is presented in Figure 2.

The prime mover, a 100-kW diesel engine, provides power to a hydraulic pump connected directly to the engine. The pump is variable displacement type, i.e. its output flow (see  $Q_p$  of Figure 2) can be controlled both by its swash plate angle (displacement) and by the speed of the engine shaft  $n_e$ . Moreover, the pump can provide flow in both directions allowing forward and reverse motion. The produced volumetric flow is directed to 4 hydraulic motors connected to each wheel of the machine. The displacement ratios of these hub motors ( $\epsilon_m$ ) can be changed between two discrete settings, full and 50% of



Figure 1. Research platform.

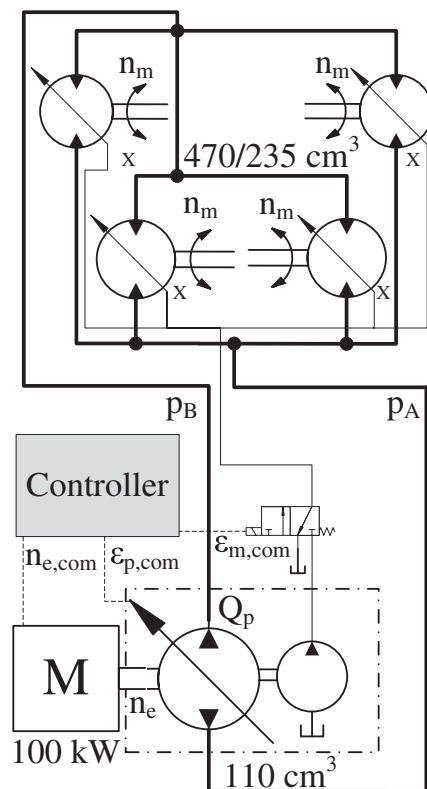


Figure 2. Hydrostatic drive transmission of the research platform machine.

the maximum. This is done by ‘short-circuiting’ feed and return ports of the motors together during half of their piston strokes. With reduced displacement, the velocity of the machine can be approximately doubled only by changing the control command of the motors  $\epsilon_{m,com}$ . However, this will reduce the maximum available output torque the same proportion. The steady-state equations of the system are presented in Section 2.2.2. The maximum displacements of the HSD pump ( $V_p$ ) and motors ( $V_m$ ) are 110 and 470  $\text{cm}^3$ , respectively. Variables  $p_A$  and  $p_B$  are the pressures of volumes  $A$  and  $B$ , respectively.

#### 2.1.2. Control electronics

The devised controller is realised in Matlab Simulink environment and implemented in the research platform with an embedded PC board running xPC target. The low level actuator controllers of the HSD pump and diesel engine are designed by their manufacturer. Both the command of the pump ( $\epsilon_{p,com}$ ) and the engine ( $n_{e,com}$ ) are transmitted via CAN bus to the on-board-electronics of these components that implement the closed loop control of the displacement ratio of HSD pump ( $\epsilon_p$ ) and the rotational speed of engine. The command of HSD motors is amplified with a commercial control unit which operates the control valve of Figure 2.

#### 2.1.3. On-line fuel consumption measurement

In contrast to majority of fuel economy researches, we present measured real-time fuel consumption data. The utilized hardware is a KMA Mobile by AVL. This device

enables measuring fuel flows from 0.16 to 75 l/h also in transient situations, because its rise time (10–90%) is smaller than 125 ms. The flow metre is based on the Pierburg measuring principle, and its measurement uncertainty is 0.1% of reading. (AVL 2009) The acquired data is sent to CAN bus with 20-Hz frequency. Use of the unit increases the accuracy and reliability of data for short tests.

## 2.2. Problem formulation

In this section, we derive the necessary equations for the fuel optimal control of HSD. First, we describe the inputs and outputs of the system. Then utilized cost function is introduced, from which we proceed to the equations that can be evaluated with the measured values of the states of the system.

### 2.2.1. Control objectives

Our control objective in words can be expressed as follows. Given a geometrical path to follow and a reference speed profile,

- (1) Minimise the amount of fuel consumed.
- (2) Minimise the velocity error for given reference trajectory.

The optimal controller attempts to meet these objectives by determining the control combination  $\mathbf{u}$  that minimises a cost function  $J(\mathbf{x}, \mathbf{u})$ , where  $\mathbf{x}$  and  $\mathbf{u}$  are vectors of system states and control signals, respectively. Optimal control combination is referred to as  $\mathbf{u}^*(\mathbf{x})$ . Mathematically stated as

$$\mathbf{u}^*(\mathbf{x}) = \underset{\mathbf{u} \in U}{\operatorname{argmin}} J(\mathbf{x}, \mathbf{u}), \quad (1)$$

subject to  $|\dot{\mathbf{u}}| < \dot{\mathbf{u}}_{\max}$

where  $U$  is a set of all admissible actuator commands and  $\dot{\mathbf{u}}_{\max}$  is a vector that defines the maximum values of the rate of change of the control commands. The values for  $\dot{\mathbf{u}}_{\max}$  can be determined based on actuator dynamics. Absolute and comparison operators in Equation (1) act element wise. The cost function  $J(\mathbf{x}, \mathbf{u})$  consists of components related to fuel economy and estimated velocity

error of the system. Because the controller optimises the cost for one sample interval at a time, the cost has to be power type, instead of energy. Therefore, the first component is the estimated consumption per travelled distance. One sample interval optimisation is also referred as instantaneous optimisation (Paganelli *et al.* 2000). The results obtained with this method will be restricted to local optimality. The costs are evaluated with

$$J(\mathbf{x}, \mathbf{u}) = q_1 \frac{\hat{m}_f(\mathbf{x}, \mathbf{u})}{\hat{v}(\mathbf{x}, \mathbf{u})} + q_2 |v_{\text{ref}} - \hat{v}(\mathbf{x}, \mathbf{u})| \quad (2)$$

where  $q_1$  and  $q_2$  are weighting coefficients,  $v_{\text{ref}}$  is the velocity reference,  $\hat{m}_f(\mathbf{x}, \mathbf{u})$  and  $\hat{v}(\mathbf{x}, \mathbf{u})$  refer to the estimated mass flow of fuel and velocity, respectively. In actual implementation, we will translate actuator constraints  $|\dot{\mathbf{u}}| < \dot{\mathbf{u}}_{\max}$  to penalising  $|u(t) - u(t - i)|$ , for  $i = 1, 2, 3$ .

### 2.2.2. System model

In the previous section, we defined a cost function that requires estimating the fuel consumption and velocity of the machine. In this section, we derive appropriate equations that can be evaluated with measured variables of HSD and show how the cost is calculated. The interactions of the system components are presented in Figure 3. The figure also shows the control commands of the engine  $n_{e,\text{com}}$ , HSD pump  $\varepsilon_{p,\text{com}}$  and motors  $\varepsilon_{m,\text{com}}$ , entering to the diagram from the top. All these 3 inputs have an effect on the velocity of the machine  $v$  (output) (see Equation (5)). The control vector of the research platform is therefore defined by  $\mathbf{u} = \begin{bmatrix} n_{e,\text{com}} & \varepsilon_{p,\text{com}} & \varepsilon_{m,\text{com}} \end{bmatrix}$ .

To overcome the load forces  $F_L$ , the pressure difference  $\Delta p = p_B - p_A$  over the hydraulic motors has to be high enough. The pump provides flow  $Q_p$  that both pressurises the volumes A and B (see Figure 3), and determines the rotational speed of the motors. This eventually defines the torque exerted on the engine (see Equation (4) for  $T_e$ ). In steady-state conditions, i.e.  $\dot{\mathbf{x}} = 0$ , the fuel mass flow of the engine  $\dot{m}_f(\mathbf{x})$  depends on its output power  $P_e(\mathbf{x})$  and efficiency. The latter is commonly described with BSFC, which states how much fuel has to be injected in order to produce a unit of energy. The fuel consumption of engine can be calculated with

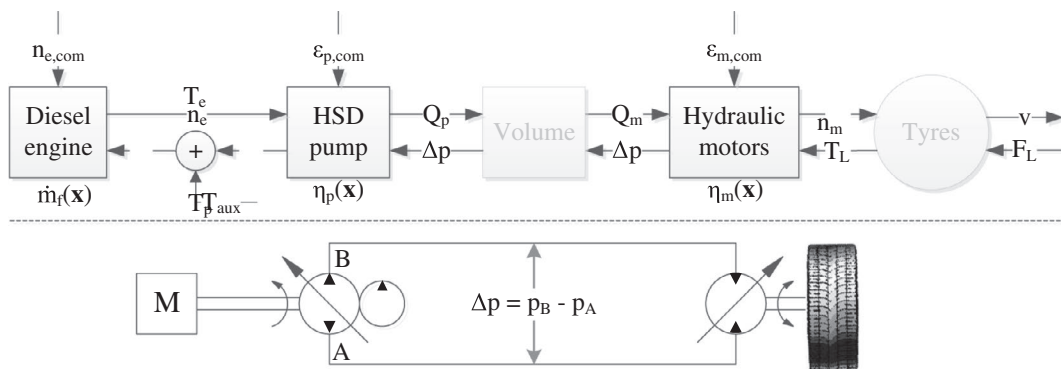


Figure 3. Interactions of HSD components.

$$\begin{aligned} \dot{m}_f(\mathbf{x}) &= P_e(\mathbf{x}) \times BSFC(T_e(\mathbf{x}), n_e) \\ &= 2\pi n_e T_e(\mathbf{x}) \times BSFC(T_e(\mathbf{x}), n_e) \end{aligned} \quad (3)$$

From the variables of Equation (3), rotational speed of the engine is easy and inexpensive to measure. However, measuring the torque  $T_e(\mathbf{x})$  requires sensors not applicable for cost-conscious machine manufactures. Therefore, the required torque has to be calculated with

$$T_e(\mathbf{x}) = T_p(\mathbf{x}) + T_{aux}(\mathbf{x}) = \frac{\varepsilon_p V_p \Delta p}{2\pi \eta_{hm,p}(\mathbf{x})} + T_{aux}(\mathbf{x}), \quad (4)$$

where  $T_p(\mathbf{x})$  and  $T_{aux}(\mathbf{x})$  denote the required torques of HSD pump and auxiliary devices, respectively. Here auxiliary devices include e.g. boost pump (see Figure 2), hydraulic steering pump and charger.  $\Delta p$  is the pressure difference over the HSD pump and motors.  $\eta_{hm,p}(\mathbf{x})$  represents the hydromechanical efficiency of HSD pump. This variable includes mechanical losses such as frictions.

The other variable required in the cost function (Equation (2)) is the velocity of machine  $v(\mathbf{x})$ . For the HSD of the research platform, this can be calculated with

$$\begin{aligned} v(\mathbf{x}) &= \frac{d_t}{2} 2\pi \frac{n_m}{60}(\mathbf{x}) \\ &= \underbrace{d_t \pi V_p \varepsilon_p \frac{n_e}{60} \eta_{vol,p}(\mathbf{x})}_{\text{pump}} \frac{\eta_{vol,m}(\mathbf{x})}{4V_m \varepsilon_m}, \end{aligned} \quad (5)$$

where  $d_t$  is the diameter of the tyre,  $n_m$  is the rotational speed of the motor,  $\eta_{vol,p}(\mathbf{x})$  and  $\eta_{vol,m}(\mathbf{x})$  are volumetric efficiencies of HSD pump and motors, respectively. This efficiency accounts for volumetric losses, for example leakages.

In order to determine the optimal control combination  $\mathbf{u}^*(\mathbf{x})$ , we need to know the loading conditions of the machine. At constant speed, i.e.  $\dot{v} = 0$ , they are defined only by load torque  $T_L = F_L \frac{d_t}{2}$  (see Figure 3), namely frictions, the effect of gravity, air resistance etc. Therefore, as  $\Delta p$  can be measured, we are able to calculate  $T_L$  with

$$m\dot{v} = \frac{T_m - T_L}{\frac{d_t}{2}} \stackrel{\dot{v}=0}{\Rightarrow} T_L = \varepsilon_m \frac{V_m}{2\pi} \Delta p \eta_{hm,m}(\mathbf{x}), \quad (6)$$

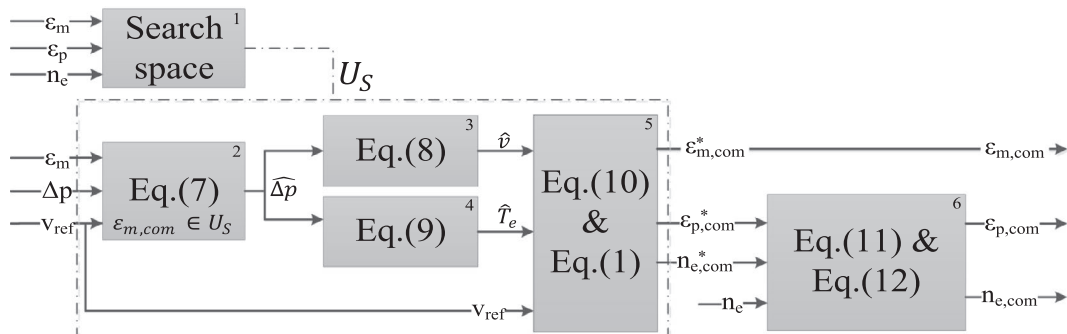


Figure 4. Implementation structure of the optimal controller.

where  $T_m$  and  $\eta_{hm,m}(\mathbf{x})$  are the torque and hydromechanical efficiency of the HSD motors, respectively. The same equation is also used to estimate  $\Delta p$  for the other  $\varepsilon_m$ , having estimated  $T_L$ . Details are presented in Section 3.2.

In this paper, we need the following simplifying assumptions on the system operation:

- Pressure loss and leakage of the hoses are considered insignificant i.e.  $\Delta p_p = \Delta p_m$  and  $Q_p = Q_m$ .
- No slip or slide of the wheels (See Equation (5)).
- Temperature/viscosity is assumed constant, that is, we assume it does not have an effect on hydraulic efficiencies.
- Load torque remains unchanged regardless of  $v_{ref}$  changes for the next control cycle.

### 3. Controller implementation

The purpose of the devised controller is to improve the fuel economy of the HSD, while preserving the controllability of the system and tracking the velocity reference of the operator. This is achieved by selecting the optimal control combination  $\mathbf{u}^*$  based on Equation (1). Recall that  $\mathbf{u}^*$  includes the optimal control commands of the engine  $n_{e,com}^*$ , HSD pump  $\varepsilon_{p,com}^*$  and motors  $\varepsilon_{m,com}^*$ .

The hydraulic efficiencies of HSD pump (see Equations (4) and (5)) are estimated based on steady-state laboratory measurements. The estimates of BSFC of the engine (see Equation (3)) and the efficiencies of HSD motors (see Equations (5) and (6)) are based on the data provided by their manufacturers.

#### 3.1. Structure of controller

Figure 4 presents the block diagram of the main parts of the controller. The inputs of the controller are  $v_{ref}$ ,  $\Delta p$ ,  $n_e$ ,  $\varepsilon_p$  and  $\varepsilon_m$ . For numerical calculation purposes, we discretize the control space. The set of discrete admissible control commands is then called

$U_D, U_D \subset U$ .  $U_D$  is defined by

- $U_e: \{1000, 1010, \dots, 2200\} \text{r/min}$ ,
- $U_p: \{0, 0.01, \dots, 1\}$  and
- $U_m: \{0.5, 1\}$ ,



i.e.

$$U_D = U_e \times U_p \times U_m \\ = \left\{ \left( n_{e,\text{com}}^*, \varepsilon_{p,\text{com}}^*, \varepsilon_{m,\text{com}}^* \right) \mid n_{e,\text{com}}^* \in U_e, \varepsilon_{p,\text{com}}^* \in U_p, \varepsilon_{m,\text{com}}^* \in U_m \right\}.$$

This choice was made to improve calculation efficiency and to match  $U_D$  to the resolution of the CAN interface. However, optimisation search space is reduced to  $U_S$ , a subset of  $U_D$ . Details are defined in Section 3.5. This is depicted in Block 1, Figure 4. These choices enable the implementation of the controller also to control units with significantly lower calculation power e.g. commercial PLCs.

In Block 2, first the loading condition is estimated. In Block 3 and 4, machine velocities and required engine torques for every control combination are calculated (with the discretization choices  $U_D$  includes  $121 \times 101 \times 2 = 24,442$  combinations in total). Finally, in Block 5, the optimal control combination is calculated (see Equation (12)) and transmitted to the actuators. Block 6 is added for controllability, to be detailed in Section 3.6. Obviously, consumption optimisation is as accurate as the accuracy of the models allow. The cycle time of the optimisation  $t_{\text{opt}}$  (Figure 4 blocks 1–5) is 48 ms. In the next few sections, each block is presented in detail.

### 3.2. Load estimation

This section describes Figure 4, block 2. Restating Equation (6) in terms of the systems states, we have  $\hat{T}_L = \frac{V_m}{2\pi} \hat{\eta}_{\text{hm},m}(n_{m,\text{ref}}, \varepsilon_m, \Delta p) \varepsilon_m \Delta p$ . We can see that if the motor displacement remains the same, constant load assumption translates to constant pressure  $\Delta p$ . Thus for forthcoming blocks, we will use  $\Delta p$  to represent the load and all we need to do is to estimate  $\Delta p$  for all feasible motor displacements. However, given  $\varepsilon_m$  solving above equation for  $\Delta p$  is rather complex. We thus approximately solve it based on the observation that for relatively flat efficiency curve (based on measurement data) the pressure change will be proportional to the motor displacement change, that is,  $\varepsilon_m / \varepsilon_{m,\text{com}} \Delta p$  will be used to estimate hydromechanical efficiency of HSD motors  $\hat{\eta}_{\text{hm},m}$ . Putting all together, we can write

$$\hat{\Delta p} = \frac{\hat{T}_L}{\hat{\eta}_{\text{hm},m} \frac{V_m}{2\pi} \varepsilon_{m,\text{com}}} \\ = \frac{\hat{\eta}_{\text{hm},m}(n_{m,\text{ref}}, \varepsilon_m, \Delta p) \varepsilon_m}{\hat{\eta}_{\text{hm},m}(n_{m,\text{ref}}, \varepsilon_{m,\text{com}}, \frac{\varepsilon_m}{\varepsilon_{m,\text{com}}} \Delta p) \varepsilon_{m,\text{com}}} \Delta p, \forall \varepsilon_{m,\text{com}} \in U_S \quad (7)$$

where  $n_{m,\text{ref}} = 60v_{\text{ref}} / (\pi d_t)$ . Notice that estimated pressure difference  $\hat{\Delta p}$  for the current  $\varepsilon_m$  is simply the same as the measured  $\Delta p$ .

In Equation (7),  $\hat{\eta}_{\text{hm},m}$  is estimated based on manufacturer data as a function of rotational speed, motor

displacement and pressure difference. Since we assume that load remains unchanged and perform the calculations in steady-state, it is better to low pass filter  $\Delta p$  before utilization to reduce its high dynamic components. A modified version of the filter engineered by Luomaranta (1999) is utilized for this purpose.

### 3.3. Steady-state velocity and torque estimates

Having calculated the pressure differences for both  $\varepsilon_{m,\text{com}}$  with Equation (7), it is possible to calculate the velocity of the machine and the required output torque of the engine with Equations (5) and (4), respectively. This section describes how these variables are estimated for all 24,442 control combinations.

#### 3.3.1. Machine velocity estimates

This section describes Figure 4, block 3. Equation (5) determines the velocity of the machine as a function of  $\eta_{\text{vol},p}$  and  $\eta_{\text{vol},m}$ . Replacing the coefficients with their estimates in Equation (5), we have

$$\hat{v} = \pi d_t \frac{V_p}{V_m} \frac{n_{e,\text{com}}}{60} \frac{\varepsilon_{p,\text{com}}}{\varepsilon_{m,\text{com}}} \hat{\eta}_{\text{vol},p}(n_{e,\text{com}}, \varepsilon_{p,\text{com}}) \hat{\eta}_{\text{vol},m}(n_{m,\text{ref}}, \varepsilon_{m,\text{com}}) \\ , \forall (n_{e,\text{com}}, \varepsilon_{p,\text{com}}, \varepsilon_{m,\text{com}}) \in U_S \quad (8)$$

To reduce computational costs, tabulated velocity estimates are used instead of calculating them again for every execution cycle. As seen from Equation (8), the effect of  $\Delta p$  on volumetric efficiency is not considered even though pressure is known to have a strong effect on the leakages. Instead,  $\hat{\eta}_{\text{vol}}$  are calculated with a  $\Delta p$  that corresponds a value of steady-state driving with an appropriate  $\varepsilon_{m,\text{com}}$ . If measured pressure values were utilized, increasing  $\Delta p$  would result in increasing leakages (decreasing  $\eta_{\text{vol}}$ ), which would have to be compensated by increasing  $Q_p$ . This would raise pressure even more and cause oscillations that also decrease the fuel economy of the machine. This implementation was chosen to reduce oscillations during the acceleration of the machine. However, it increases velocity reference tracking error.

#### 3.3.2. Engine output torque estimates

This section describes Figure 4, block 4. Required  $T_e$  can be calculated with Equation (4). Final estimate values  $\hat{T}_e$  are determined with

$$\hat{T}_e = \begin{cases} \infty & , \hat{T}_e > T_{e,\text{max}}(n_{e,\text{com}}) \\ \varepsilon_{p,\text{com}} \frac{V_p}{2\pi} \frac{\hat{\Delta p}(\varepsilon_{m,\text{com}})}{\hat{\eta}_{\text{hm},p}(n_{e,\text{com}}, \varepsilon_{p,\text{com}}, \hat{\Delta p}(\varepsilon_{m,\text{com}}))} + T_{\text{aux}} & , \text{otherwise} \end{cases} \quad (9)$$

$$, \forall (n_{e,\text{com}}, \varepsilon_{p,\text{com}}, \varepsilon_{m,\text{com}}) \in U_S$$

$\hat{T}_e$  assumes a bounded value only if a certain control combination is feasible i.e. the maximum torque curve of the engine ( $T_{e,\max}(n_{e,\text{com}})$ ) is not exceeded. For an unfeasible combination, the required torque is set to infinity, which results in infinite cost.  $T_{\text{aux}}$  is considered constant.

Exceeding the maximum torque curve should especially be avoided when  $n_e$  is below the speed of maximum torque (usually in the middle of operation region). In this rising part of the torque curve, high load can easily stall the engine. This originates from the basic operation of diesel engines, because with constant throttle setting their rotational speed decreases when load increases. If the engine operates at this region, it will generate less torque for lower speed, thus the speed will drop even more. Eventually, this results in the stall of the engine, if the load is not reduced accordingly. This will be addressed in Section 3.6.2.

### 3.4. Cost function

In the cost function of Equation (2), the penalised variables included consumed fuel for travelled distance ([g/m]) and estimated velocity error. Equation (3) is utilized in the evaluation of  $\hat{m}_f$ , in which BSFC is estimated based on manufacturer data.

In addition, the initial optimisation problem (see Equation (1)) was constrained with the maximum values of control command derivatives. For the investigated HSD system, this yields  $|\dot{n}_{e,\text{com}}| < \dot{n}_{e,\text{max}}$ ,  $|\dot{\epsilon}_{p,\text{com}}| < \dot{\epsilon}_{p,\text{max}}$  and  $|\dot{\epsilon}_{m,\text{com}}| < \dot{\epsilon}_{m,\text{max}}$ . The hard constraints  $\dot{n}_{e,\text{max}}$ ,  $\dot{\epsilon}_{p,\text{max}}$  and  $\dot{\epsilon}_{m,\text{max}}$  describe the maximum rates of change for the rotational speed of the engine and displacements of HSD pump and motors, respectively.

Approximating the control command derivatives with

$$|\dot{\mathbf{u}}| \approx \left| \frac{\mathbf{u}(t) - \mathbf{u}(t-1)}{t_{\text{opt}}} \right| \quad (10)$$

yields

$$\frac{\dot{\mathbf{u}}}{\dot{\mathbf{u}}_{\text{max}}} \approx \frac{\mathbf{u}(t) - \mathbf{u}(t-1)}{t_{\text{opt}} \dot{\mathbf{u}}_{\text{max}}} = \frac{\mathbf{u}(t) - \mathbf{u}(t-1)}{\Delta \mathbf{u}_{\text{max}}} \quad (11)$$

where  $\Delta \mathbf{u}_{\text{max}}$  is the maximum control command change in one calculation cycle. This can be utilized in implementing the limits as soft constraints. Therefore, limit can be defined also for  $|\dot{\epsilon}_{m,\text{com}}|$  which would not be otherwise applicable for motors with 2 discrete displacement settings. Our implementation defines  $\dot{\epsilon}_{m,\text{max}}$  in terms of maximum switching frequency i.e. we penalise the number of switches made in 3 calculation cycles ( $i_{\text{max}} = 3$  in Equation (12)).

The normalised costs of feasible control combinations are evaluated with

$$\begin{aligned} J(\mathbf{x}(t), \mathbf{u}(t)) = & q_1 \frac{\hat{m}_f(t)/\hat{v}(t)}{(\hat{m}_f/v)_{\text{max}}} + q_2 \frac{|v_{\text{ref}}(t) - \hat{v}(t)|}{\Delta v_{\text{max}}} \\ & + r_1 \sum_{i=1}^{i_{\text{max}}} \frac{|\epsilon_{m,\text{com}}(t) - \epsilon_{m,\text{com}}(t-i)|}{i_{\text{max}} \Delta \epsilon_{m,\text{max}}} \\ & + r_2 \sum_{i=1}^{i_{\text{max}}} \frac{|\epsilon_{p,\text{com}}(t) - \epsilon_{p,\text{com}}(t-i)|}{i_{\text{max}} \Delta \epsilon_{p,\text{max}}} \\ & + r_3 \sum_{i=1}^{i_{\text{max}}} \frac{|n_{e,\text{com}}(t) - n_{e,\text{com}}(t-i)|}{i_{\text{max}} \Delta n_{e,\text{max}}} \end{aligned} \quad (12)$$

$$, \forall (n_{e,\text{com}}, \epsilon_{p,\text{com}}, \epsilon_{m,\text{com}}) \in U_S$$

where  $r_1$ ,  $r_2$  and  $r_3$  are weighting coefficients. In addition,  $(\hat{m}_f/v)_{\text{max}}$  and  $\Delta v_{\text{max}}$  are maximum values for consumption and velocity error, respectively. Maximum values for control command changes (i.e.  $\Delta \epsilon_{m,\text{max}}$ ,  $\Delta \epsilon_{p,\text{max}}$  and  $\Delta n_{e,\text{max}}$ ) are defined with search space (see Section 3.5). This results in normalised cost.

Following values have been chosen for the weighting factors:  $q_1 = 0.65$ ,  $q_2 = 0.31$ ,  $r_1 = 0.0025$ ,  $r_2 = 0.0095$  and  $r_3 = 0.028$ , which sum up to 1. The control combination that results in the lowest cost is selected as the output of the optimal controller  $\mathbf{u}^*$  (see Figure 4, block 5).

Penalising command changes reduces e.g. pressure variations and the wear of the actuators as the changing frequency is lower. Experiments show that fuel economy is also improved. This might originate from the fact that every time  $n_e$  is increased and again decreased some amount of energy cannot be recuperated back from rotational energy.

### 3.5. Search space

This section describes Figure 4, block 1. The block enables the reduction of computational effort by reducing the number of investigated control combinations. This is important especially if the controller is implemented to a control unit with lower calculation power because the costs of all control combinations within the search space are evaluated in every execution.

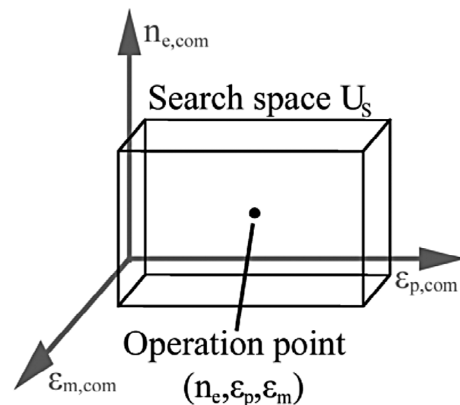


Figure 5. Search space of the optimal controller.

The size of this search space  $U_S$  can be freely defined in advance and separately for  $n_{e,com}$ ,  $\varepsilon_{p,com}$  and  $\varepsilon_{m,com}$ ;  $U_S \subset U_D$ . This facilitates successful real-time implementation. A graphical illustration is presented in Figure 5.

The following choices have been made. If the search space does not cover all the possible control combinations ( $U_S \neq U_D$ ), evaluated combinations depend on current operation point. The number of feasible command values above and below the measured value of a control variable is independent, but their sum is always constant  $\Delta \mathbf{u}_{max}$ . For example, if  $\varepsilon_p$  is at maximum, the number of feasible commands below the measured value is increased correspondingly. This also limits the maximum rate of change of the control variables for one evaluation cycle of the controller. With the appropriate selection of the maximum values of the control command changes, the constraint of Equation (1) can be fulfilled as  $|\dot{\mathbf{u}}| \leq \Delta \mathbf{u}_{max} / \Delta t_c < \dot{\mathbf{u}}_{max}$ .

This has an effect on the functionality of the machine in a similar way as the costs of the command changes in Equation (12). In practice,  $\hat{T}_e(\mathbf{u}) = \infty$ ,  $\mathbf{u} \notin U_S$ , i.e. if a control combination is outside the search space, it is made unfeasible by setting the corresponding torque to infinity. This is similar to the case where maximum torque value is exceeded in Equation (9).

$$\varepsilon_{p,com} = \begin{cases} \varepsilon_{p,com}^* & , n_{e,com}^* - n_e \leq K_{droop} n_{e,com}^* \\ \min\left(\varepsilon_{p,max} - \frac{\min(n_{e,com}^* - n_e, \Delta n_{e,max})}{\Delta n_{e,max}}, \varepsilon_{p,com}^*\right) & , \text{otherwise} \end{cases} \quad (14)$$

### 3.6. Additional parts of the controller for improved functionality

Because the optimal controller utilizes only the steady-state equations of the system, some additional strategies are implemented to improve controllability. Firstly, engine droop is compensated by increasing the  $n_{e,com}^*$ , according to the estimated load. Secondly, the load of the engine is limited by limiting the  $\varepsilon_{p,com}^*$ . Both are evaluated every time the inputs of the controller are acquired, i.e. at 4-ms cycle. The faster cycle time (compared to optimisation) enables more rapid reactions for the changes of load (see Figure 4, block 6).

In addition, the rate of change of  $\varepsilon_{p,com}$  has to be limited during motor displacement change and  $\varepsilon_{m,com}$  is set to 1 in the high loading conditions of HSD. Both of these features reduce the unwanted switching of  $\varepsilon_{m,com}$ , which oscillates also other control commands.

#### 3.6.1. Feedforward to compensate engine droop

The electronic control units of diesel engines have closed loop control for rotational speed. However, usually a certain amount of error is allowed. This is called engine droop and it is proportional to the load of the engine. Droop dampens the response and stabilizes engine controller. For example, with  $n_{e,com} = 1000$  r/min and 5% maximum droop,  $n_{e,com}$  will be 950 r/min in full load

condition. In governor controlled diesel engines, droop is determined with the spring rate of governor.

When  $\mathbf{u}^*$  is determined based on the model of the machine,  $n_{e,com}^*$  (i.e. the optimal point) cannot be reached without compensating engine droop. This is done with a feedforward compensator implemented with

$$n_{e,com} = \left(1 + K_{droop} \frac{\hat{T}_e(\mathbf{u}^*)}{T_{e,max}(n_{e,com}^*)}\right) n_{e,com}^* \quad (13)$$

where  $K_{droop}$  is a parameter that defines maximum droop value ( $[K_{droop}] = \%$ ). The compensator increases  $n_{e,com}^*$  based on estimated load torque ( $\hat{T}_e(\mathbf{u}^*)$ ) and parameter  $K_{droop}$ . As a result, the compensated command  $n_{e,com}$  should decrease the error between the measured  $n_e$  and the optimal command  $n_{e,com}^*$ .

#### 3.6.2. Limiting fast load

The optimal controller is only valid for quasi-static situations, because of the models used. The bandwidth of the controller is also limited by low-pass filtering the measured  $\Delta p$ . To address fast dynamic situations, e.g. when the machine is driven to a hill or accelerated rapidly, the maximum displacement command of the HSD pump is limited to a value  $\varepsilon_{p,com}$  to restrict load on the engine. Otherwise, fast load transient might stall the engine. The displacement of HSD pump is limited with

where  $\varepsilon_{p,com}$  is the command value send to the pump, and  $\varepsilon_{p,max} = 1$  is the maximum displacement of the HSD pump. The condition on the first row is equivalent to maximum allowed engine droop for maximum available torque, see Equation (11). In the second row, that is, when the engine speed error  $n_{e,com}^* - n_e$  is too high, pump displacement is reduced proportional to the engine speed error and a maximum allowed error  $\Delta n_{e,max}$ . Notice that if  $n_{e,com}^* - n_e \geq \Delta n_{e,max}$ , then  $\varepsilon_{p,com} = 0$ . Additionally, this function facilitates accelerating the rotational speed of the engine, because of increased available torque and the engine operating in regions with better dynamic characteristics. Notice that in Equation (14),  $n_{e,com}^*$  is used instead of  $n_{e,com}$  not including the inverse function of Equation (13) when limiting the  $\varepsilon_p$ .

#### 3.6.3. Rate limiter for pump command during motor displacement change

In simulation studies reported in (Backas *et al.* 2014), motor dynamics were not considered. However, in the real machine, motor displacement change has considerable dynamic (approximately 300 ms from 50 to 100%). We need to synchronise the pump displacement and that of the motor. This has dramatic effect on the performance of the control system since motor displacement

is discrete, and thus causes large changes in speed and pressures. Different ramp functions are used for increasing and decreasing motor commands.

This feature evidently prevents optimal control commands reaching the actuators while active.

### 3.6.4. Feasible motor displacements at a steep uphill

The manufacturer of the HSD pump has included a function that limits the  $\varepsilon_p$  when  $p_B$  or  $p_A$  exceeds a pre-defined limit. This feature, called pressure cut-off, was not included in the simulation model of the machine utilized in the experiments of Backas *et al.* (2014) yet in the real machine it has a dramatic effect on performance near maximum pressure.

When pressure increases too high, for example at a steep uphill,  $\varepsilon_p$  decreases due to pressure cut-off, but as soon as the corresponding pressure ( $p_B$  in forward motion) drops,  $\varepsilon_p$  is increased again. This leads to oscillations in the displacement of the HSD pump and pressures in this kind of situations. More importantly, because  $\mathbf{u}^*$  is determined based on  $\Delta p$ , motor command  $\varepsilon_{m,com}^*$  starts to oscillate between 0.5 and 1 values, further degrading the performance of the machine. To prevent the described phenomenon, we set the displacement of hydraulic motor to full (i.e.  $\varepsilon_{m,com} = 1$ ), when  $\Delta p$  exceeds 300 bars. Reduced displacement is again enabled when  $\Delta p < 80$  bars, for example when the machine has reached the hill top.

## 4. Architecture

The computer running the compiled Simulink code in xPC Target environment has 2.53 MHz Intel Core i7 CPU with 2 GB RAM (see QM-57 in Figure 6). The collected data is saved with 2-ms sample time to a 16 GB SSD drive before downloading it after every experiment.

The computer is connected to three of the four main CAN buses of the machine. Currently, all data related to the engine, e.g. the control command  $n_{e,com}$  and the measured speed  $n_e$ , is transmitted to a commercial control unit BODAS RC36 by Bosch Rexroth which forwards them to appropriate buses. The architecture of HSD control hardware is presented in Figure 6.

The outputs of the optimal controller are first sent to RC36, which transmits them to the HSD actuators.

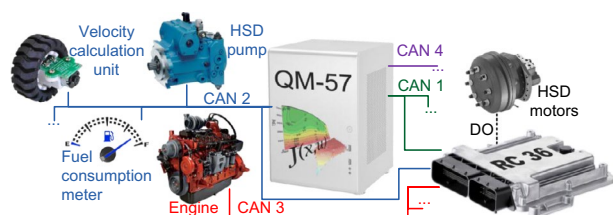


Figure 6. Architecture of HSD control hardware.

This guarantees isochronous transmission of control commands and facilitates implementing safety features, because all commands can be reset in one unit.

## 5. Real-world experiments

The optimal controller was initially developed in a real-time simulator. The controller was implemented in similar xPC Target environment that is used also in the real machine. The simulation results are presented in Backas *et al.* (2014), where a constant rotational speed controller was used as baseline.

Presented tests include only driving, but the controller can also be utilized as a part of the control system of the entire machine that has a client-server structure described in Ahopelto *et al.* (2012). This does not have an effect on the results if the power of HSD is not limited e.g. due to the operation of implement hydraulics.

### 5.1. Description of the tests & testing area

The experimental tests were conducted with the wheel loader described in Section 2.1 in the testing area of IHA. Figure 7 presents an overview of the site.

In this paper, two different kinds of tests are presented to evaluate the efficacy and functionality of the devised optimal controller.

*Test 1.* Improved fuel economy is verified by driving autonomously around the area along the multicolour path described in Figure 7. This test includes both asphalt (flat:red and uphill:blue) and gravel (downhill:green and flat:magenta) sections. Velocity reference for the red and blue parts (flat) is 4 m/s, for the green (downhill) 1 m/s, and for the magenta part (flat) 2 m/s. The machine starts from standstill at every lap at the point marked with the black X. Autonomous control of a similar machine is described in (Ghabcheloo *et al.* 2009).

*Test 2.* In addition, in a second test scenario, the functionality of the controller is demonstrated in hill climbing tests, in which the machine is driven along straight path (see orange arrow in Figure 7) to such a steep hill that without initial kinetic energy, its climbing capacity would be insufficient. This test is conducted with constant velocity references 4, 5 and 6 m/s.

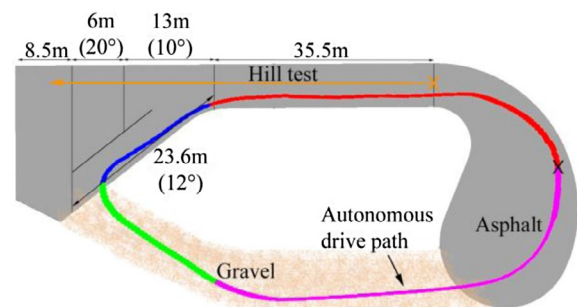


Figure 7. Overview of the testing area with the paths of hill and autonomous tests.



## 5.2. Rule-based controller

The optimal controller is compared to a rule-based controller that is very similar to algorithms used in commercial wheel loaders (Bosch Rexroth AG 2003, Korane 2004, Eaton Corporation 2007). Algorithms resulting to global optimality e.g. dynamic programming (DP) were not utilized here, because they require knowledge about the complete cycle. In empirical testing, gathering this data is not a trivial matter.

Optionally, DP could be utilized as benchmark with a pure simulation experiment. However, all simulation models include assumptions and simplifications which would cause uncertainty to the results. For example, consumption of engine in transient situations is uncertain to model. Moreover, the focus of this research is to demonstrate real measured fuel economy benefits, and therefore simulations were excluded.

The most widely used HSD structure for wheel loaders has one variable displacement hydraulic motor and mechanical drive shafts. The 2-speed hub motors installed in our research platform are rarely utilized. For these reasons, our rule-based controller is not identical to commercial algorithm, but their main principles are the same.

Figure 8 presents how the control commands are determined. The velocity reference of operator sets directly the command of the engine  $n_{e,com}$  as shown in Figure 8. Immediately after  $v_{ref}$  exceeds a minimum value,  $n_{e,com}$  is increased from idle speed to 1100 r/min. After this, the engine command is directly proportional to  $v_{ref}$ . With 5-m/s reference,  $n_{e,com}$  is set to 1650 r/min. The displacements of the hydraulic components are set based on measured and filtered engine speed  $n_e$  (not  $n_{e,com}$ ) using a function visualized in the middle and right hand side plots.

As stated above, rules of the controller are based on commercial algorithms and it is tuned to minimise the steady-state velocity error of the machine on level ground. It is clear that the rules can be changed to achieve better fuel economy, but then it would not correspond to the mentioned widely used hydromechanical controllers.

If the hydraulic motor was variable displacement type,  $\varepsilon_{m,com}$  would be decreased as  $\varepsilon_{p,com}$  increases. With 2-speed motors, the point where  $\varepsilon_{m,com}$  changes from 1 to 0.5 is problematic when it is set based on engine speed. This is because it can easily start switching up and down as the engine load depends on pump displacement according to Equation (4) and  $n_e$  varies based on the load. For this reason, we have implemented a hysteresis to avoid oscillation around this region. This is presented with parallel arrows in the middle and lower plot of Figure 8. Even though this type of algorithm would not be ideal for controlling the machine, it provides better baseline for fuel economy than e.g. a controller that uses constant (or even maximum)  $n_{e,com}$  throughout the velocity range.

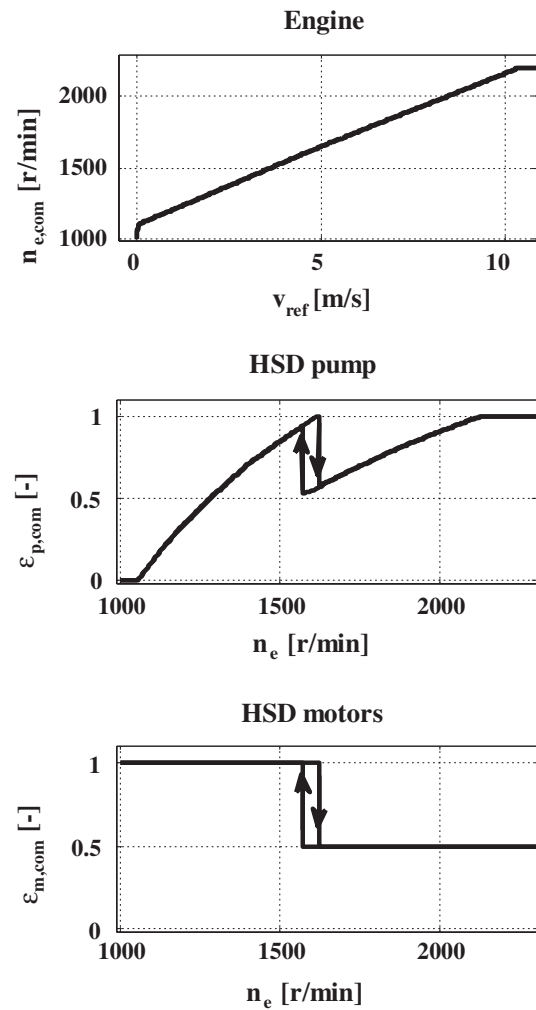


Figure 8. Control commands of the baseline controller.

In addition to the rules above,  $\varepsilon_{m,com}$  is set to 1 if filtered  $\Delta p$  exceeds 300 bars; setting  $\varepsilon_{m,com} = 0.5$  is again enabled when  $\Delta p$  falls below 80 bars. This maximises the climbing capacity of the machine and prevents unintended switching of the control command. This control rule is similar to the one of the optimal controller described in Section 3.6.4.

## 5.3. Results

Figure 9 presents measured fuel consumption for five different velocities at steady-state situation for both controllers. In all the figures of this section, rule-based and optimal controllers are referred as RB and OPT, respectively.

As shown in Figure 9, the optimal controller provides drastic improvements to the fuel efficiency in steady-state driving. The consumption is decreased at least 22.7% and up to 46.9% compared to the rule-based controller. In the presented measurement pairs, the velocity of the machine is not exactly the same with both controllers. For this reason, the consumption is presented by litres per 100 km. Recall that consumption per travelled distance was in the cost for optimisation. As explained

in Section 5.1, the fuel economy improvements of the optimal controller were demonstrated by driving 3 times around the test area along the path in Figure 7. The same test was conducted with and without load; a 1000-kg load was used. Subplots of Figure 10 present an approximate altitude profile of the driven path (GPS data), the measured velocity, control commands and fuel

consumption of the machine. One should notice that the horizontal axis of the figure is distance instead of time. This choice was made to ease the comparison between the controllers, because now the changes occur at the same point of the horizontal axis. However, the presented consumption values (ml/m) are uncertain during transient states as velocity (m/s) and consumption (ml/s) data are not synchronised. Nevertheless, the accuracy of total amounts of fuel consumed in each test (see  $m_f$  values in Table 1) is not compromised because they are integrated values of KMA mobile (see Section 2.1.3) according to time. The curves of Figure 10 describe only a single lap around the area.

The optimal controller accelerates the machine by increasing the engine speed to 1350 r/min and pump displacement to 99% during the first 7 m. After this, it reduces the motor displacement to 50%. At the same time, the commands of the engine and pump are also reduced, because required volumetric flow is lower. During this steady-state phase, rule-based controller uses almost 500 r/min higher engine speed. Lower  $n_e$  leads to lower power consumption (due to constant  $T_{aux}$ ). Therefore, fuel economy is improved with the optimal controller.

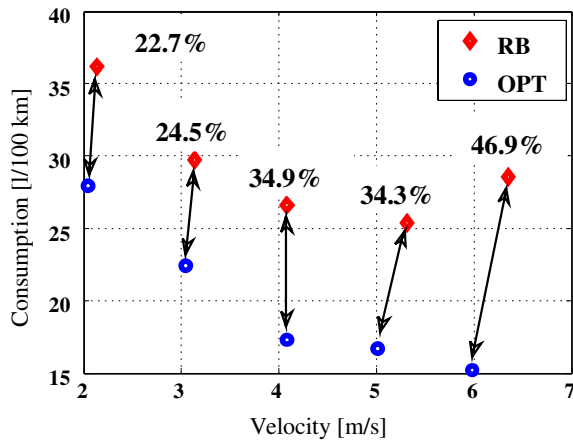


Figure 9. Steady-state consumptions with the rule-based and optimal controllers.

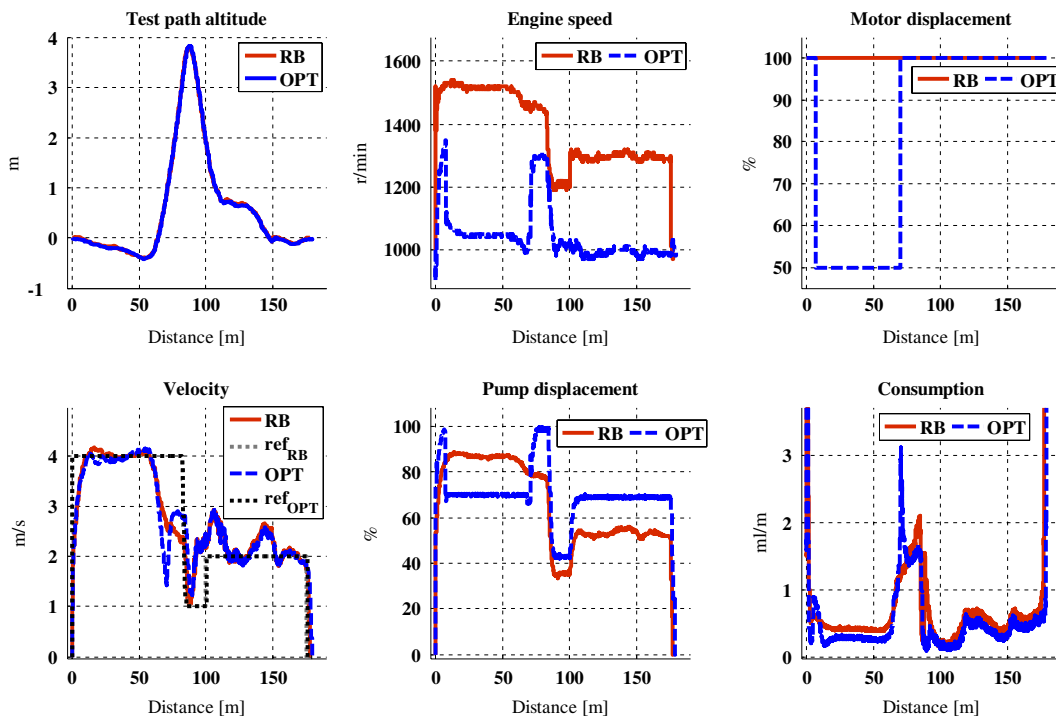


Figure 10. Autonomous drive test around the test area without load.

Table 1. Comparison of fuel consumptions in all tests.

| Test             | Mass [kg] | Optimal controller |            |              |              |                    | Rule-based controller |            |              |              |  |
|------------------|-----------|--------------------|------------|--------------|--------------|--------------------|-----------------------|------------|--------------|--------------|--|
|                  |           | Time [s]           | $m_f$ [ml] | Distance [m] | Cons. [ml/m] | $\Delta$ cons. [%] | Time [s]              | $m_f$ [ml] | Distance [m] | Cons. [ml/m] |  |
| Autonomous drive | 5000      | 229.3              | 290.4      | 550.9        | 0.53         | -16.6              | 228.7                 | 346.5      | 548.1        | 0.63         |  |
|                  | 6000      | 235.4              | 329.4      | 538.8        | 0.61         | -12.4              | 233.6                 | 375.5      | 538.2        | 0.70         |  |
| Hill, 6 m/s      | 5000      | 23.8               | 72.9       | 71.9         | 1.01         | 0.6                | 21.7                  | 70.4       | 69.8         | 1.01         |  |
| Hill, 5 m/s      | 5000      | 24.4               | 65.1       | 72.3         | 0.90         | -0.9               | 21.9                  | 63.0       | 69.3         | 0.91         |  |
| Hill, 4 m/s      | 5000      | 29.6               | 73.2       | 70.6         | 1.04         | 8.4                | 26.3                  | 68.4       | 71.4         | 0.96         |  |

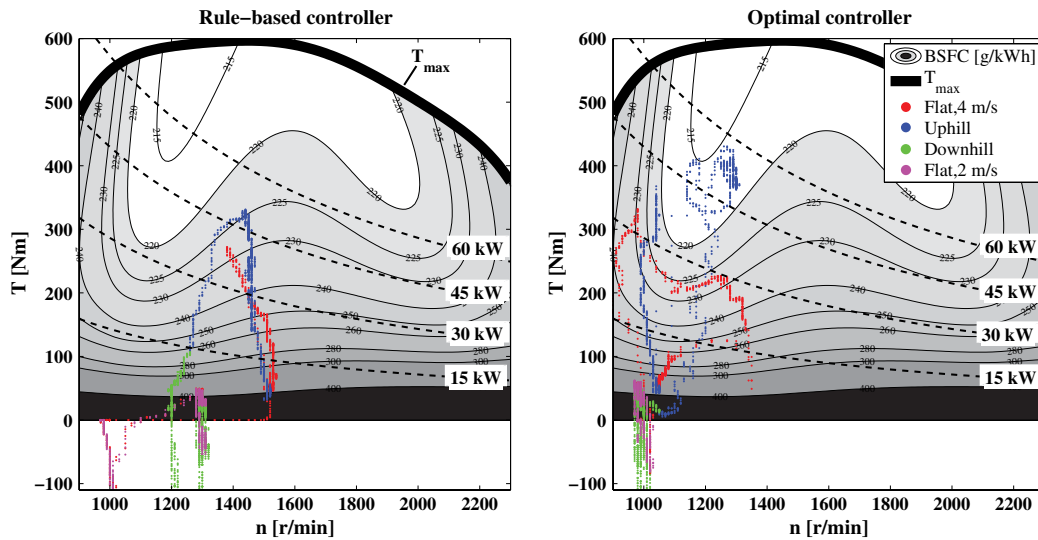


Figure 11. Operation points of the engine in the autonomous drive test without load.

However, as the machine reaches uphill, the torque generated by the hydraulic decreases rapidly with the optimal controller. Because of this,  $\varepsilon_{m,com}$  is increased, which requires also higher  $\varepsilon_{p,com}$  and  $n_{e,com}$ . Accelerating the engine under high load (uphill) requires substantial fuel injection rate. It is evident that the resulting efficiency is momentarily below the one of the rule-based controller. Recall that the engine rotation is already higher in rule-based control.

At the downhill, both controllers exceed the 1-m/s velocity reference and their consumption is the same. In flat gravel ( $v_{ref} = 2$  m/s), the fuel economy of the optimal controller is again notably better than the one reached with the rule-based controller. As both the controllers set  $\varepsilon_m$  to 100%, this difference originates from the higher  $\varepsilon_p$  (better efficiency) and lower  $n_e$  chosen by the optimal controller. Figure 11 describes the engine operation points ( $n_e, \hat{T}_e$ ) in the same autonomous drive test plotted on top of the BSFC map of the engine. Same colours are used to mark different parts of the path in Figure 7. In these plots, engine torque ( $\hat{T}_e$ ) is calculated based on measured  $\Delta p$  and Equation (4). In addition, curves indicating constant powers 15, 30, 45 and 60 kW are shown.

It can be seen from Figure 11 that the BSFC values of the engine are lower (i.e. lighter regions, better fuel economy) and regions with low rpm are used with the optimal controller. This is particularly clearer on flat ground with  $v_{ref} = 4$  m/s (red points), when the lower  $\varepsilon_{m,com}$  results in higher  $\hat{T}_e$  and lower BSFC. Moreover, in this part of the path, maximum engine power with the optimal and rule-based controllers are 34 and 40 kW, respectively. On the other hand, in uphill, the same value for the optimal controller is 57 kW and for the rule-based controller 50 kW.

In *Test 2* series, the functionality of the controllers was evaluated with an extreme test where the machine was driven to a hill that it cannot climb without initial speed. These tests were conducted without load. Velocity

reference was kept constant during the tests. Figure 12 presents the same variables as Figure 10 with the exception that fuel consumption is replaced with pressure difference and horizontal axis, contrary to the previous plots, is time instead of distance. This facilitates investigating the functionality of the controllers.

During the acceleration phase, the optimal controller increases the  $n_e$  to 1960 r/min and  $\varepsilon_p$  to 100%. The rule-based controller chooses slightly lower engine speed, and reduces the  $\varepsilon_{m,com}$  to 50% at time 3.3 s. Up to this point, the acceleration of the machine is the same with both controllers, but acceleration naturally decreases together with  $\varepsilon_m$ .

At time 4.4 s, the optimal controller reduces  $\varepsilon_{p,com}$ , but keeps it only for 0.5 s as it decides to change the  $\varepsilon_{m,com}$  to 50%. This is because the controller does not predict the system behaviour or plan the future controls at all.

When the machine enters the hill (at time 10 s), both controllers have  $\varepsilon_{m,com} = 50\%$ , which does not provide enough torque to reach the top. Therefore,  $\varepsilon_{m,com}$  is changed in the middle of the hill. Now more flow is needed and also other command values have to be increased. The optimal controller increases  $n_{e,com}$ , because the high value of  $\Delta p$  implies high power demand. On the contrary, the rule-based controller changes  $\varepsilon_{p,com}$ , since its  $n_{e,com}$  is only based on velocity reference.

The most demanding situation occurs when  $\Delta p$  reaches the pressure cut-off limit of the HSD pump. When activated, the pressure cut-off reduces  $\varepsilon_p$  as long as  $\Delta p$  exceeds the limit. This dynamic behaviour is not considered in either controller, and it causes severe oscillation in the steepest part of the hill. The optimal controller is even more sensitive to this, because it utilizes measured pressure values in calculations. Constantly changing  $\varepsilon_p$  results in alternating pressures which eventually causes also unwanted  $n_{e,com}$  changes.

Table 1 summarises the fuel consumptions of all the conducted tests. As stated earlier, *Test 1* series shows

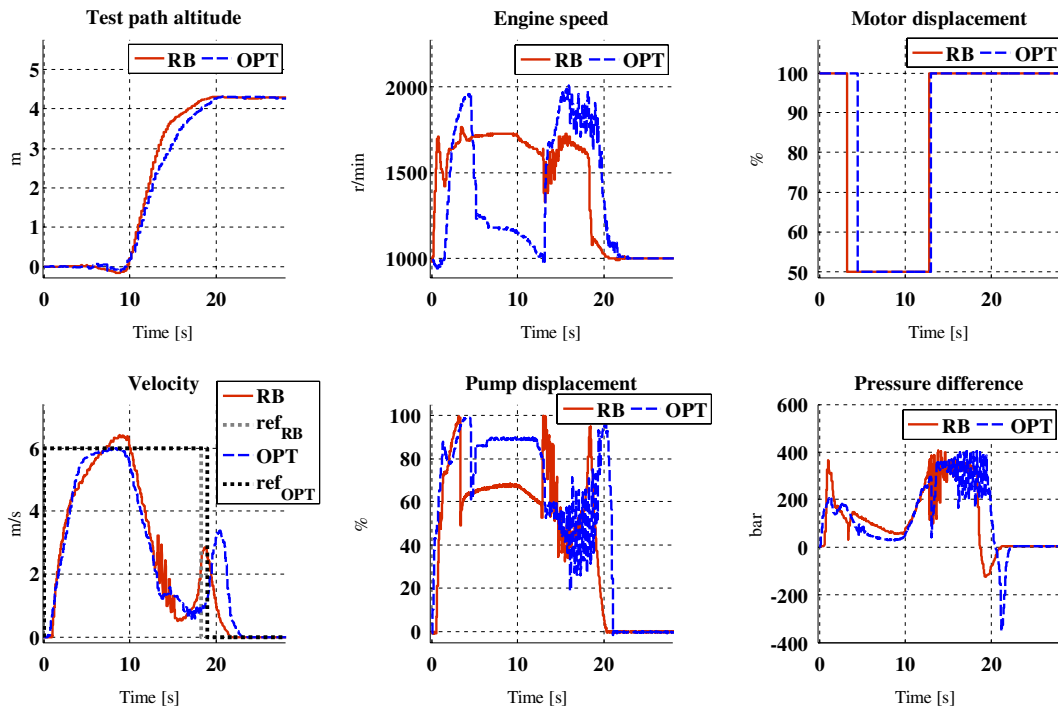


Figure 12. Hill test with constant velocity reference of 6 m/s.

fuel economy of the optimal controller compared to the rule-based, and *Test 2* series is designed to demonstrate the functionality of the controllers in extreme situation. As reference drive cycles for NRMM are not available, *Test 1* demonstrates typical transport drive situations of wheel loaders. In *Test 1* series (autonomous drive tests), measured fuel economy improvement with the optimal controller is 16.6% without load and 12.5% with 1000-kg load. See the boldface column ( $\Delta cons.$ ) of Table 1 for the relative consumption differences of all conducted tests. Main reason why these values differ is the uphill. When the machine is heavier, more fuel has to be injected to generate enough torque with the engine.

The optimal controller uses lower rotational speeds especially in flat surface and therefore,  $n_e$  has to be increased dramatically in uphill. This deteriorates the fuel efficiency even more with load. In addition, when looking at the BSFC-map of the engine (see Figure 11), it is clear that decreasing the  $n_e$  with high constant power (e.g. 60 kW) does not improve BSFC as much as it would with lower power (e.g. 15 kW).

Even though *Test 2* series (the hill climbing tests) mainly demonstrates the functionality of the controllers, Table 1 includes also the consumed fuel amounts of steady-state situations (see Figure 9), the extreme hill tests show that the optimal controller cannot reach the lowest consumption in dynamic situations. In fact, when climbing the hill with 4-m/s reference, it consumed 8.4% more fuel than the rule-based controller. This is mainly due to the fact that the rule-based controller keeps the displacement of the hydraulic motors full throughout the test. In addition, the optimal controller accelerates of the engine under high load which decreases fuel economy.

In the other hill tests, the total fuel consumptions of the controllers are almost the same, because both controllers reduce  $\varepsilon_{m,com}$  to 0.5. With the optimal controller, less fuel is consumed in steady-state driving, but this amount is lost when entering the hill as described above. Eventually, these are quite expected results, because the optimal controller is based on steady-state equations of the system.

## 6. Conclusions and future work

In this paper, we presented a fuel optimal controller for HSD based on the steady-state equations of the system, while including parts that consider dynamic situations as well. The devised controller was implemented in a 5-ton wheel loader to verify its efficacy and functionality. The fuel consumption of the machine was measured online with a state-of-the-art device.

The results of the optimal controller were compared to the ones obtained with a much simpler rule-based controller that is very similar to algorithms used in commercial wheel loaders. In steady-state driving, the optimal controller improved fuel economy at least 22.7% and up to 46.9%. Autonomous drive tests, including hills, different surfaces and loads, were also conducted, and the consumption was decreased up to 16.6%. Functionality of the controllers was proven in extreme hill climbing tests.

Even though the performance of the optimal controller was satisfactory at the conducted tests, it did not provide optimal behaviour in all situations. Especially, operation under rapidly increasing load was inefficient. However, further improvements require utilizing the dynamic equations of the system in the controller. Moreover, one important challenge is that the efficiency



curves of hydraulic components and BSFC curves of engines are only tested and provided in steady-state situations. It is known, as we also showed, that in dynamic situations actual consumption differs from steady-state curves. In the future, we will investigate MPC and consider dynamic equations of the HSD systems together with state and input constraint. This should provide better overall fuel economy, adequate velocity tracking, and no need for auxiliary functions at the output. In addition, we will also conduct complete work cycle experiments instead of pure driving in empirical tests.

### Disclosure statement

No potential conflict of interest was reported by the authors.

### Notes on contributors



**Joni Backas** graduated (MSc) from Tampere University of Technology in 2010, majoring in machine automation. Currently, he is a PhD student at the Department of Intelligent Hydraulics and Automation (IHA). His research interests lie in the control of hydrostatic drive transmissions, especially improving their fuel economy.



**Reza Ghabcheloo** received his PhD degree from Technical University of Lisbon, Portugal in 2007. He is currently an associate professor with the Department of Intelligent Hydraulics and Automation, Tampere University of Technology, Finland. His research interests include guidance and motion control for mobile robots, and optimal motion planning and control in particular for energy efficiency of hydraulic powertrains.



**Seppo Tikkanen** Seppo Tikkanen (MSc. 1995, Mech.Eng. Dr.Tech. 2000) is a professor of machine automation (energy efficient drives) in Department of Hydraulics and Automation at Tampere University of Technology. Previously he has worked as CTO at FIMECC Ltd., as group manager at Bosch Rexroth AG and as a researcher in Tampere University of Technology.



**Kalevi Huhtala** was born in August 1957. Received his Dr.Tech. degree from Tampere University of Technology (Finland) in 1996. He is currently working as a professor in the Department of Intelligent Hydraulics and Automation (IHA) at Tampere University of Technology. He is also the head of the department. His primary research fields are intelligent mobile machines and diesel engine hydraulics.

### ORCID

Joni Backas  <http://orcid.org/0000-0002-0553-5990>

Reza Ghabcheloo  <http://orcid.org/0000-0002-6043-4236>

Seppo Tikkanen  <http://orcid.org/0000-0003-2973-094X>  
Kalevi Huhtala  <http://orcid.org/0000-0003-4055-0392>

### References

- Ahopelto, M., *et al.*, 2013. Improved energy efficiency and controllability of mobile work machines by reduced engine rotational speed. *Proceedings of the ASME 2013 international mechanical engineering congress & exposition, IMECE2013*, San Diego, California, USA.
- Ahopelto, M., Backas, J., and Huhtala, K., 2012. Power management in a mobile work machine: reduced diesel rpm for better energy efficiency. *Proceedings of the 7th FPNI PhD Symposium on Fluid Power*, June 27–30 2012, Reggio Emilia, Italy.
- Arcadis, 2010. *Study in view of the revision of directive 97/68/EC on non-road mobile machinery (NRMM) (module I - an emissions inventory)*.
- AVL, 2009. *AVL product description KMA mobile* [online]. Available from: [https://www.avl.com/c/document\\_library/get\\_file?uuid=168caf92-827a-44ab-9dd2-33281cb4eb3d&groupId=10138&download](https://www.avl.com/c/document_library/get_file?uuid=168caf92-827a-44ab-9dd2-33281cb4eb3d&groupId=10138&download) [Accessed 4 February 2015].
- Backas, J., *et al.*, 2011. IHA-machine: a future mobile machine. *The proceedings of the twelfth scandinavian international conference on fluid power*. Tampere, Finland.
- Backas, J., Ghabcheloo, R., and Huhtala, K., 10–12 September 2014. Fuel optimal controller for hydrostatic drives - a simulation study and model validation. *Proceedings of the Bath/ASME 2014 symposium on fluid power & motion control*, Bath, United Kingdom.
- Bosch Rexroth AG, 2003. *Easy machine operation with rexroth automotive drive and anti stall control*. Elchingen: Bosch Group.
- Caterpillar Inc., 2013. *336E H hydraulic excavator* [online]. Available from: <http://s7d2.scene7.com/is/content/Caterpillar/C811713> [Accessed 20 April 2016].
- Daher, N. and Ivantysynova, M., 2014. Energy analysis of an original steering technology that saves fuel and boosts efficiency. *Energy conversion and management*, 86, 1059–1068.
- Deppen, T.O., Alleyne, A.G., Stelson, K.A. and Meyer, J.J., 2012. Optimal energy use in a light weight hydraulic hybrid passenger vehicle. *Journal of dynamic systems, measurement, and control*, 134 (4), 041009-1–041009-11. doi:<http://dx.doi.org/10.1115/1.4006082>.
- Deppen, T.O., *et al.*, 2015. Comparative study of energy management strategies for hydraulic hybrids. *Journal of dynamic systems, measurement, and control*, 137 (4), 041002-1–041002-11. doi:<http://dx.doi.org/10.1115/1.4028525>.
- Eaton Corporation, 2007. *ETAC: electronic transmission automotive control user's manual*. Eden Prairie, MN: Eaton Corporation.
- Feng, D., Huang, D. and Li, D., 2011. Stochastic model predictive energy management for series hydraulic hybrid vehicle. *Proceedings of the 2011 IEEE international conference on mechatronics and automation*, Beijing, China.
- Filipi, Z., *et al.*, 2004. Combined optimisation of design and power management of the hydraulic hybrid propulsion system for the 6 × 6 medium truck. *International journal of heavy vehicle systems*, 11 (3/4), 372–402.
- Ghabcheloo, R., *et al.*, 2009. Autonomous motion control of a wheel loader. *ASME dynamic systems and control conference*, Hollywood, CA, USA.

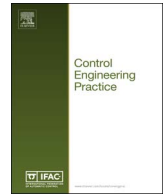
- Hippalgaonkar, R. and Ivantysynova, M., 2012. Fuel savings of a mini-excavator through a hydraulic hybrid displacement controlled system. *8th international fluid power conference, 8. IFK*, Dresden, Germany.
- Huova, M., et al., 2010. Energy efficient control of multiactuator digital hydraulic mobile machine. *7th international fluid power conference, 7. IFK*, Aachen, Germany.
- Jalil, N., Kheir, N., and Salman, M., 1997. A rule-based energy management strategy for a series hybrid vehicle. *Proceedings of the American control conference*, Albuquerque, New Mexico.
- Jähne, H., et al., 2008. Drive line simulation for increased energy-efficiency of off-highway-machines. *6th international fluid power conference, 6. IFK*, Dresden, Germany.
- KCMA Corporation, 2011. *Kawasaki loaders, CONEXPO 2011 handout* [online]. Available from: [https://www.google.fi/url?sa=t&andct=j&andq=andsrc=sandsource=webandcd=7&andved=0CDYQFjAGahUKEwiAwZSgi7XHahUF\\_HIKHdlrAGYandurl=http%3A%2F%2Fkawasakiloaders.com%2FdownloadFile.aspx%3Ffile%3D%2Fpublic%2FCONEXPO2011%2Fpdf%2FKawasaki\\_CONEXPO\\_Handout.pdf&andei=j27UVcC9HoX4ywPZ1](https://www.google.fi/url?sa=t&andct=j&andq=andsrc=sandsource=webandcd=7&andved=0CDYQFjAGahUKEwiAwZSgi7XHahUF_HIKHdlrAGYandurl=http%3A%2F%2Fkawasakiloaders.com%2FdownloadFile.aspx%3Ffile%3D%2Fpublic%2FCONEXPO2011%2Fpdf%2FKawasaki_CONEXPO_Handout.pdf&andei=j27UVcC9HoX4ywPZ1) [Accessed 19 August 2015].
- Kermani, S., et al., 2011. Predictive energy management for hybrid vehicle. *Control engineering practice*, 20 (4), 408–420.
- Korane, K., 2004. *Machine design* [online]. Available from: <http://machinedesign.com/archive/getting-more-mobile-machines> [Accessed 21 December 2015].
- Kum, D., Peng, H., and Bucknor, N. K., 2011. Supervisory control of parallel hybrid electric vehicles for fuel and emission reduction. *Journal of dynamic systems, measurement, and control*, 133 (6), 061010-1–061010-10. doi: <http://dx.doi.org/10.1115/1.4002708>.
- Kumar, R. and Ivantysynova, M., 2011. An instantaneous optimization based power management strategy to reduce fuel consumption in hydraulic hybrids. *International journal of fluid power*, 12 (2), 15–25.
- Luomaranta, M., 1999. A stable electrohydraulic load sensing system based on a microcontroller. *The proceedings of the sixth Scandinavian international conference on fluid power*, 26–28 May 1999, Tampere, 419–432.
- Meyer, J., et al., 2010. Power management strategy for a parallel hydraulic hybrid passenger vehicle using stochastic dynamic programming. *Proceedings of the 7th international fluid power conference*, Aachen, Germany.
- Opila, D., et al., 2013. Real-time implementation and hardware testing of a hybrid vehicle energy management controller based on stochastic dynamic programming. *Journal of dynamic systems, measurement, and control*, 135 (2), 021002-1–021002-11. doi: <http://dx.doi.org/10.1115/1.4007238>.
- Paganelli, G., et al., 2001. General supervisory control policy for the energy optimization of charge-sustaining hybrid electric vehicles. *SAE review*, 22 (4), 511–518.
- Paganelli, G., et al., 2000. Simulation and assessment of power control strategies for a parallel hybrid car. *Proceedings of the institution of mechanical engineers, part D: journal of automobile engineering*, 214 (7), 705–717.
- Pfiffner, R., Guzzella, L., and Onder, C., 2003. Fuel-optimal control of CVT powertrains. *Control engineering practice*, 11 (3), 329–336.
- Sciarretta, A., Back, M., and Guzzella, L., 2004. Optimal control of parallel hybrid electric vehicles. *IEEE transactions on control systems technology*, 12 (3), 352–363.
- Sciarretta, A. and Guzzella, L., 2007. Control of hybrid electric vehicles. *IEEE control systems magazine*, 27 (2), 60–70.
- Serrao, L., Onori, S., and Rizzoni, G., 2011. A comparative analysis of energy management strategies for hybrid electric vehicles. *Journal of dynamic systems, measurement, and control*, 133 (3), 031012-1–031012-11. doi: <http://dx.doi.org/10.1115/1.4003267>.
- Srivastava, N. and Haque, I., 2009. A review on belt and chain continuously variable transmissions (CVT): dynamics and control. *Mechanism and machine theory*, 44 (1), 19–41.
- The Lubrizol Corporation, 2013. *John Deere adopts hybrid technology* [online]. Available from: <http://drivelinenews.com/off-highway-insights/john-deere-adopts-hybrid-technology/> [Accessed 19 August 2015].
- Wang, Y., Zhang, H., and Sun, Z., 2013. Optimal control of the transient emissions and the fuel efficiency of a diesel hybrid electric vehicle. *Proceedings of the institution of mechanical engineers part D: journal of automobile engineering*, 227 (11), 1547–1561.
- Williamson, C. A., 2010. *Power management for multi-actuator mobile machines with displacement controlled hydraulic actuators*. Thesis (PhD). Purdue University.

## **Publication P.III**

Backas, J., Ghabcheloo, R. & Huhtala, K. 2017. Gain Scheduled State Feedback Velocity Control of Hydrostatic Drive Transmissions. *Control Engineering Practice* 58. DOI: 10.1016/j.conengprac.2016.10.016. pp. 214-224.

© Elsevier. Reprinted with permission.

The color print of this publication is available online (DOI: 10.1016/j.conengprac.2016.10.016)



# Gain scheduled state feedback velocity control of hydrostatic drive transmissions



Joni Backas\*, Reza Ghabcheloo, Kalevi Huhtala

Tampere University of Technology, Department of Intelligent Hydraulics and Automation, P.O. Box 589, FI-33101 Tampere, Finland

## ARTICLE INFO

### Keywords:

Gain scheduling  
D-implementation  
Powertrain  
State-dependent model  
Model based control  
Nonlinear control

## ABSTRACT

In this paper, a velocity tracking controller for hydrostatic drive transmissions is developed. The solution is based on a state-dependent model that incorporates nonlinear characteristics of the system. A full state feedback controller is devised and the gains are scheduled on measured speed and pressures, together with approximated volumetric flow. The effects of uncertainties, especially those related to equilibrium values of pressures, are eliminated by utilizing so-called D-implementation. This technique eliminates the need for equilibrium values, which are model based and thus uncertain.

To demonstrate the efficacy of the controller, the solution is implemented on a 4.5-ton wheel loader. For comparison purposes, a constant gain state feedback controller with integral action is devised, and also a linear PID controller is tuned. The results show that the benefits of the devised controller are significant when it is compared to these two controllers. Moreover, the controllability of the machine is maintained in every situation.

## 1. Introduction

Non-road mobile machines are a fundamental part of several fields of industry. They are a requisite for modern agriculture, the construction and mining industries, increasing productivity of numerous essential and hazardous tasks. Even though some autonomous systems are in operation even today, e.g. in mining (Bills & Cherrington, 2013) and ports (Freundlich, 2013), the majority of these machines are operated by humans. Moreover, skilled operators are a scarce resource. Thus, operator assistance functions have emerged as key factors in the competition between manufacturers. Closed loop velocity control, also known as cruise control in the automobile industry, is one example of such systems.

One can argue that cruise control is not a required functionality for manually operated work machines. However, it improves the quality of work with inexperienced drivers and also enables experts to concentrate better on their work. Nevertheless, autonomous and cooperative machines are the main motivation for this research work. Agricultural tasks that need regular speeds such as combine-tractor synchronization and also convoying in mining machinery are just a few examples of where accurate speed tracking is essential for safety and performance.

Several sources of nonlinearities exist in hydrostatic drive transmissions (HSD) (Merritt, 1967). Gain scheduling is a widely used control scheme for nonlinear systems, possibly due to its relative simplicity. It has been shown in several different applications, e.g. vapor compres-

sion (Yang, Pollock & Wen, 2015), wind turbine control (Jafarnejadsani and Pieper, 2015), air-fuel ratio of engines (Postma and Nagamune, 2012) and autonomous underwater vehicles (Silvestre and Pascoal, 2007) that this method works well in practice. In addition to gain scheduling, state-dependent (SD) system models are a common practice in the modeling of hydraulic systems in this community. For example, Strano and Terzo based their feedback controller on the state-dependent Riccati equation, which they utilized for the pole placement of a hydraulic actuation system (symmetric cylinder) (Strano and Terzo, 2015). Also Taylor and Robertson assigned poles for a hydraulic manipulator control with SD model (Taylor and Robertson, 2013). Nevertheless, research on the control of hydraulic rotary actuators is limited as the majority of investigated hydraulic systems include only hydraulic cylinders. The number of moving parts and gaps is multiple in hydraulic piston motors or pumps used in the HSD of this study. This makes, e.g. the efficiency models of cylinders substantially simpler. In fact, it is common to consider cylinders leakless, or model their volumetric efficiency with a constant value.

Knowledge about the operation point of the system is essential for successful state feedback, i.e. in hydraulic systems pressure information is required. Balkan, Caliskan, Dolen, Kilic and Koku (2014) stated that it is difficult to estimate the pressure dynamics of hydraulic systems if flow rate measurement is not available (Kilic et al., 2014). Moreover, they investigated the chamber pressures of a hydraulic cylinder. A standard practice is to utilize a system model for pressure

\* Corresponding author.

E-mail addresses: [joni.backas@tut.fi](mailto:joni.backas@tut.fi) (J. Backas), [reza.ghabcheloo@tut.fi](mailto:reza.ghabcheloo@tut.fi) (R. Ghabcheloo), [kalevi.huhtala@tut.fi](mailto:kalevi.huhtala@tut.fi) (K. Huhtala).



calculations, but this leads to inaccurate estimates due to, e.g. the uncertainties of friction modeling. To tackle this challenge, the so-called D-implementation developed by Coleman, Kaminer, Kahrgonekar and Pascoal (1995) is used in this paper. D-implementation replaces the calculation of some of the operation points with the derivatives of the states. This is realized by placing a derivative and integral at a certain points in the control loop. It is shown that this operation does not change the closed loop properties of the design, yet constant operation points vanish by derivation.

Several research teams have developed cruise control systems and some of these are intended for HSDs, such as the MPC solution for combine harvesters by Baerdemaeker, Coen, Missotten and Saeys, (2008), who controlled both engine speed and pump displacement, but they presented results only for one step response with 6-km/h velocity reference. Guo and Hu utilized an adaptive fuzzy-PD method for the velocity control of a tractor (Guo and Hu, 2014). Their approach requires defining many rules and membership functions for the controller, which is quite common for fuzzy systems. The demonstrated operating speed in this research was 0.8–1.4 m/s. In both of these studies, control design was validated with field tests in which the HSD was composed of variable pump, hydraulic motor and mechanical transmission.

However, most cruise control solutions are developed for on-road vehicles with no hydraulic components. For example, Askari, Ordys and Shakouri (2012) used an approach similar to SD in their nonlinear model predictive control (Shakouri et al., 2012) and detailed their design to switch between velocity and distance tracking modes in (Shakouri & Ordys, 2014). Yadav and Gaur combined internal model control and fuzzy logic for speed control of heavy duty vehicles (Yadav & Gaur, 2015).

In this paper, a gain scheduled velocity controller (GSVC) for hydrostatic drive transmissions is designed. The solution is based on full state feedback and D-implementation. Utilization of D-implementation ensures that the uncertain friction model of the system does not impair the response, and steady-state accuracy together with disturbance rejection are preserved. In addition, the presented control concept does not include an excessive amount of tunable parameters as the only required information is the dynamic equations of the system and parameter values as functions of the states. Therefore, the GSVC is easy to design and tune for machines of different sizes and HSD layouts. It can also be extended for throttling control of hydraulic cylinders: see Jelali and Kroll (2003) for dynamics models of such systems.

The SD parameters of the utilized system model are the volumetric and hydro-mechanical efficiencies of the motors and pump of HSD. Although the efficiencies are functions of the states, the variation is not great and allows for the employment of gain scheduled pole placement using full state feedback. Overall, ignoring time variations in the system during the design is justified for slowly varying system parameters and scheduling (Shamma and Athans, 1992). In general, the accuracies of SD parameters impact the performance of state feedback controllers and some retuning might be required due to changing conditions. For example, if the effects of temperature are not considered, some adjustments might be necessary, e.g. according to seasonal weather. The devised GSVC is not that sensitive to inaccuracies of the model because D-implementation lifts the requirement of constant operating points as measured states are replaced by their derivatives.

Next, we summarize the contributions of this paper. The presented research addresses the control problem of velocity tracking of hydraulic rotary actuators. The initial simulation results and proof of concept were presented in a conference paper (Backas, Ghabcheloo & Huhtala, 2015). Here, the design is extended and the controller is implemented to a real research platform, a 4.5-ton wheel loader. The efficacy of the controller is demonstrated under disturbance and with multiple velocity reference values up to 5 m/s. To the best of our knowledge, this is the first time these control techniques have been experimented

in HSD systems, although many of these aspects have been covered separately in different studies: mostly on throttling control, less on rotary actuators. Hydraulic pumps and motors are significantly more complex (i.e. more difficult to model) than hydraulic cylinders utilized in the majority of studies related to hydraulic systems. Nonlinearities of HSDs make their control much more demanding than mechanical power trains of on-road vehicles, for which most cruise control systems have been devised. Moreover, testing the control system in field experiments in several different operating points, and under positive and negative disturbances, means that the utilized models will not match the plant exactly and guarantees a certain level of robustness.

The rest of the paper is organized as follows. Section 2 presents the hydraulic system and dynamic equations of the research platform machine. A detailed presentation of the GSVC is provided in Section 3. Section 4 describes different implementation aspects related to the controller. In Section 5, the experimental field test results are presented, in which the functionality of the GSVC is compared with the ones obtained with a linear proportional-integral-derivative (PID) controller and a constant gain full state feedback controller with integral term.

## 2. System description and modeling

In this section, the research platform machine - namely its HSD and control systems - is introduced. For more detailed description of the systems of the machine, an interested reader is referred to Backas et al. (2011). Moreover, the dynamic equations of translational motion of the machine to be used by the GSVC are presented.

### 2.1. Research platform machine

The utilized research platform was engineered at the Department of Intelligent Hydraulics and Automation (IHA) in Tampere University of Technology (TUT). The machine is presented in Fig. 1.

The HSD of the machine is a closed hydraulic circuit. This means that the fluid utilized in the transfer of power is fed back to the pump from the motors instead of being circulated through a tank. A hydraulic diagram of HSD, including control commands, is presented in Fig. 2.

The prime mover (denoted M in Fig. 2), a 100-kW diesel engine, provides power to a hydraulic pump connected directly to the engine. The pump is a variable displacement type, i.e. its output flow (see  $Q_p$  of Fig. 2) can be controlled both by its swash plate angle (displacement ratio  $\epsilon_p$ ) and by the speed of the engine shaft  $n_e$ . Subscript *com* indicates command variables in Fig. 2. Moreover, the pump can provide flow in both directions, allowing forward and reverse motion. The produced volumetric flow is directed to 4 hydraulic motors connected to each wheel of the machine. The displacement ratios of these hub motors ( $\epsilon_m$ ) can be changed between two discrete settings, full and 50% of the maximum. The maximum displacements of the HSD pump ( $V_p$ ) and motors ( $V_m$ ) are 110 and 470 cm<sup>3</sup>, respectively. Variables  $p_A$  and  $p_B$  are the pressures of volumes A and B, respectively.

In this HSD system, the flow through the flush valve (in the middle of Fig. 2) always comes from the volume that has the lower pressure and the flow of the boost pump (see  $Q_b$  of Fig. 2) is also directed to this



Fig. 1. Research platform.

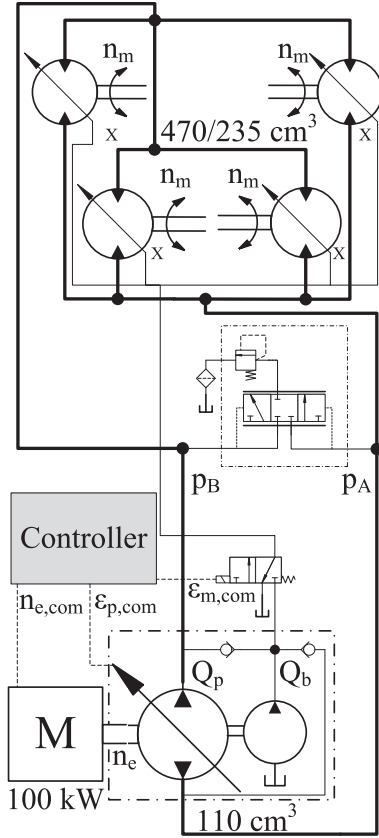


Fig. 2. Hydrostatic drive transmission of the research platform machine.

volume.

The main benefits of HSDs compared to mechanical transmissions are that both traction force and velocity of the machine are decoupled from the rotational speed of the engine. Therefore, high torque values can be achieved even in situations where the machine is barely moving. This is enabled by constantly variable transmission ratio which results in constantly applied traction force, whereas in mechanical transmissions this is not possible due to discrete gear steps.

Installed sensors enable the measurement of several variables, of which the most significant for this research are the rotational speed of the motors  $n_m$  together with  $p_A$ ,  $p_B$ ,  $\epsilon_p$  and  $n_e$ . All of these are converted to digital values and sent via CAN-bus to the control computer of the machine (see Fig. 6 for the architecture of the control system).

## 2.2. Dynamic model of the translational motion of the machine

The dynamic model of the machine includes viscous  $F_v$  and coulomb  $F_C$  frictions, together with the traction forces of the machine  $F_T$  and disturbance force from a hill  $F_h$ . In deriving the model it is assumed that the wheels do not slip and all motors rotate at the same speed; therefore, the velocity of the machine is proportional to the rotational speed of the motors, i.e.,  $v_{mach}=2\pi r_i n_m$ . The torque balance equation of the machine can be obtained using Newton's second law. By solving that for acceleration of the hydraulic motor, the translational motion of the machine is described with

$$\dot{n}_m = - \underbrace{\frac{b}{m} n_m}_{F_v} + \underbrace{\frac{\epsilon_m V_m}{\pi^2 r_i^2 m} \eta_{hm,m} p_B - \frac{\epsilon_m V_m}{\pi^2 r_i^2 m} \eta_{hm,m} p_A}_{F_T} - \underbrace{\frac{g}{2\pi r_i} \mu_{fric}}_{F_C} - \underbrace{\frac{g}{2\pi r_i} \sin \theta_h}_{F_h} \quad (1)$$

where

$b$  is the viscous friction coefficient [Ns]

$m$  is the mass of the machine [kg]

$n_m$  is the rotational speed of the motors [1/s]

$\epsilon_m$  is the relative displacement of the motor [-]

$V_m$  is the displacement of the motors [ $m^3/r$ ]

$r_i$  is the radius of the tyres [m]

$\eta_{hm,m}$  is the hydromechanical efficiency of the motors [-]

$p_{B/A}$  is the pressure of volume B/A<sup>1</sup> [Pa]

$g$  is the gravitational constant [ $m/s^2$ ]

$\mu_{fric}$  is the coulomb friction coefficient

$\theta_h$  is the slope angle of hill

Utilizing the continuity equation<sup>2</sup> (Merritt, 1967), the derivatives of pressures of volumes B and A in forward motion can be described with

$$\dot{p}_B = - \frac{\beta_{eff}}{V_B} 4\epsilon_m V_m \eta_{vol,m} n_m - \frac{\beta_{eff}}{V_B} K_{v,fv} C_{pB} p_B + \frac{\beta_{eff}}{V_B} Q_p + Q_b C_{pB}$$

$$C_{pB} = \begin{cases} 0 & p_A \leq p_B \\ 1 & p_A > p_B + 0.5 \text{ MPa} \end{cases} \quad (2)$$

$$\dot{p}_A = \frac{\beta_{eff}}{V_A} 4\epsilon_m V_m n_m - K_{v,fv} \frac{\beta_{eff}}{V_B} C_{pA} p_A - \frac{\beta_{eff}}{V_A} \frac{1}{\eta_{vol,p}} Q_p + Q_b C_{pA}$$

$$C_{pA} = \begin{cases} 1 & p_A \leq p_B - 0.5 \text{ MPa} \\ 0 & p_A > p_B \end{cases} \quad (3)$$

where

$\beta_{eff}$  is the effective bulk modulus of the system [Pa]

$V_B$  is the B side volume [ $m^3$ ]

$\eta_{vol,m}$  is the volumetric efficiency of the motors [-]

$K_{v,fv}$  is the flow coefficient of the flush valve [ $(m^3/s)/Pa$ ]

$C_{pB/A}$  is the coefficient defining the flush valve opening [-]

$Q_p$  is the volumetric flow of the HSD pump [ $m^3/s$ ]

$Q_b$  is the volumetric flow of the boost pump [ $m^3/s$ ]

$\eta_{vol,p}$  is the volumetric efficiency of HSD pump [-]

A simplified first order dynamics of the flow of HSD pump is presented in

$$\dot{Q}_p = - \frac{1}{\tau_p} Q_p + \frac{1}{\tau_p} Q_{p,com} \equiv - \frac{1}{\tau_p} Q_p + \frac{V_p}{\tau_p} \eta_{vol,p} u_Q \quad (4)$$

where

$\tau_p$  is the time constant of the HSD pump displacement [s]

$u_Q$  is the control input of the system [1/s] and

$$u_Q = n_{e,com} \epsilon_{p,com} \quad (5)$$

where

$n_{e,com}$  is the control command of the rotational speed of the engine

$\epsilon_{p,com}$  is the control command of the relative displacement of the HSD pump

In the research platform, also displacement of the hydraulic motors can be controlled. However, the dynamics of these components are neglected in Eqs. (1)–(3), and therefore here  $\epsilon_m = \epsilon_{m,com}$ . This does not have an effect on the results because in this study  $\epsilon_{m,com}=100\%$  throughout the tests.

**Definition.** : System models

<sup>1</sup> In this paper, the symbol"/" is used to compact the notation. In this case, B/A means B or A and  $p_{B/A}$  means  $p_B$  or  $p_A$ .

<sup>2</sup> Continuity equation states that the rate of change of pressure in a volume is proportional to flows entering and exiting that volume.

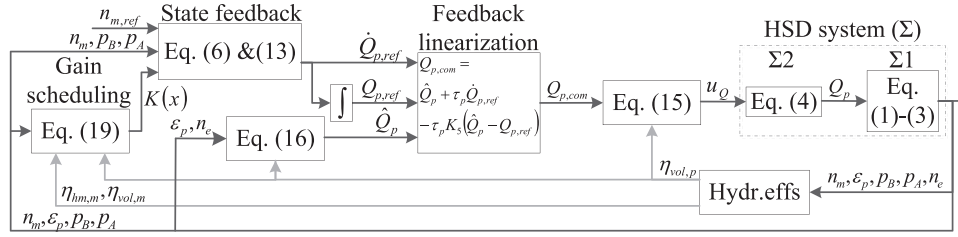


Fig. 3. Control system for HSD velocity tracking.

- **$\Sigma$  (HSD system model):** Eqs. (1)–(4) define equations of translational motion of the machine, with input  $u_Q$  and states  $(n_m, P_B, P_A, Q_p)$
- **$\Sigma 1$  (HSD subsystem model):** Eqs. (1)–(3) define a subset of equations of translational motion of the machine with input  $Q_p$  and states  $(n_m, P_B, P_A)$
- **$\Sigma 2$  (HSD pump model):** Eq. (4) defines the equation of motion of the HSD pump, with input  $u_Q$  and state  $Q_p$

**Remark 1.** As is clear from the above definition, system  $\Sigma$  is split into two subsystems. The reason will become clear in the next section. Notice that coupling between  $\Sigma 1$  and  $\Sigma 2$  is through efficiency coefficient  $\eta_{vol,p}$  in Eq. (4). In the controller, this coefficient is approximated as a function of  $P_A, P_B, \epsilon_p$  and  $n_e$ , i.e.  $\eta_{vol,p}(P_B - P_A, \epsilon_p, n_e)$  (see Section 4.5 for details). This coupling is not shown in Fig. 3 for clarity of the figure.

**Problem definition (speed tracking):** Given system  $\Sigma$  with all states measured, devise a control law such that speed  $n_m$  tracks reference trajectory  $n_{m,ref}$  in the presence of disturbances.

**Remark 2.** Inputs to real machine are  $n_{e,com}, \epsilon_{p,com}$  and  $\epsilon_{m,com}$ , which are commands of rotational speed of the engine, and displacements of the HSD pump and motors, respectively. In the experiments presented in Section 5.2,  $n_{e,com}$  and  $\epsilon_{m,com}$  are held constant, and  $\epsilon_{p,com}$  is calculated with Eq. (5), given  $u_Q$ .

### 3. Control system architecture

For the control architecture, an inner – outer loop structure (shown on Fig. 3) is proposed. A gain scheduling controller is devised to control system  $\Sigma 1$  assuming that the flow  $Q_p$  can be controlled perfectly. To distinguish between state  $Q_p$  and control signal  $Q_p$ , the latter is named  $Q_{p,ref}$ . At the inner loop, a feedback linearization based controller is devised to control system  $\Sigma 2$ . The objective of the latter controller is to guarantee that  $Q_p$  tracks  $Q_{p,ref}$  generated by the outer loop controller.

In Fig. 3, the signals of the outer and inner control loops (e.g. control commands and measurements) are indicated with black lines. The grey lines depict the approximated state-dependent parameters of system. The presented numbers of equations in the blocks indicate control and system dynamics.

#### 3.1. Gain scheduling controller- the outer loop

First, an additional integral state  $z$  is defined as follows

$$\dot{z} = n_m - n_{m,ref} \quad (6)$$

where  $n_{m,ref} = n_{m0}$  is the equilibrium state. Next, the equations of motion (system  $\Sigma 1$ ) - augmented by extra integral state - are arranged into matrix form.

$$\dot{x} = \begin{bmatrix} -\frac{b}{m} & K_m \eta_{hm,m}(n_m, P_B, P_A) & -K_m \eta_{hm,m}(n_m, P_B, P_A) & 0 \\ -\frac{\beta_{eff}}{V_B} A \epsilon_m V_m & -\frac{\beta_{eff}}{V_B} K_{v,fv} C_{pB}(P_B, P_A) & 0 & 0 \\ \eta_{vol,m}(n_m, P_B, P_A) & 0 & 0 & 0 \\ \frac{\beta_{eff}}{V_A} A \epsilon_m V_m & 0 & -K_{v,fv} \frac{\beta_{eff}}{V_B} C_{pA}(P_B, P_A) & 0 \\ 1 & 0 & 0 & 0 \end{bmatrix} x + \begin{bmatrix} 0 \\ \frac{\beta_{eff}}{V_B} \\ -\frac{\beta_{eff}}{V_A} \eta_{vol,p}(n_e, \epsilon_p, P_B, P_A) \\ 0 \end{bmatrix} u + \begin{bmatrix} -\frac{g}{2\pi r_f} \mu_{fric} - \frac{g}{2\pi r_f} \sin \theta_h \\ Q_b C_{pB} \\ Q_b C_{pA} \\ -n_{m,ref} \end{bmatrix} \quad (7)$$

where  $K_m = \frac{\epsilon_m V_m}{(\pi^2 r_f^2 m)}$  or in compact form

$$\dot{x} = A(x)x + B(x)u + d, \quad (8)$$

where

$$x = \begin{bmatrix} n_m \\ P_B \\ P_A \\ z \end{bmatrix}, \quad u = Q_p \quad (9)$$

Note that  $A(x), B(x)$  and  $d$  describe state-dependent system matrix, input vector and disturbance input, respectively.

Since the HSD system is stable, for constant input  $u=u_0$ , Eq. (7) will converge to steady-state, that is,

$$A(x_0)x_0 + B(x_0)u_0 + d=0 \quad (10)$$

for some constant point  $x_0$ . It is worth mentioning that variation of  $A(x)$  and  $B(x)$  with respect to  $x$  is small in the region of interest for the HSD system. This enables scheduling of the control gains on the measured states  $x$ . For the pair  $(x_0, u_0)$ , a full state feedback is calculated

$$u = -K(x_0)(x - x_0) + u_0 \equiv \delta u + u_0 \quad (11)$$

where  $K(x_0)$  is designed using pole placement techniques. Some details are provided in Section 4.2. Fig. 4 presents the block diagram of standard state feedback implementation of Eq. (11), for which Eq. (10) needs to be solved at every execution cycle of the controller. Beside the need for a numerical solver, the solution will be far from correct, since the solution will heavily depend on the friction, which is very uncertain. Next, the concept of D-implementation that eliminates the need to solve Eq. (10) is introduced.

#### D-implementation.

The D-implementation by Kaminer et al. (1995) addresses the problem of gain scheduling controller implementation in nonlinear plants. It requires the same number of additional states to be added to the original system as the number of inputs. That is why one integral state was added to the system  $\Sigma$  in Eq. (7). This extra state  $z$  is aimed at driving the steady-state error to zero.

Fig. 5 illustrates the D-implementation version of the standard state feedback implementation presented in Fig. 4. Notice how the deriva-

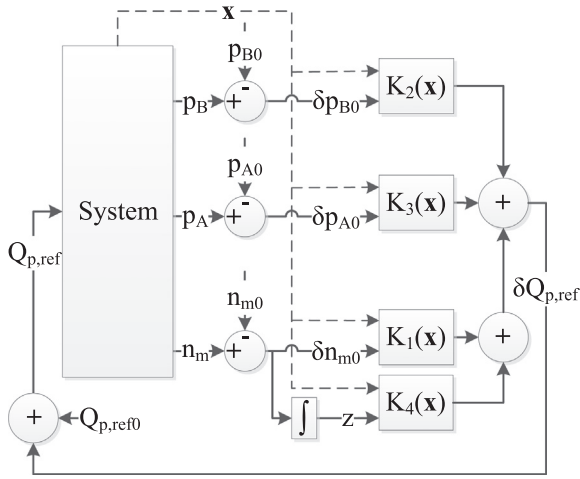


Fig. 4. Standard state feedback control implementation.

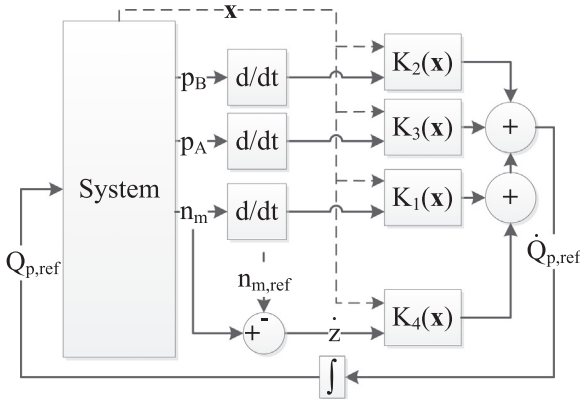


Fig. 5. State feedback with D-implementation.

tives are added to the loop right before the control gains and an integrator is added to the loop right after the gains. As explained in (Kaminer et al., 1995), this operation does not introduce any unstable pole-zero cancellations and the eigenvalues of the closed loop system remain unchanged.

Thus, the derivative of control command can be calculated from Eq. (11) with

$$\dot{u} = -K(x_0)\dot{x} \quad (12)$$

assuming constant equilibrium state  $x_0$ , control input  $u_0$  and state feedback vector  $K(x_0)$ . Notice that D-implementation has eliminated the need for calculation of equilibrium pair  $(x_0, u_0)$ . Eq. (12) is presented elementwise as follows

$$\dot{u} = \dot{Q}_{p,ref} = -K_1(x)\dot{n}_m - K_2(x)\dot{p}_B - K_3(x)\dot{p}_A - K_4(x)(n_m - n_{m,ref}) \quad (13)$$

and  $Q_{p,ref}$  is simply an integral of  $\dot{Q}_{p,ref}$ . Equilibrium control value  $Q_{p,ref0}$  is considered as the initial condition of the integrator and its accuracy is not important. In fact, the integrator acts as an estimator, estimating the correct steady-state control values. In summary,  $Q_{p,ref}$  and  $\dot{Q}_{p,ref}$  are outputs of the outer-loop controller, which are in turn the inputs of the inner-loop controller. Notice from Eq. (13) and also from Fig. 5 that only  $n_{m,ref}$  is required.

**Remark 3:** Differentiating the system outputs is not possible in practice, and in most cases derivatives of the states cannot be measured, because they do not have physical meaning. In real implementation, the derivations are replaced by an approximate derivative, a causal transfer function  $s/(\tau s + 1)$  with small enough  $\tau$  (Kaminer et al., 1995).

### 3.2. Pump control- the inner loop

In this section, the solution for tracking control of system  $\Sigma_2$  is elaborated. In short, given reference  $Q_{p,ref}$ , design control signal  $u_Q$ , such that  $Q_p$  follows the reference. Let  $e = Q_p - Q_{p,ref}$  be the error to minimize. By substitution of Eq. (14) in Eq. (4), it is easy to show that with the control signal

$$Q_{p,com} = Q_p + \tau_p \dot{Q}_{p,ref} - \tau_p K_5 (Q_p - Q_{p,ref}) \quad (14)$$

the closed loop dynamic for  $e$  is governed by  $\dot{e} = -K_5 e$ , that is, an exponentially fast dynamics. Notice that the control law of Eq. (14) is simply a proportional controller with a feedforward gain. Control input of  $u_Q$  is then solved by

$$u_Q = \frac{Q_{p,com}}{V_p \eta_{vol,p} (n_e, \epsilon_p, P_B, P_A)} \quad (15)$$

However, to implement Eq. (14), the volumetric flow of the HSD pump  $Q_p$  is needed. Due to lack of robust and compact sensors for non-road mobile machines,  $Q_p$  is not measured. Nevertheless, utilizing pressures  $p_B$  and  $p_A$ , pump displacement and engine speed,  $Q_p$  can be approximated with

$$\hat{Q}_p = \epsilon_p n_e V_p \eta_{vol,p} (n_e, \epsilon_p, P_B, P_A) \quad (16)$$

Moreover, for practical reasons (for example, bounded control signals), following control law instead of Eq. (14) is implemented

$$Q_{p,com} = \begin{cases} \hat{Q}_p + \dot{Q}_{p,ref} - K_5 \text{sat}(\hat{Q}_p - Q_{p,ref}), & \text{if } |v_{ref}| \geq 0.1 \frac{m}{s} \\ 0, & \text{if } |v_{ref}| < 0.1 \frac{m}{s} \end{cases} \quad (17)$$

where  $\text{sat}()$  is a saturation function. In this case, the error dynamics is given by  $\dot{e} = -K_5 \text{sat}(e)$ , which is still stable and exponentially fast when  $|e|$  is smaller than the saturation bound. The method above is referred to as feedback linearization. Interested readers are invited to see Khalil (2002) for more details.

## 4. Control implementation

### 4.1. Control hardware of the machine

The devised controller is realized in the Matlab Simulink environment and implemented in the research platform with an embedded PC board running xPC target. Both the command of the pump ( $\epsilon_{p,com}$ ) and the engine ( $n_{e,com}$ ) are transmitted via Controller Area Network (CAN bus) to the on-board-electronics of these components that implement the closed loop control of  $\epsilon_p$  and  $n_e$ . These low level actuator controllers are designed by their manufacturers. The command of the HSD motors is amplified with a commercial control unit (RC36 in Fig. 6), which operates the control valve of Fig. 2.

The computer running the compiled Simulink code (QM-57 in Fig. 6) in xPC Target environment has a 2.53 MHz Intel Core i7 CPU with 2 GB RAM. The collected data is saved with 2-ms sample rate to a 16 GB SSD drive before being downloaded after every experiment.

The QM-57 is connected to three of the four main CAN buses of the machine. Currently, all the data related to the engine, e.g. the control command  $n_{e,com}$  and the measured speed  $n_e$ , is transmitted to the RC36, which forwards it to the buses from which the QM-57 is receiving messages. The architecture of HSD control hardware is presented in Fig. 6.

The outputs of the controller are first sent to RC36, which transmits them to the HSD actuators with 6-ms rate. This guarantees isochronous transmission of control commands and facilitates the implementing of safety features, because all commands can be reset in one unit.



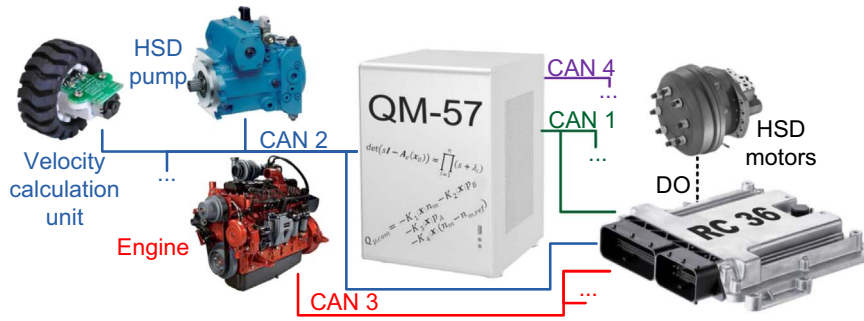


Fig. 6. Architecture of HSD control hardware.

#### 4.2. Pole placement, calculation of gains $K(x)$

Control gains  $K(x) = [K_1(x) \ K_2(x) \ K_3(x) \ K_4(x)]$  are calculated at each sample time by solving

$$\det(sI - A_c(x)) = \prod_{i=1}^4 (s + \lambda_i) \quad (19)$$

where  $A_c(x) = A(x) - B(x)K(x)$ . This operation will place the closed-loop poles at desired locations  $\lambda_{1,2,3,4}$ . Closed form solutions were found using Matlab symbolic toolbox and used in real-time implementation. We set  $\lambda_{1,2,3,4} = -6$  in all of the experiments.

#### 4.3. Control parameters

The GSVc utilizes measured states to calculate the efficiencies and the flush flow coefficients ( $C_{PB}$ ,  $C_{PA}$ ) of Eq. (7). The following choices were made for the controller.

1. The control commands of the engine  $n_{e,com}$  and hydraulic motors  $n_{m,com}$  are 1650 1/min and 100%, respectively.
2. The flush valve model is simplified for the control design as the minimum 0.5-MPa pressure difference given by Eqs. (2) and (3) is neglected in gain scheduling.
3. The derivative is approximated with  $s/(\tau s + 1)$ , where  $\tau = \tau_p$ .
4. The tuneable gain of Eq. (17)  $K_5 = 1/\tau_p$ .
5. The saturation function used in Eq. (17) is set to 10% of the maximum  $Q_p$ .
6. The poles of the closed loop system are all placed to  $s = -6$  (i.e.  $\lambda_{1,2,3,4} = -6$ ) to calculate the gains  $K_{1,2,3,4}(x)$ .
7. The execution cycle of the GSVc is 6 ms.

#### 4.4. Sensor data

The velocity of the machine is measured with sensors integrated in the hydraulic motors. Two of these were malfunctioning during the tests, and therefore this value is calculated as an average of the rotational speeds of the rear tires. This has an effect on the control command in situations where the front wheels are slipping or sliding. In the conducted tests, there was only a minor slippage when the machine reached the hilltop. However, this did not have an effect on the response of the system nor contributed to  $\epsilon_{p,com}$ .

The steering mechanism of the research platform (described in Section 2.1) is articulated steering, which creates kinematic constraints among speeds of the wheels of the front and rear units of the body and articulation angle. These constraints can be used to detect slipping/sliding wheel (thus removed from calculation) as well as to improve machine (let say front unit) speed calculation using least squares optimization. See (Ghabcheloo et al., 2009) for details. The method was not employed in this study.

The rotational speed sensors are connected to a custom made module (see Velocity calculation unit in Fig. 6) that sends the data to a CAN bus with 10-ms rate and the resolution of  $1/2\pi$  1/s. This value is

filtered in the GSVc with 4-Hz low pass filter.

The HSD pump includes several integrated sensors, from which the devised controller utilizes pressures  $p_A$  and  $p_B$  (resolution: 1 bar), as well as pump displacement ratio  $\epsilon_p$  (0.1%). These data are sent in one message with 10-ms rate. The pressures are filtered in the controller with 40-Hz low pass filter.

As stated in Section 4.1, the computer running the controller code (QM-57) is not connected to the same bus with the engine. For this reason, the RC36 reads the data and sends it forward, which causes a slight delay for  $n_e$ . This value has 20-ms rate and resolution of 10 1/min. However, because the engine has much lower dynamics than the HSD pump or the pressures, this is not specially considered in the controller.

All the data filters operate in a 2-ms cycle, but the actual calculations of control commands are executed every 6 ms.

#### 4.5. Approximation of hydraulic efficiencies

In this study, the hydraulic efficiencies are interpolated from tabulated values to determine control gains  $K(x)$  at every execution cycle of the controller.  $\eta_{vol,p}$ ,  $\eta_{hm,m}$  and  $\eta_{vol,m}$  are modelled as a function of pressure difference  $|p_B - p_A|$ , component displacements  $\epsilon_p$  and  $\epsilon_m$ , and the rotational speed of the engine and motor shafts  $n_e$  and  $n_m$ , respectively.

The efficiency models of HSD pump and motors are based on laboratory measurements and the data provided by the manufacturer, respectively. However, these values were determined in constant oil temperatures (60 °C for the pump and 50 °C in the motor test), whereas in the experiments presented in Section 5.2 the temperature was approximately 40 °C.

### 5. Real-world experiments

The GSVc was tested with a 4.5-ton wheel loader in the test area of IHA. Two different types of experiments (both depicted in Fig. 7) were conducted.

- Disturbance test
- Velocity sequence test

In the disturbance test (orange path in Fig. 7), the velocity reference

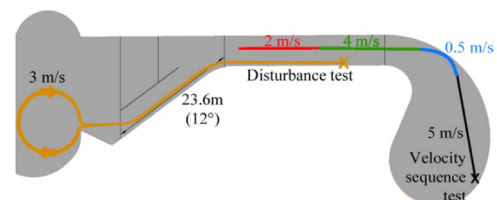


Fig. 7. Approximate paths of the disturbance (orange path) and velocity sequence (multicolor path) tests. (For interpretation of the references to color in this figure legend, the reader is referred to the web version of this article.)

was kept constant at 3 m/s throughout the test and the machine was driven to an approximately 12-degree hill. The hill was both climbed and descended. The second test included driving with four different speeds on flat asphalt. This is referred to as the velocity sequence test (multicolor path in Fig. 7). The distance driven in this test was limited by the flat road of the test area.

For comparison purposes, a constant gain state feedback controller with integral action was devised and also a linear PID controller was tuned. A brief description of these controllers is provided in Section 5.1.

Both tests were driven by a human driver, who manually steered the machine and decided when to change the velocity reference to the next pre-determined value in the velocity sequence test. For this reason, reference changes do not occur at the same time for different controllers, and therefore it is clearer to present the responses in separate figures. With all the controllers, velocity reference is filtered with a first degree filter (time constant: 0.5 s), in which the maximum rate of reference change is limited to  $\pm 2 \text{ m/s}^2$ .

### 5.1. Comparative controllers

To evaluate the performance of the GSVC, two additional controllers were devised based on a time invariant representative model.

- A state feedback controller with extra integral state and D-implementation. This is referred to as Constant Gain state feedback Controller (CGC)
- a PID controller

The model used to design CGC and PID controllers was a linear time invariant system  $\dot{x} = A(x_{0,v3})x + B(x_{0,v3})u$ , where  $x_{0,v3} = (0.88 \ 55 \times 10^5 \ 25 \times 10^5 \ 0)^T$ , which represents steady-state driving on level ground with 3-m/s velocity. At this operation point, the hydraulic efficiencies are  $\eta_{vol,m} = 0.95$ ,  $\eta_{hm,m} = 0.85$  and  $\eta_{vol,p} = 0.87$ .

#### 5.1.1. Constant Gain state feedback Controller

Implementation of CGC is the same as GSVC except for the gains, that is, CGC uses constant gains, while GSVC uses gain scheduling. In particular, D-implementation is also part of CGC to retain the benefits gained from it.

Also CGC is based on pole placement. Thus, the calculation method described in Section 4.2 applies together with the chosen values of the poles in Section 4.3. The derivative of control input (see Eq. (13)) is determined with constant state feedback vector  $K(x_{0,v3})$ .

#### 5.1.2. PID controller

In order to provide a baseline with a standard practice in hydraulic literature, a PID controller was devised. The structure of the controller is depicted with

$$K_p + K_i \frac{1}{s} + K_d \frac{N}{1 + N \frac{1}{s}} \quad (20)$$

Where

- $K_p$  is the proportional gain of the controller
- $K_i$  is the integral gain of the controller
- $K_d$  is the derivative gain of the controller
- $N$  is the filter coefficient of the controller

The objective of the tuning process was to acquire a set of control coefficients that results in as close as possible rise time from standstill to 3 m/s as compared with the GSVC while retaining acceptable overshoot. The results of this kind of test are presented in Fig. 8. Matlab tools were used to automate this tuning process. The values obtained are  $K_p = 6.23 \times 10^{-3}$ ,  $K_i = 1.04$ ,  $K_d = 9.35 \times 10^{-6}$ .  $N$  was set to 100.

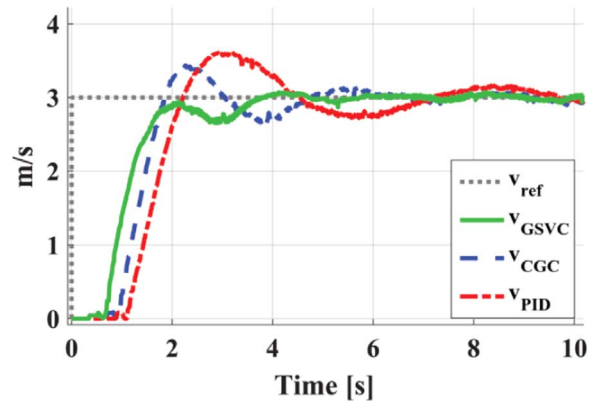


Fig. 8. Acceleration test of the machine with all the controllers.

Naturally, this set is merely a good compromise between, e.g. speed and stability, as is customary when nonlinear systems are controlled with linear controllers.

As can be seen from Fig. 8, the acceleration of the machine is very similar with all the tested controllers. The response of the GSVC is the fastest, with practically no overshoot. The experimental results are thoroughly analyzed in Section 5.2.

### 5.2. Experiment results

#### 5.2.1. Disturbance test

In this test, the machine is accelerated to a velocity of 3 m/s. After reaching steady-state, it climbs a 12-degree hill. At the hilltop, a complete circle is made and the same hill is driven downwards. Shortly after the downhill, the machine is stopped. An approximate path is presented in Fig. 7 in orange. The velocity reference is kept at 3 m/s throughout the test. Notice that this is also the value used in the model utilized in the comparative controllers. Therefore, it should provide the best possible response.

Fig. 9 presents the described test driven with the GSVC. It can be seen from the middle plot that the reference is reached ( $\pm 5\%$ ) in 3.4 s with no overshoot. There is a small delay in the speed response when the machine is accelerated as pressure builds up, eventually reaching 366 bars (see the lowest plot). The GSVC slightly overcompensates the increase of the state derivatives, which results in a slight decrease of speed at  $t = 2.5 - 3.5$  s. Without this, the settling time ( $\pm 5\%$ ) would be approximately 2 s. Before the uphill, steady-state velocity error remains very small ( $< 0.05 \text{ m/s}$ ).

The start of the uphill is quite gentle, but as it steepens velocity error increases. In the upper plot, one can notice oscillation in the control signal in the steeper part of the hill. This is mildly reflected in velocity, but the driver is not able to observe variations of speed. However,  $n_e$  changes because of alternating load, which is discernible also to the driver.

At the hilltop ( $t = 20$  s), velocity error is at its maximum (apart from acceleration and deceleration). There is also some oscillation of  $p_B$ , caused by slipping of the front tires. This is not seen in the velocity curve because of the sensor malfunction explained in Section 4.4.

In between the uphill and downhill parts, the machine is constantly turning, which causes pressure variations that the GSVC attempts to compensate with  $\epsilon_{p,com}$ . Eventually, this results in slowly oscillating velocity.

While driving downhill, there are visible oscillations in the control command. These low amplitude ( $\pm 1.5\%$ ) variations are significantly faster (2 Hz) than the ones observed during turning, and they are caused by gain scheduling (i.e. changing hydraulic efficiencies). However, velocity error remains very small. Deceleration is smooth and the machine is completely stopped 3.3 s after the reference change.

A similar test was driven also with CGC and the collected data is

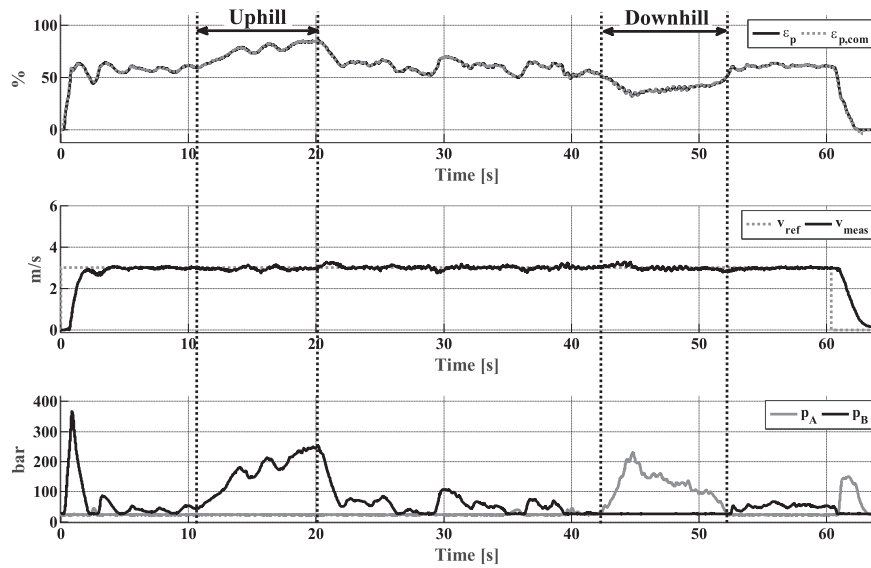


Fig. 9. Disturbance test with GSVC.

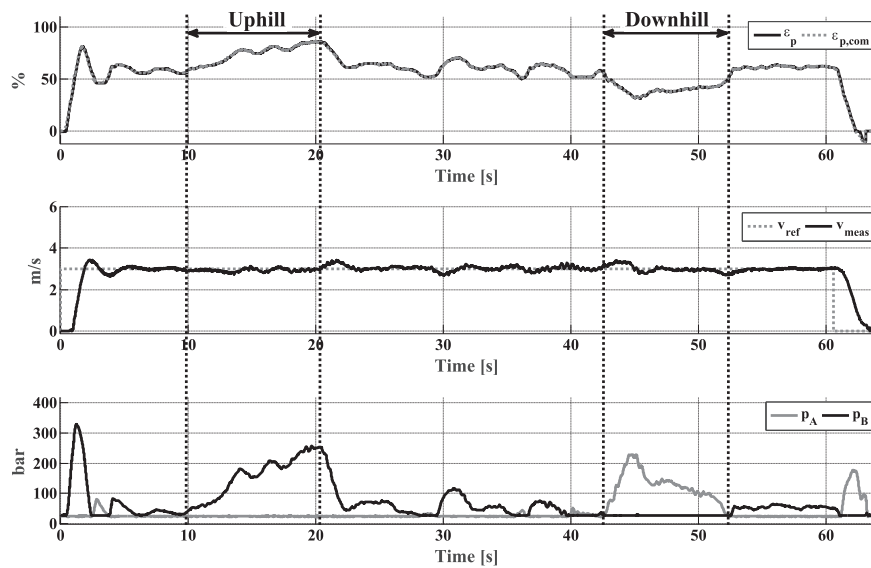


Fig. 10. Disturbance test with CGC.

presented in Fig. 10. The main difference compared to the one obtained with GSVC is the visible overshoot at the end of the acceleration. Obviously, this originates from the constant gains, because the CGC is not able to consider the nonlinear relationship that the pressures and displacement of the pump have on the hydraulic efficiencies. Hence, the model utilized in the GSVC causes overcompensation at the end of acceleration (see Fig. 9), but also improves the transient response of the system.

The settling time with the CGC is 4.3 s. In addition, the velocity error is larger at the hilltop both after uphill and at the beginning of the downhill. At the downhill part, no oscillations of control command are observed with CGC, which is natural because they originate from the gain scheduling part of GSVC.

When the machine is brought to standstill with CGC, the displacement of the HSD pump is set to negative values. Interestingly, the measured displacement does not change before the  $\epsilon_{p,com}$  has decreased to  $-5\%$ . Presumably, this is caused by the wearing of the component. Increased frictions of the displacement setting mechanism restrain the movement, and pressure has to reach higher values to overcome static friction and the forces of the piston centering springs. If the control

command is held constant for a longer period of time, also displacement values between  $\pm 5\%$  can be achieved. However, the HSD pump would have to be detached to confirm the reason for this.

In Fig. 11, the disturbance test is driven with the PID controller (see Section 5.1.2). Initial acceleration is very close to the one achieved with the GSVC, but there is an even larger overshoot with the PID than with the CGC and the 5-% settling time is 6.6 s. In the uphill, the control command of PID does not oscillate as much as with the GSVC. However, maximum velocity error is the largest among the tested controllers both at the beginning and at the end of the hill.

Between the hills, as the machine is turned around, the PID controller is not able to stabilize the speed and  $\epsilon_{p,com}$  oscillates slowly. At the beginning of the downhill, velocity error increases significantly. After this, the control command changes quite smoothly. The efficiencies do not have an effect on the  $\epsilon_{p,com}$  with the PID; therefore, no such low amplitude oscillations as found with the GSVC are observed. When the machine is stopped, also the control command of PID is set to negative values just before the filtered reference falls below the minimum attempted value (0.1 m/s), which forces the  $\epsilon_{p,com}$  to 0%. Despite the sudden change, the machine stops quite smoothly due to

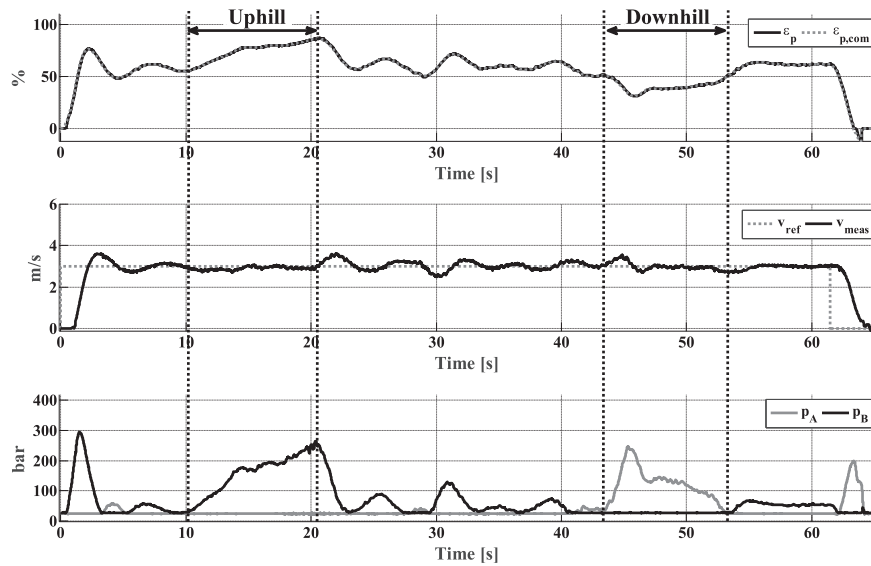


Fig. 11. Disturbance test with PID controller.

low velocity.

5.2.2. Velocity sequence

The second test includes four different values for velocity reference (see multicolor path in Fig. 7). At the beginning, the machine is accelerated to 5-m/s speed (black path in Fig. 7), which is the maximum with the chosen  $n_{e,com}$  and  $\epsilon_{m,com}$ . This is followed by deceleration to 0.5 m/s (light blue), after which the reference is increased to 4 m/s (green). Before stopping, also operation at 2-m/s velocity (red) is demonstrated. The test is driven on level ground. Because of the shape of the test area (see Fig. 7), the machine is steered when driving at 0.5-m/s velocity.

Fig. 12 presents the velocity sequence test with the GSVC. Initial acceleration starts rapidly as the  $\epsilon_{p,com}$  is increased to 59.1% in 0.79 s. Because of this,  $p_B$  raises to 360 bars, and thus the rate of control command is decreased. Recall that derivatives of the states decrease  $\dot{Q}_{p,ref}$  (see Eq. (13)). The displacement of the HSD pump saturates to 100%, but during  $t=3.8-4.8$  the GSVC reduces it up to 5 %-units, mainly because the volumetric efficiency is estimated higher as  $\Delta p$  drops. Velocity error falls within a 5-% margin in 3.5 s

When the velocity reference is set to 0.5 m/s, it takes 4.7 s to reach

$\pm 5$ -% error. However, 0.25-m/s error (5% of 5 m/s) is reached in 3.7 s. No undershoot is observed, but as the machine is turning with this velocity, minor oscillations can be noticed. This is similar to the phenomena in the disturbance test described above.

The acceleration from 0.5 to 4 m/s resembles the one in the disturbance test (see Fig. 9) as the GSVC overcompensates the state derivatives. Also here  $\epsilon_{p,com}$  is temporarily decreased before the steady-state phase. The settling time is 4.0 s ( $\pm 5$ %).

The last two decelerations (4→2 m/s and 2→0 m/s) are quite similar, except that just before the machine is completely stopped the GSVC sends negative control commands to the pump. In these decelerations, the settling and stopping times are approximately 2.1 and 2.5 s, respectively with no undershoot.

Fig. 13 presents the velocity sequence test with the CGC. The performance of CGC is quite similar to GSVC, but there are some clear differences. All the accelerations are as fast, but due to the overshoots (and undershoots) of CGC, the 5-% settling times are significantly longer. There is no overshoot in the first acceleration, because  $\epsilon_p$  saturates. Furthermore, the response of CGC does not seem to reach steady-state with 0.5-m/s velocity reference. Depending on the application, this impaired performance might be acceptable, but the

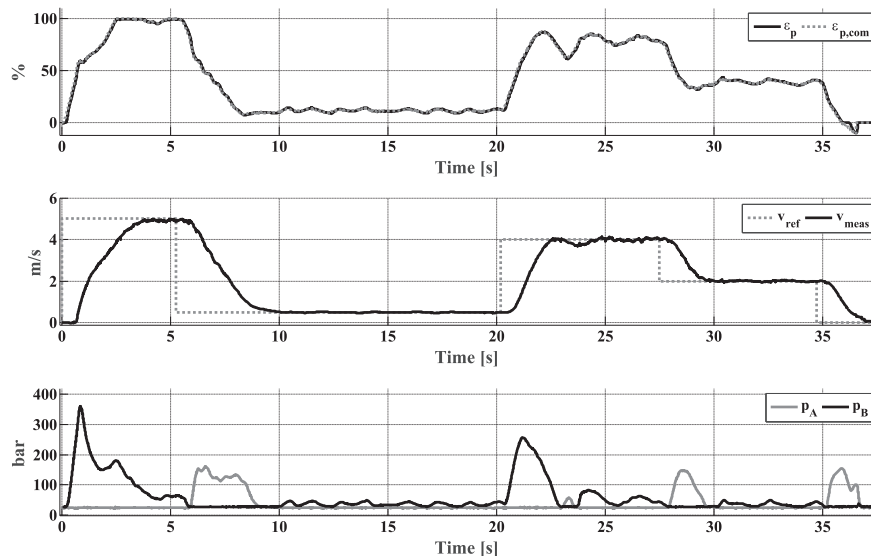


Fig. 12. Velocity sequence with GSVC.



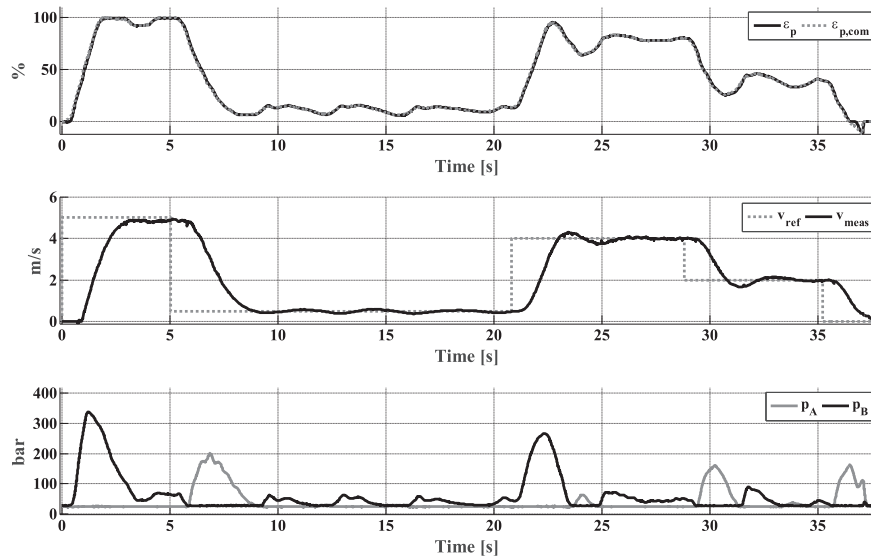


Fig. 13. Velocity sequence with the CGC.

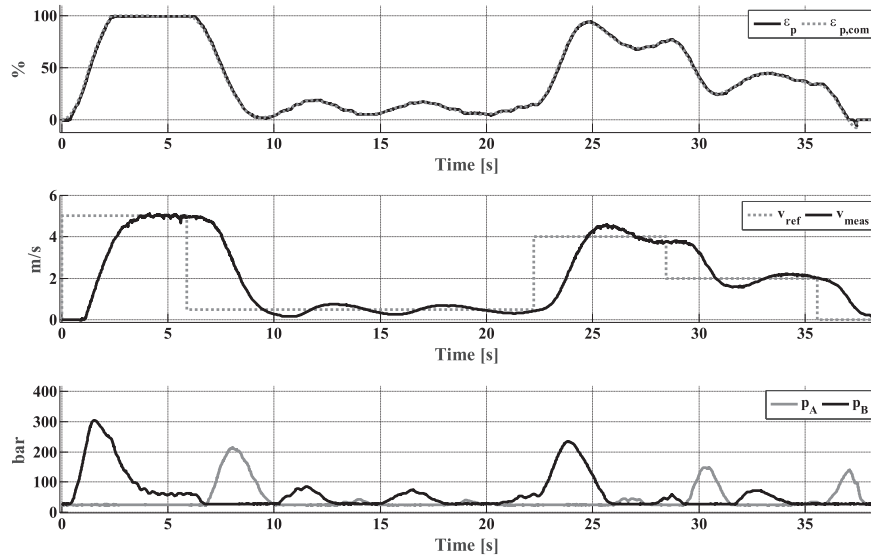


Fig. 14. Velocity sequence with the PID controller.

difference between GSVC and CGC is in any case very explicit.

Finally, the velocity sequence test was driven also utilizing the PID controller. The recorded control command, pump displacement, velocity response and HSD pressures are presented in Fig. 14. When looking at the velocity curve, it is clear that the performance of this linear controller is not as good as the one of the GSVC. Recall that the machine model was linearized to 3-m/s steady-state velocity for the tuning of the PID controller.

Despite the overall response, the first acceleration is quite good as the settling time of the velocity is 3.3 s ( $\pm 5\%$ ) and the overshoot is under 0.1 m/s. Similarly to CGC, this is completely due to the saturating  $\epsilon_p$ . Reference changes to other operating points clearly show that the performance of the PID controller is not as good as with the GSVC. Throughout the test, the velocity response does not completely settle with any utilized reference. However, similar durations of constant reference values were used also with the GSVC that could reach steady-state noticeably before all the reference changes.

## 6. Conclusion

In this study, a velocity tracking controller for hydrostatic drive

transmissions was designed utilizing gain scheduled full state feedback. Hydraulic systems are extremely nonlinear by nature, and thus a state-dependent system model was used to calculate the feedback gains of the controller. In particular, the hydraulic efficiencies are functions of the states. In addition, in order to guarantee zero steady-state error and adequate disturbance rejection, D-implementation (Kaminer et al., 1995) that lifts the requirement of constant operating points, was utilized. This is extremely useful, as especially pressures are difficult to estimate. The presented approach (displacement control) is simple to modify also for valve controlled hydraulic cylinders (throttling control).

The GSVC was implemented in a 4.5-ton wheel loader, and its performance was evaluated in two different tests against two controllers. The first controller included constant gain state feedback with integral term. In addition, a PID controller was tuned. The disturbance test included both uphill and downhill parts driven manually with a constant velocity reference. In the second test, operation was evaluated with reference values ranging from 0.5 to 5 m/s on flat asphalt. The results of the conducted experiments prove the concept of the GSVC. Despite the simplified model (with uncertain parameters), it can be confidently stated that the tracking performance is adequate, e.g. for conveying vehicles.

In the future, the presented controller will be integrated with the fuel optimal controller proposed by the authors in Backas, Ghabcheloo & Huhtala (2014) in order to improve its velocity tracking under load. For this, the controller presented in this paper has to be modified to also consider variable command of the engine and reduced displacement of the hydraulic motors.

## References

- Backas, J., Ghabcheloo, R. & Huhtala, K., (2014). Fuel optimal controller for hydrostatic drives - a simulation study and model validation. In: *Proceedings of the Bath/ASME 2014 symposium on fluid power & motion control*, Bath, United Kingdom, 10–12 September 2014.
- Backas, J., Ghabcheloo, R. & Huhtala, K., (2015). Gain scheduling full state feedback with D-implementation for velocity tracking of hydrostatic drive transmission. In: *Proceedings of the fourteenth scandinavian international conference on fluid power, SICFP15*, May 20–22, 2015, Tampere, Finland.
- Backas, J., Ahopelto, M., Huova, M., Vuohijoki, A., Karhu, O., Ghabcheloo, R. & Huhtala, K., (2011). IHA-machine: A future mobile machine. In: *Proceedings of the twelfth scandinavian international conference on fluid power*, Tampere, Finland
- Bills, K., & Cherrington, M. (2013). The mining factory. *Solid Ground*, 9, 22–27.
- Coen, T., Saeys, W., Missotten, B., & Baerdemaeker, J. (2008). Cruise control on a combine harvester using model-based predictive control. *Biosystems Engineering*, 99, 47–55.
- Freundlich, T. (2013). Straddling the world. *Kalmar Global*, 1, 32–35.
- Ghabcheloo R., Hyvönen M., Uusisalo J., Karhu O., Järä J. & Huhtala K., (2009). Autonomous motion control of a wheel loader. In: *Proceedings of the ASME dynamic systems and control conf. conference and bath/asme symposium on fluid power & motion control*. Hollywood, CA, USA, 12–14 October 2009.
- Guo, N. & Hu, J. (2014). Velocity control system with variable universe adaptive fuzzy-PD method for agricultural vehicles. In: *Proceeding of the 11th world congress on intelligent control and automation*, Shenyang, China.
- Jafarnejadsani, H., & Pieper, J. (2015). Gain-scheduled  $\lambda_1$ -optimal control of variable-speed-variable-pitch wind turbines. *IEEE Transactions on Control Systems Technology*, 23(1), 372–379.
- Jelali, M., & Kroll, A. (2003). *Hydraulic Servo-systems: Modelling, Identification and Control* London, UK: Springer Science Business Media.
- Kaminer, I., Pascoal, A. M., Kahrgonekar, P. P., & Coleman, E. E. (1995). A velocity algorithm for the implementation of gain-scheduled controllers. *Automatica*, 31(8), 1185–1191.
- Khalil, H. (2002). *Nonlinear Systems* Upper Saddle River, New Jersey, USA: Prentice Hall.
- Kilic, E., Dolen, M., Caliskan, H., Koku, A. B., & Balkan, T. (2014). Pressure prediction on a variable-speed pump controlled hydraulic system using structured recurrent neural networks. *Control Engineering Practice*, 26, 51–71.
- Merritt, H. E. (1967). *Hydraulic control systems* New York, USA: John Wiley Sons.
- Postma, M., & Nagamune, R. (2012). Air-fuel ratio control of spark ignition engines using a switching LPV controller. *IEEE Transactions on Control Systems Technology*, 20(5), 1175–1187.
- Shakouri, P., & Ordys, A. (2014). Nonlinear model predictive control approach in design of adaptive cruise control with automated switching to cruise control. *Control Engineering Practice*, 26, 160–177.
- Shakouri, P., Ordys, A., & Askari, M. R. (2012). Adaptive cruise control with stop & go function using the state-dependent nonlinear model predictive control approach. *ISA Transactions*, 51, 622–631.
- Shamma, J., & Athans, M. (1992). Gain scheduling: Potential hazards and possible remedies. *IEEE Control Systems Magazine*, 12(3), 101–107.
- Silvestre, C., & Pascoal, A. (2007). Depth control of the INFANTE AUV using gain-scheduled reduced order output feedback. *Control Engineering Practice*, 15, 883–895.
- Strano, S., & Terzo, M. (2015). A SDRE-based tracking control for a hydraulic actuation system. *Mechanical Systems and Signal Processing*, 60–61, 715–726.
- Taylor, J. C., & Robertson, D. (2013). State-dependent control of a hydraulically actuated nuclear decommissioning robot. *Control Engineering Practice*, 21, 1716–1725.
- Yadav, A. K., & Gaur, P. (2015). Intelligent modified internal model control for speed control of nonlinear uncertain heavy duty vehicles. *ISA Transactions*, 56, 288–298.
- Yang, Z., Pollock, D. T., & Wen, J. T. (2015). Gain-scheduling control of vapor compression cycle for transient heat-flux removal. *Control Engineering Practice*, 39, 67–89.

## **Unpublished Manuscript P.IV**

Backas, J. and Ghabcheloo, R. Nonlinear Model Predictive Energy Management of Hydrostatic Drive Transmissions.

Tampereen teknillinen yliopisto  
PL 527  
33101 Tampere

Tampere University of Technology  
P.O.B. 527  
FI-33101 Tampere, Finland

ISBN 978-952-15-4177-3

ISSN 1459-2045